

POLITECNICO DI TORINO

Master's Degree in Physics of Complex Systems



# Dynamics for large $q$ -*Potts* model in $2d$

Supervisor

Dr. Marco PICCO

Co-Supervisor

Dr. Luca DALL'ASTA

Candidate

Francesco CHIPPARI

2019-2020



*Don't worry about a thing, 'cause every little thing is gonna be all right :)*

## Abstract

This Master's thesis aims to study, via massive numerical simulations and analytical considerations, the dynamical properties of the *2d Ferromagnetic Potts* model, after extremely rapid quenches to sub-critical temperatures. In particular, we are interested in the case in which the model has a large number of states  $q$  (interesting results are obtained for  $q \geq 10^3$ ) and it is built on a square lattice topology. The starting point is a fully disordered configuration with completely uncorrelated spins (infinite temperature,  $T \rightarrow \infty$ ). The quench mechanism, drives the large  $q$ -*Potts* model through a 1<sup>st</sup> order *ferromagnetic-paramagnetic* phase transition (*FOT*).

We want to understand how the final temperature  $T$  and the number of states  $q$  influence the dynamical behaviour of the relaxation towards equilibrium process.

It is known that, depending on  $q$ , this model shows different kinds of *critical behaviour* [1] and, consequently, different dynamical properties. In *2d*, for a *Potts* model with  $q \leq 4$  there is a 2<sup>nd</sup> order phase transition (*SOT*) and the dynamical properties are related, for not too small temperatures, to the world of *coarsening* of domains. For very low temperatures, instead, *blocked* states are observed.

Regarding the case deepened in this thesis, with  $q$  very large and a *FOT*, the dynamical properties are more complex. In fact, varying the two parameters  $T$  and  $q$ , different dynamical behaviours are found. In particular, it is known, for a *FOT*, that order and disorder coexist close to the transition. This results, in a certain range of temperatures, in the birth of *metastable* states. After a quench below  $T_c$  disordered *metastable* states are observed. These can survive for a rather long time. This, then, gives rise to many phenomena concerning *nucleation* and *coarsening* dynamics. *Blocked* states are found, again, in the large  $q$  case.

We study these dynamical behaviours with *Monte Carlo* numerical methods and analytical considerations. The *heat-bath* transition rates have been brought into play to define the stochastic dynamics in the *Continuous time Monte carlo algorithm*.

The most important result is that, while studying how the equilibrium configuration is reached, an *universal behaviour* of the dynamics, in  $T$  and  $q$  has been sought and found for some large  $q$  value and in a particular final temperature  $T$  range. The *universal behaviour* in  $T, q$  certifies that, for any large  $q$ -*Potts model* quenched to any final temperatures  $T$  (belonging to that particular range), the dynamics is the same for each of them.

Beyond the numerical description of the *metastable* states, we attack the problem also analytically: using a large  $q$  expansion for the *heat-bath* dynamics it is possible to obtain some interesting information about this phenomenon. In particular we have found a range in which, for sub-critical quenches and in the infinite  $q$  limit, the *metastable* states are never escaped. In the finite but large  $q$  case, instead, the very same range is the unique one in which these particular states are observed.

A paper presenting the results contained in this master's thesis and other features of the dynamics of the large  $q$ -*Potts* model is in progress [2].

# Table of Contents

List of Tables	VII
List of Figures	VIII
Acronyms and Symbols	XI
<b>1 Introduction to the <i>Potts</i> model at equilibrium</b>	<b>1</b>
1.1 The <i>Potts</i> model . . . . .	1
1.1.1 Analytical solution of the <i>1d Potts</i> model . . . . .	5
<b>2 Phase transitions and out of equilibrium <i>Potts</i> model</b>	<b>10</b>
2.1 Phase transitions: few concepts . . . . .	10
2.1.1 Phase transitions in <i>2d Potts model</i> . . . . .	15
2.2 A dynamical point of view . . . . .	16
2.2.1 Out of equilibrium Statistical Physics . . . . .	17
2.2.2 How to recognize the dynamical regimes: the growing length $R(t)$ . . . . .	21
2.3 Dynamical regimes . . . . .	23
2.3.1 <i>Metastable</i> regime . . . . .	24
2.3.2 <i>Nucleation</i> regime . . . . .	27
2.3.3 <i>Coarsening</i> regime . . . . .	33
2.3.4 <i>Blocked</i> states regime . . . . .	37
<b>3 Theoretical consideration and numerical simulation of the bidi- mensional large <math>q</math> states <i>Potts</i> model</b>	<b>40</b>
3.1 Introduction . . . . .	40
3.2 <i>Heat bath</i> dynamics for the <i>Potts</i> model . . . . .	41
3.3 Characterization of the dynamics . . . . .	50
3.4 <i>Metastability</i> and dynamics for $T > T_c/2$ with the <i>heat bath</i> rules . . . . .	54
3.4.1 Infinite $q$ case . . . . .	55

3.4.2	Finite but large $q$ case . . . . .	57
3.4.3	More precise characterization of the dynamics in the $T > T_c/2$ regime . . . . .	59
3.5	Equilibration for $T \leq T_c/2$ . . . . .	59
3.5.1	Geometry of the clusters for infinite $q$ . . . . .	59
3.5.2	Dynamics at finite $T \leq T_c/2$ with infinite $q$ and at finite $q$ but zero temperature: the <i>blocked</i> states . . . . .	61
3.6	Dynamics in the $T/T_c \leq 1/2$ regime: the <i>universal behaviour</i> . . . .	63
3.7	Snapshots and geometrical properties of the clusters . . . . .	73
<b>4</b>	<b>Conclusions and future research</b>	<b>77</b>
	<b>Bibliography</b>	<b>79</b>

# List of Tables

3.1	Measurements of some interesting geometrical observables for $q = 10^2$ and $L = 10^2$ and $L = 10^3$ . . . . .	75
3.2	Measurements of some interesting geometrical observables for $q = 10^4$ and $L = 10^2$ and $L = 10^3$ . . . . .	76

# List of Figures

1.1	Example of a generic configuration of the <i>Potts</i> model defined on a square lattice with side $L = 1000$ , $N = L^2$ spins each one with $q = 25$ possible colours. . . . .	3
2.1	Phase diagram for the <i>liquid-gas FOT</i> and for the <i>ferromagnetic-paramagnetic SOT</i> in the <i>Ising</i> model. . . . .	11
2.2	Disordered and ordered configuration in the <i>2d ferromagnetic Ising</i> model with <i>nearest neighbour</i> interaction. We used the <i>Wolff algorithm</i> [17] to obtain the equilibrium configuration. . . . .	14
2.3	Example of initial and final configuration for a <i>Potts model</i> with $q = 10^4$ , $T = 0.98T_c$ and $L = 1000$ . . . . .	16
2.4	Example of $R(t)$ for the <i>Potts</i> model defined on a square lattice: $q = 10^4$ , $L = 1000$ with snapshot of the lattice to characterize the different regimes. The dotted line is $t^{1/2}$ . . . . .	23
2.5	Generic disordered <i>metastable</i> state and $R(t)$ vs. $t$ for $q = 10^4$ with $L = 10^3$ at different temperatures given in the key. . . . .	24
2.6	<i>Metastable</i> , stable, unstable equilibrium. Taken from [37]. . . . .	26
2.7	<i>Potts</i> model with $q = 10^4$ , $T = 0.85T_c$ , $L = 1000$ . . . . .	27
2.8	$R(t)$ vs. $t$ at $T = 0.85T_c$ for a <i>Potts</i> model with $q = 10^4$ and $L = 10^3$ . . . . .	28
2.9	Example of flat and curve interfaces. . . . .	33
2.10	<i>Coarsening</i> of domains for a <i>Potts</i> model with $q = 10^3$ , $T = 0.80T_c$ , $L = 1000$ . . . . .	34
2.11	$R(t)$ vs. $t$ at $T = 0.80T_c$ for a <i>Potts</i> model with $q = 10^3$ and $L = 1000$ . . . . .	35
2.12	$R(t)$ vs. $t$ at $T = 0.4T_c$ for a <i>Potts</i> model with $q = 10^4$ and $L=1000$ . . . . .	37
2.13	Snapshots of the lattice to see a <i>blocked state</i> for the <i>Potts</i> model at $T = 0.40T_c$ with $q = 10^4$ , $L = 1000$ . The last two figures have been zoomed to see better the interfaces. In <i>fig.(c)</i> , the presence of T-junctions, flat interfaces and corners it is evident. . . . .	38
2.14	Another kind of <i>blocked-striped</i> state. . . . .	39

3.1	Example of spins configuration. . . . .	43
3.2	All the 12 possible local configurations, taken from [44]. . . . .	44
3.3	Flat interface configuration, the spins with a yellow background corresponds to a (1) vertex. . . . .	45
3.4	$R(t)$ vs. $t$ for $L = 10^3$ at fixed (large) $q$ increasing from top to bottom at different reduced temperatures $T/T_c$ , given in the keys, for the characterization of the dynamics. . . . .	52
3.5	Snapshots of the lattice for $T = 0.80T_c$ , $q = 10^4$ and $L = 10^3$ at various times and $R(t)$ vs. $t$ to see the escaping from the <i>metastable</i> state. . . . .	58
3.6	Snapshots of the lattice for $T = 0.80T_c$ , $q = 10^6$ and $L = 10^3$ at various times and $R(t)$ vs. $t$ to see the escaping from the <i>metastable</i> state. . . . .	58
3.7	Snapshot of the lattice after equilibration with $q \rightarrow \infty$ at $T < T_c/2$ with $L = 10$ for <i>fig.(a)</i> and at $T < T_c/2$ with $L = 100$ for <i>fig.(b)</i> to show the squared/rectangular shaped clusters. . . . .	60
3.8	$R(t)$ vs. $t$ in lattices with $L = 10^3$ to show the similitude between the dynamics with infinite $q$ and finite $T \leq T_c/2$ and the dynamics with finite $q$ and zero temperature. $R(t)$ is averaged over 10 samples. We plot also curves related to the honeycomb and triangular lattices. . . . .	61
3.9	$R(t/t_s)$ vs. $t/t_s$ for $L = 10^3$ at fixed (large) $q$ , increasing from top to bottom and specified in the caption. The different final temperatures of the quenches are given in the keys. A dotted line in correspondence of the plateau has been plotted in addition to the usual one representing $t^{1/2}$ . . . . .	66
3.10	$T/T_c = 0.30$ . . . . .	67
3.11	$R(t/t_s)$ vs. $t/t_s$ , for $L = 10^3$ at fixed $T/T_c$ equal to 0.30,0.40,0.50 (from top to bottom) for different $q$ , averaged over 10 samples. . . . .	68
3.12	Universal behaviour for $L = 10^3$ both in $q$ and $T/T_c$ , the legend gives information about the various values of $q$ and $T/T_c$ used in the simulations. . . . .	69
3.13	$t_{R(t)=R^*}$ vs. $T/T_c$ for $L = 10^3$ at fixed $q$ , given in the legend, averaged over 10 samples. . . . .	70
3.14	$t_{R(t)=5}$ vs. $q^{-1}$ for $L = 10^3$ at $T/T_c = 0.40$ averaged over 10 samples. . . . .	71
3.15	Snapshots with $q = 100$ and $L = 10^2$ at $R(t) = 5,10,20,40,80$ from left to right with $T/T_c = 0.20,0.25,0.30,0.40,0.50,0.60,0.70,0.80$ from top to bottom. . . . .	73
3.16	Snapshots with $q = 10^3$ and $L = 10^2$ at $R(t) = 5,10,20,40,80$ from left to right with $T/T_c = 0.25,0.30,0.40,0.50,0.60,0.70,0.80$ from top to bottom. . . . .	74

3.17 Snapshots with  $q = 10^4$  and  $L = 10^2$  at  $R(t) = 5, 10, 20, 40, 80$  from left to right with  $T/T_c = 0.3, 0.40, 0.50, 0.60, 0.70, 0.80$  from top to bottom. . . . . 74

# Acronyms and Symbols

**PT** Phase transition.

**FOT** First order phase transition.

**SOT** Second order phase transition.

**w.r.t.** With respect to.

**pdf** Probability distribution function.

**SSB** Spontaneous symmetry breaking.

**QFT** Quantum field theory.

**CNT** Classical theory of nucleation.

$\xi$  Correlation length.

**a** Lattice spacing.

**MCMC** Monte Carlo Markov Chain.

**MC** Markov Chain.



# Chapter 1

## Introduction to the *Potts* model at equilibrium

### 1.1 The *Potts* model

The *Potts* model [1, 3] is a mathematical model describing interacting spins on a lattice, with a certain coordination number and a certain topology. It is characterized by the fact that each spin has  $q \in \mathbb{N}$  possible states<sup>1</sup>. It was introduced by *Potts* in his thesis research in 1951 and, even if at first it was not deeply considered, it has gained an incredible importance now. It is used as an important testing ground for the study of methods and approaches suitable to be applied in the analysis of *Phase transitions*.

Indeed, its *critical behaviour*<sup>2</sup> is extremely rich: for different values of  $q$  we have two kinds of *phase transitions*: 1<sup>st</sup> and 2<sup>nd</sup> order *paramagnetic-ferromagnetic* phase transition<sup>3</sup>. The *critical behaviour* could be modified also by the eventual addition of disorder. Above all, the *Potts* model is a generalization of the renowned *Ising* model to an arbitrary number of states  $q$  of the spin variables  $s_i$ . Below, the energy functions of these two models:

$$H_J^{Ising}(\{s_i\}) = -J \sum_{\langle i,j \rangle} s_i s_j \text{ with } s_i \in \{-1,1\}, i \in \{1, \dots, N\} \quad (1.1)$$

$$H_J^{Potts}(\{s_i\}) = -J \sum_{\langle i,j \rangle} \delta_{s_i, s_j} \text{ with } s_i \in \{1, \dots, q\}, i \in \{1, \dots, N\} \quad (1.2)$$

---

<sup>1</sup>Usually, a colour is associated to each state.

<sup>2</sup>Behaviour in the "vicinity" of the transition.

<sup>3</sup>See chapter 2.

Where  $N$  is the number of spins on the lattice and  $\sum_{\langle i,j \rangle}$  means that the sum is restricted to the nearest neighbours of each spin avoiding double counting.

The *Potts* model is mapped into an *Ising* one doing these steps :

- Choose  $q = 2$ .
- Translate the "colour" interval in order to have  $s_i \in \{-1,1\}$ .
- Use the identity:  $\delta_{s_i,s_j} = \frac{1}{2}(1 + s_i s_j)$ .
- Discard a meaningless constant.
- Call  $J' = \frac{J}{2}$ .

$$\begin{aligned}
 H_J^{Potts}(\{s_i\}) &= -J \sum_{\langle i,j \rangle} \delta_{s_i,s_j} \\
 &= -J \sum_{\langle i,j \rangle} \frac{1}{2}(1 + s_i s_j) \\
 &= -\frac{J}{2} - \frac{J}{2} \sum_{\langle i,j \rangle} s_i s_j \\
 &= \text{const} - J' \sum_{\langle i,j \rangle} s_i s_j \\
 &= -J' \sum_{\langle i,j \rangle} s_i s_j \\
 &= H_{J'}^{Ising}(\{s_i\})
 \end{aligned} \tag{1.3}$$

The *Potts* model is widely studied since it can be applied to describe not only ferromagnetic systems but also several phenomena regarding very different topics: from soap foams [4] and metallic grain systems [5] to *FOT* of the quark-gluon plasma in heavy ion collision [6] but also biological morphogenesis, active cell movement [7], protein folding [8] and eventually real world social networks [9]. It is, also, the ideal model to numerically simulate thermal first order phase transitions.

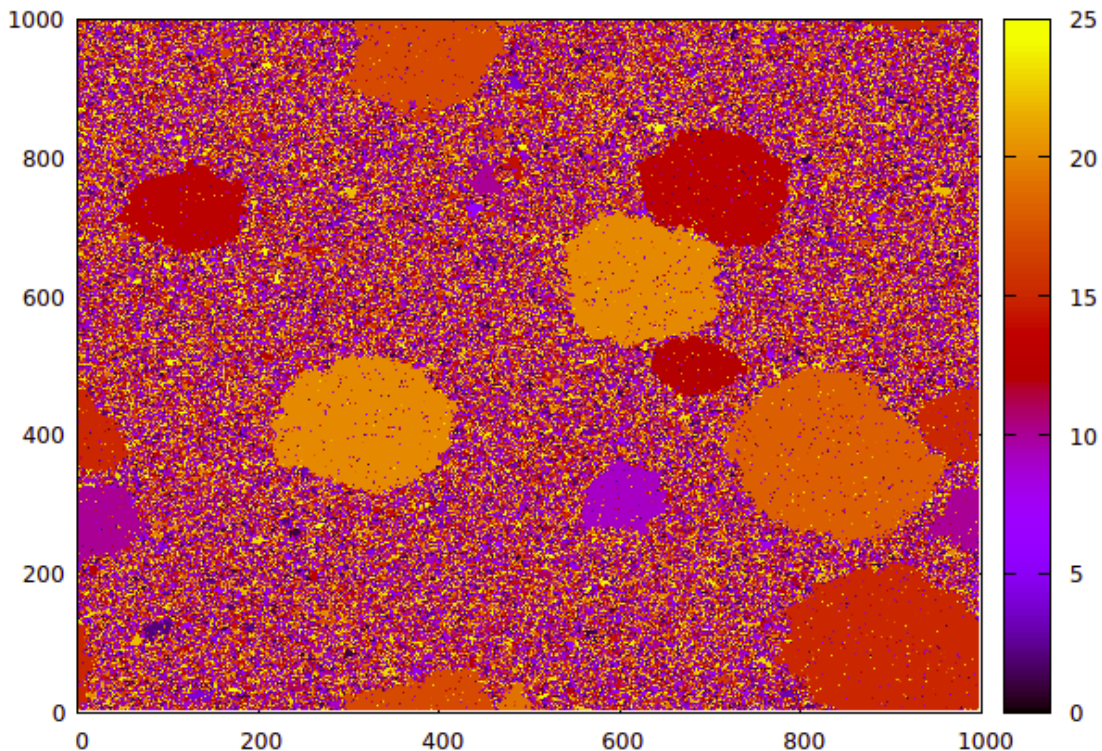


**Figure 1.1:** Example of a generic configuration of the *Potts* model defined on a square lattice with side  $L = 1000$ ,  $N = L^2$  spins each one with  $q = 25$  possible colours.

In this thesis we will study a *Potts* model defined on a  $2d$  square lattice with *coordination number*<sup>4</sup>  $c_{number} = 4$ , side  $L$  and *periodic boundary conditions*. There are  $N$  spins<sup>5</sup> on the lattice which are coupled by means of a *nearest neighbours ferromagnetic interaction*:  $J > 0$ . This kind of interaction, as could be inferred by the form of the Hamiltonian, favours the "alignment"<sup>6</sup> of neighbouring spins. In particular, neighbouring spins with the same colour interact between each other lowering the energy of the system by a value  $-J$ . If two neighbouring spins do not have the same value, the *Kronecker delta*, in the energy function, gives zero and the energy is not lowered. This lets the *ferromagnetic-paramagnetic* phase transitions happen.

<sup>4</sup>*i.e.* the number of nearest neighbours and it is related to the topology of the lattice.

<sup>5</sup>With  $N = L^2$ .

<sup>6</sup>Two spins are aligned if they have the same colour *i.e.*  $s_i = s_j$ .

Let us write the *canonical*<sup>7</sup> partition function for this model:

$$\begin{aligned}
 Z &= \sum_{\{s_i\}} e^{-\beta H_{Potts}(\{s_i\})} \\
 &= \sum_{\{s_i\}} e^{+\beta J \sum_{\langle i,j \rangle} \delta_{s_i, s_j}} \\
 &= \sum_{\{s_i\}} \prod_{\langle i,j \rangle} e^{\beta J \delta_{s_i, s_j}}
 \end{aligned} \tag{1.4}$$

where  $\sum_{\{s_i\}}$  means sum over all the possible spin configurations and  $e^{-\beta J}$  with  $\beta = \frac{1}{k_B T}$  is the so called *Boltzmann weight*, crucial in the definition of the *canonical ensemble* with *pdf*:

$$P_{canonical}(\{s_i\}) = \frac{1}{Z} e^{-\beta H_{Potts}(\{s_i\})} \tag{1.5}$$

The *Potts* model could be also defined in the *anti-ferromagnetic* version [10, Chapter 8.13], simply choosing a coupling constant  $J < 0$  which favours the non-alignment of the spins<sup>8</sup>.

The *2d-Potts* model has not yet been analytical solved<sup>9</sup>. Nevertheless, some important features could be extracted, at the critical point and for certain lattices (like the square one), by some duality arguments. Indeed, with a particular mapping, that goes beyond the purpose of this thesis, it can be shown the *Potts* model is nothing but an *Ice-type* one [10]. Thus, the exact position of the critical point for the square lattice can be extrapolated:

$$T_c = \frac{J}{\ln(1 + \sqrt{q})} \simeq \frac{2J}{\ln(q)} \text{ in the large } q \text{ limit} \tag{1.6}$$

We will often use physical units in which  $J = 1$  but it is important to emphasize the coupling strength dependence of the critical temperature. Exactly at this point the *2d Potts* model undergoes a *paramagnetic-ferromagnetic* phase transition in temperature which is of the 1<sup>st</sup> order if  $q > 4$  and of the 2<sup>nd</sup> order if  $q \leq 4$ .

<sup>7</sup>It is the statistical ensemble which represents the possible states of a system in thermal equilibrium with a heat bath at a fixed temperature. The system can exchange energy with the heat bath, so that the states of the system can differ in total energy.

<sup>8</sup>Choosing  $\beta J = -\infty$  we have a mapping between *q-Potts* and the *q-colouring problem*, very famous in computer science. For some particular *q* values and for some special graphs the *q-colouring* problems are solvable in polynomial time (*P* class). Nevertheless, the vast majority of them are contained in the *NP - complete* class.

<sup>9</sup>For  $q \neq 2$ , since for  $q = 2$  we have *Ising* which is solved by Onsager in *2d* [11], [12].

### 1.1.1 Analytical solution of the $1d$ Potts model

To warm up and become familiar with this model, we solve the  $1d$  version of it. We calculate the *canonical partition function*  $Z$  and the *free energy density*  $f$  with different boundary conditions.

#### Open boundary conditions

Let us solve the  $1d$  Potts model with  $N$  spins,  $q$  states and coordination<sup>10</sup>  $c_{number} = 2$  on an open chain:

$$H_{1d-Potts}^{OBC_s} = -J \sum_{i=1}^{N-1} \delta_{s_i, s_{i+1}} \quad (1.7)$$

$$\begin{aligned} Z &= \sum_{\{s_i\}} e^{-\beta H_{1d-Potts}^{OBC_s}} \\ &= \sum_{\{s_i\}} e^{\beta J \sum_{i=1}^{N-1} \delta_{s_i, s_{i+1}}} \\ &= \sum_{\{s_i\}} \prod_{i=1}^{N-1} e^{\beta J \delta_{s_i, s_{i+1}}} \quad (1.8) \\ &= \sum_{s_1=1}^q \sum_{s_2=1}^q \dots \sum_{s_N=1}^q e^{\beta J \delta_{s_1, s_2}} e^{\beta J \delta_{s_2, s_3}} \dots e^{\beta J \delta_{s_{N-1}, s_N}} \\ &= \sum_{s_1=1}^q \sum_{s_2=1}^q e^{\beta J \delta_{s_1, s_2}} \sum_{s_3=1}^q e^{\beta J \delta_{s_2, s_3}} \dots \sum_{s_N=1}^q e^{\beta J \delta_{s_{N-1}, s_N}} \end{aligned}$$

Now if we consider the following sum:

$$\sum_{s_2=1}^q e^{\beta J \delta_{s_1, s_2}} = e^{\beta J \delta_{s_1, 1}} + e^{\beta J \delta_{s_1, 2}} + \dots + e^{\beta J \delta_{s_1, q}} \quad (1.9)$$

We notice that, depending on the  $s_1$  value, only one term of the sum is equal to  $e^{\beta J}$  while the other  $q - 1$  terms are equal to  $e^0 = 1$ .

At this point we can write:

$$\sum_{s_2=1}^q e^{\beta J \delta_{s_1, s_2}} = e^{\beta J} + q - 1 \quad (1.10)$$

---

<sup>10</sup>To avoid double counting we let each spin interact with the one on its right.

and the same could be written for the sum on  $s_3 \dots s_N$ . Thus, going back to  $Z$  we can write:

$$\begin{aligned}
 Z &= \sum_{s_1=1}^q (e^{\beta J} + q - 1) \cdot (e^{\beta J} + q - 1) \dots (e^{\beta J} + q - 1) \\
 &= (e^{\beta J} + q - 1)^{N-1} \sum_{s_1=1}^q 1 \\
 &= q(e^{\beta J} + q - 1)^{N-1}
 \end{aligned} \tag{1.11}$$

Straightforwardly, we can evaluate the *free energy* density in the thermodynamic limit:

$$\begin{aligned}
 f &= \lim_{N \rightarrow \infty} \frac{\mathcal{F}}{N} \\
 &= \lim_{N \rightarrow \infty} -\frac{1}{N} k_B T \ln Z \\
 &= \lim_{N \rightarrow \infty} -\frac{1}{N} k_B T \ln [q(e^{\beta J} + q - 1)^{N-1}] \\
 &= \lim_{N \rightarrow \infty} -\frac{(N-1)}{N} k_B T \ln [e^{\beta J} + q - 1] - \frac{k_B T}{N} \ln(q) \\
 &= \lim_{N \rightarrow \infty} -k_B T \ln(e^{\beta J} + q - 1) + O(1/N) \\
 &\simeq -k_B T \ln(e^{\beta J} + q - 1)
 \end{aligned} \tag{1.12}$$

where the thermodynamic limit  $N \rightarrow \infty$  justifies the fact that we neglect the term proportional to  $1/N$ .

$$f = -k_B T \ln(e^{\beta J} + q - 1) \text{ in the thermodynamic limit.} \tag{1.13}$$

## Periodic boundary conditions

Let us solve the same model with the periodic boundary conditions *i.e.*  $s_1 = s_{N+1}$

$$H_{1d-Potts}^{PBCs} = -J \sum_{i=1}^N \delta_{s_i, s_{i+1}} \tag{1.14}$$

To calculate the *canonical partition function*  $Z$  we use the *transfer matrix method*:

$$\begin{aligned}
 Z &= \sum_{\{s_i\}} e^{-\beta H_{1d-Potts}^{PBC_s}} \\
 &= \sum_{\{s_i\}} e^{\beta J \sum_{i=1}^N \delta_{s_i, s_{i+1}}} \\
 &= \sum_{\{s_i\}} \prod_{i=1}^N e^{\beta J \delta_{s_i, s_{i+1}}} \\
 &= \sum_{s_1=1}^q \sum_{s_2=1}^q \dots \sum_{s_N=1}^q e^{\beta J \delta_{s_1, s_2}} \dots e^{\beta J \delta_{s_N, s_1}}
 \end{aligned} \tag{1.15}$$

Let us introduce the *transfer matrix*:

$$\hat{T} = T_{s,s'} = e^{\beta J \delta_{s,s'}} \text{ with } s, s' \in \{1, \dots, q\} \tag{1.16}$$

$$\hat{T} = \begin{pmatrix} T_{s=1,s'=1} & T_{s=1,s'=2} & T_{s=1,s'=3} & \dots & T_{s=1,s'=q} \\ T_{s=2,s'=1} & T_{s=2,s'=2} & T_{s=2,s'=3} & \dots & T_{s=2,s'=q} \\ T_{s=3,s'=1} & T_{s=3,s'=2} & T_{s=3,s'=3} & \dots & T_{s=3,s'=q} \\ \vdots & \vdots & \vdots & \ddots & \vdots \\ T_{s=q,s'=1} & T_{s=q,s'=2} & T_{s=q,s'=3} & \dots & T_{s=q,s'=q} \end{pmatrix} \tag{1.17}$$

Specifying the entries values we get:

$$\hat{T} = \begin{pmatrix} e^{\beta J} & 1 & 1 & \dots & 1 \\ 1 & e^{\beta J} & 1 & \dots & 1 \\ 1 & 1 & e^{\beta J} & \dots & 1 \\ \vdots & \vdots & \vdots & \ddots & \vdots \\ 1 & 1 & 1 & \dots & e^{\beta J} \end{pmatrix} \tag{1.18}$$

which can be rewritten as<sup>11</sup>:

$$\hat{T} = (e^{\beta J} - 1) \hat{\mathbb{I}}_{q \times q} + \hat{\mathbb{U}}_{q \times q} \tag{1.19}$$

We can write the *partition sum* as:

$$Z = \sum_{s_1=1}^q \sum_{s_2=1}^q \dots \sum_{s_N=1}^q T_{s_1, s_2} T_{s_2, s_3} \dots T_{s_{N-1}, s_N} T_{s_N, s_1} \tag{1.20}$$

<sup>11</sup> $\hat{\mathbb{I}}_{q \times q}$  is the identity matrix and  $\hat{\mathbb{U}}_{q \times q}$  is a matrix made of entries all equal to 1:  $U_{i,j} = 1 \forall i, j$ .

where  $T_{s_i, s_j}$ , with  $i, j \in \{1, \dots, N\}$ , are the  $N$  equal  $q \times q$  transfer matrices. Now considering that, saturating the final sum, we have:

$$\sum_{s_N=1}^q T_{s_{N-1}, s_N} T_{s_N, s_1} = T_{s_{N-1}, s_1}^2 \quad (1.21)$$

we can iterate, obtaining:

$$Z = \sum_{s_1=1}^q T_{s_1, s_1}^N = \text{Tr}(\hat{T}^N) = \lambda_1^N + \lambda_2^N + \lambda_3^N + \dots + \lambda_q^N \quad (1.22)$$

where  $\lambda_i$  is the  $i$ th eigenvalue of the *transfer matrix*. The invariance property of the trace has been used in the last step.

Now we can calculate the *free energy* density:

$$\begin{aligned} f &= \lim_{N \rightarrow \infty} \frac{\mathcal{F}}{N} \\ &= \lim_{N \rightarrow \infty} -\frac{1}{N} k_B T \ln(\lambda_1^N + \lambda_2^N + \lambda_3^N + \dots + \lambda_q^N) \\ &= \lim_{N \rightarrow \infty} -\frac{1}{N} k_B T \ln \left[ \lambda_{max}^N \left( \left( \frac{\lambda_1}{\lambda_{max}} \right)^N + \left( \frac{\lambda_2}{\lambda_{max}} \right)^N + \dots + \left( \frac{\lambda_q}{\lambda_{max}} \right)^N \right) \right] \\ &= \lim_{N \rightarrow \infty} -\frac{1}{N} k_B T \ln(\lambda_{max}^N) - \frac{1}{N} k_B T \ln \left[ \left( \frac{\lambda_1}{\lambda_{max}} \right)^N + \left( \frac{\lambda_2}{\lambda_{max}} \right)^N + \dots + \left( \frac{\lambda_q}{\lambda_{max}} \right)^N + 1 \right] \\ &\simeq \lim_{N \rightarrow \infty} -\frac{1}{N} k_B T \ln(\lambda_{max}^N) \\ &\simeq -k_B T \ln(\lambda_{max}) \end{aligned}$$

since  $\lim_{N \rightarrow \infty} \left( \frac{\lambda_i}{\lambda_{max}} \right)^N \rightarrow 0 \forall i \in \{1, \dots, q\}$  excluding  $\lambda_{max}$  of course. Thus, the *free energy* density in the thermodynamic limit is:

$$f = -k_B T \ln(\lambda_{max}) \quad (1.23)$$

To go on we need only to calculate the eigenvalues of the matrix  $\hat{U}_{q \times q}$  since the eigenvalues of the identity matrix are already known:

$$\lambda_{max} = (e^{\beta J} - 1 + \lambda_u^{max}) \quad (1.24)$$

To do so, let us consider:

$$\hat{U}_{q \times q} \cdot \vec{v} = \lambda_u \cdot \vec{v} \quad (1.25)$$

$$\begin{pmatrix} 1 & 1 & 1 & \dots & 1 \\ 1 & 1 & 1 & \dots & 1 \\ \vdots & \vdots & \vdots & \ddots & \vdots \\ 1 & 1 & 1 & \dots & 1 \end{pmatrix} \begin{pmatrix} v_1 \\ v_2 \\ \vdots \\ \vdots \\ v_q \end{pmatrix} = \lambda_u \begin{pmatrix} v_1 \\ v_2 \\ \vdots \\ \vdots \\ v_q \end{pmatrix}$$

where  $\mathbf{v} = (v_1; v_2; \dots v_q)^T$  is a generic eigenvector of the  $\widehat{U}_{q \times q}$  matrix. Since the matrix has rank 1, being all rows (columns) linearly dependent, we have that there are  $q - 1$  degenerate eigenvalues equal to 0. Just one eigenvalue is different from 0.

This, is easily found: consider  $\mathbf{v} = (1; 1; \dots 1)^T$  We have clearly that:

$$\begin{pmatrix} 1 & 1 & 1 & \dots & 1 \\ 1 & 1 & 1 & \dots & 1 \\ \vdots & \vdots & \vdots & \ddots & \vdots \\ 1 & 1 & 1 & \dots & 1 \end{pmatrix} \begin{pmatrix} 1 \\ 1 \\ \vdots \\ \vdots \\ 1 \end{pmatrix} = \lambda_u \begin{pmatrix} 1 \\ 1 \\ \vdots \\ \vdots \\ 1 \end{pmatrix}$$

The associated linear system is<sup>12</sup>:

$$\begin{aligned} \sum_{i=1}^q 1 &= \lambda_u 1 \\ \rightarrow q &= \lambda_u \end{aligned} \tag{1.26}$$

Since we are looking for  $\lambda_{max}$  we take only  $\lambda_u^{max}$  which is clearly equal to  $q$ . The maximum eigenvalue of the complete  $\widehat{T}$  matrix is:

$$\lambda_{max} = e^{\beta J} - 1 + q \tag{1.27}$$

At the end we can write *free energy* density:

$$f = -k_B T \ln(q + e^{\beta J} - 1) \tag{1.28}$$

Which is exactly the same of the *free energy* density calculated in the *open boundary conditions* case, demonstrating that in *1d* and in the *thermodynamic* limit these two kinds of *boundary conditions* give the same solution of the model.

---

<sup>12</sup>We have the same linear system for each row of the matrix.

## Chapter 2

# Phase transitions and out of equilibrium *Potts* model

### 2.1 Phase transitions: few concepts

Phase transitions are crucial and ubiquitous in the world of statistical physics. They are *collective phenomena* in which interactions among particles are essential. To describe phase transition in an actual thermodynamic system, we need to involve a huge number<sup>1</sup> of particles. For this reason, they are described by the branch of physics called *Statistical physics* who deals with large particle interacting systems and whose basic principles are stated in [13, Chapter 3], for example. For our purposes, we are going to use some *ensemble* physics concepts and, in particular, the *canonical ensemble*.

With the tools given by this kind of physics, we can study phenomena ranging from the "simple" gas-liquid transition to the *Bose Einstein condensation* in ultra-cold atoms [14, Chapter 12] but also percolation [15] and *paramagnetic-ferromagnetic* phase transition [14, chapter 14] which is extremely important in this thesis. These phase transitions happen when, modifying a *control parameter*<sup>2</sup>, a phase becomes unstable (in the given thermodynamic conditions) and we observe a sharp change of some *order parameter* at a certain critical point or line. This *order parameter* describes and characterizes the features of the phases<sup>3</sup>. During a certain

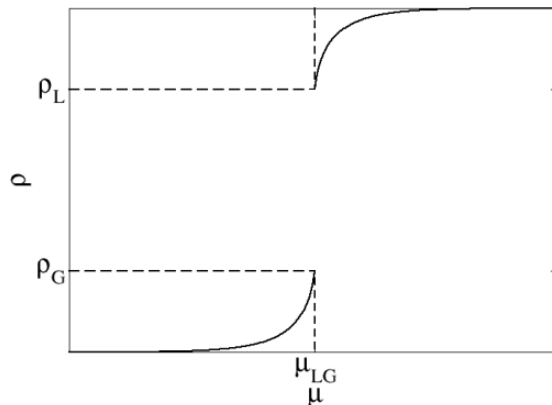
---

<sup>1</sup>Infinite in the thermodynamic limit.

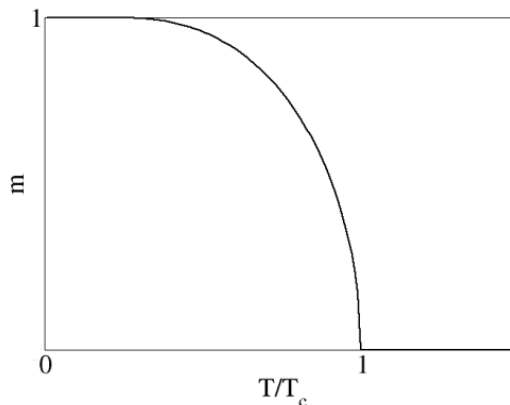
<sup>2</sup>Parameter to be varied to move from one phase to the others *i.e.* temperature, magnetic field, occupation probability and so on...

<sup>3</sup>Important observables *i.e.* magnetization, mass density, probability to be in a percolating cluster etc...

transient a phase is gradually transforming into another one. For temperature activated phase transitions<sup>4</sup>, the *order parameter* has a vanishing thermal average<sup>5</sup> on one side of the critical point and a non vanishing one on the other. Greater is the value of such thermal average deeper we are in that phase. It follows an example of phase diagrams<sup>6</sup> showing the two kinds of phase transition cited before:



(a) Discontinuity of the mass density (order parameter) during a FOT.



(b) Cusp of the magnetization density (order parameter) during a SOT.

**Figure 2.1:** Phase diagram for the *liquid-gas FOT* and for the *ferromagnetic-paramagnetic SOT* in the *Ising* model.

<sup>4</sup>Thermal phase transitions.

<sup>5</sup>Statistical average *w.r.t.* the *pdf* which defines the *ensemble*.

<sup>6</sup>*Control parameter* on the *x* vs. *order parameter* on the *y*.

$PT$ s are found mathematically in the thermodynamic limit, namely infinite volume and infinite number of particles or spins:  $V \rightarrow \infty$ ,  $N \rightarrow \infty$  with  $\frac{V}{N} = O(1)$  (the same reasoning holds for all the intensive quantities *e.g.* density of energy, density of magnetization...).

At the critical point, due to the thermodynamic limit, the thermodynamic potentials, (*e.g.* the *free energy density*) which are derivatives of the partition function<sup>7</sup>  $Z$ , are non-analytic. In particular, for a 1<sup>st</sup> order phase transition the first derivative of the chosen thermodynamic potential is non-analytic while for a 2<sup>nd</sup> order transition the second derivative of the thermodynamic potential (also called response function) is non-analytic. It can be shown that these derivatives are strictly related to the *order parameter* which indeed changes abruptly.

We can also notice a particular feature of the *order parameter*: it is related to the symmetry of the *Hamiltonian*, that is spontaneously broken during the  $PT$ <sup>8</sup>.

For example, the  $O(1)$  symmetry (spin-up, spin-down symmetry) broken in the *ferromagnetic-paramagnetic* transition, happening in the *Ising* model defined on a  $2d$  square lattice with  $N$  spins and *nearest neighbours ferromagnetic coupling*. Let us use this model to deepen some features of the  $PT$  phenomenon:

$$H_{Ising}^{ext}(\{s_i\}) = -J \sum_{\langle i,j \rangle} s_i \cdot s_j - h \sum_{i=1}^N s_i \quad (2.1)$$

In this model we see a 1<sup>st</sup> order phase transition *w.r.t* the *control parameter*  $h$  and a 2<sup>nd</sup> order phase transition *w.r.t* the *control parameter*  $T$  ( $\beta$ ).

To see mathematically the  $PT$ <sup>9</sup>, in the *Ising* model, a magnetic pinning field<sup>10</sup>  $h$  is needed. Indeed, it is required something to model the *spontaneous breaking* [16] of the  $O(1)$  symmetry of the Hamiltonian:  $H_{Ising}(\{s_i\}) = H_{Ising}(\{-s_i\})$ . This *SSB* drives the system to the selection of one of the two possible ground states:

- Ordered state with all the spins up.
- Ordered state with all the spins down.

---

<sup>7</sup>Depending on the chosen ensemble the partition function has different formulation *i.e.*, in the canonical ensemble, the sum of the Boltzmann weights:  $e^{-\beta H(\{s_i\})}$  of each possible spin configuration.

<sup>8</sup>For transition with *SSB*.

<sup>9</sup>Experimentally a transition between the two phases is observed. Of course, experimental physicists do not see the singularity of the measured *order parameter*, since the thermodynamic limit is not applicable in laboratory. Anyway, even if they deal with a finite number of elementary elements, the theoretical description is perfectly coherent with experiments.

<sup>10</sup>It models a small residual magnetic field not detectable by instruments and normally present during the experiments.

Without this mathematical trick, we would have a vanishing *order parameter* in the ordered phase too. We sent  $h$  to zero after the *thermodynamic* limit to come back to the *Ising* model without external field: For this model, the magnetization density  $m = \langle s_i \rangle$  is the *order parameter*.

$$\lim_{h \rightarrow 0} \lim_{N \rightarrow \infty} \langle s_i \rangle_h = m \neq 0 \text{ in the ordered phase.}$$

Calling the Boltzmann factor  $\beta$ :

$$\beta = \frac{1}{k_B T} \tag{2.2}$$

we have that the magnetization density is computed as following:

$$m = \frac{1}{N} \sum_{i=1}^N s_i = \frac{1}{\beta N} \frac{\partial \ln(Z)}{\partial h} = -\frac{1}{N} \frac{\partial \mathcal{F}}{\partial h} \tag{2.3}$$

with:

$$Z = \sum_{\{s_i\}} e^{-\beta H_{Ising}^{ext}(\{s_i\})} \tag{2.4}$$

the partition function in the *canonical ensemble* and:

$$\mathcal{F} = -\frac{1}{\beta} \ln(Z) \tag{2.5}$$

the *Helmholtz free energy*<sup>11</sup>.

We know that, on the right of the critical point, the configuration is completely disordered and the *order parameter* is vanishing due to the  $O(1)$  symmetry:  $\langle s_i \rangle = 0$ . There is, on average, the same number of spin up and down. Below  $T_c$ , instead, the configuration is ordered and the magnetization is no more vanishing even if there is not a magnetic field which selects one of the two possible ground states:  $\langle s_i \rangle \neq 0$ , the  $O(1)$  has been broken: *spontaneous symmetry breaking*<sup>12</sup> [16].

---

<sup>11</sup>Notice that, the *order parameter* is the derivative of the *Helmholtz free energy w.r.t. h*.  $m(h)$  as a jump, thus the transition is a discontinuous one.

<sup>12</sup>This does not happen in a *FOT*.

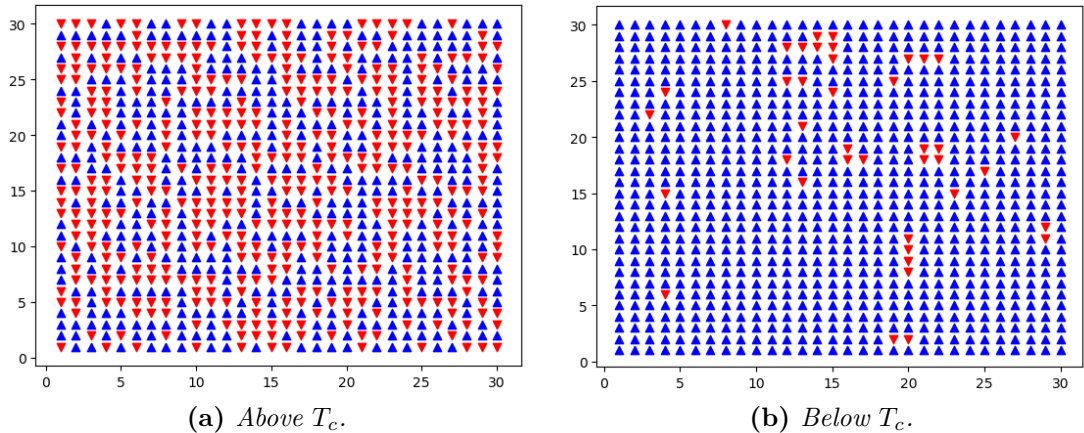


**Figure 2.2:** Disordered and ordered configuration in the  $2d$  ferromagnetic Ising model with *nearest neighbour* interaction.

We used the *Wolff algorithm* [17] to obtain the equilibrium configuration.

We can deal, also, with phase transitions which manifest themselves without *order parameter*. These kind of transitions are called *topological phase transitions* and the most important example is the *Berezinsky-Kosterlitz-Thouless transition* [16] [18, 19] [20, 21] in the  $2d$  *XY-model* defined by:

$$H_{XY}(\{\mathbf{s}_i\}) = H_{XY}(\{\theta_i\}) = -J \sum_{\langle i,j \rangle} \mathbf{s}_i \cdot \mathbf{s}_j = -J \sum_{\langle i,j \rangle} \cos(\theta_i - \theta_j)$$

where  $\mathbf{s}_i$  lives on the unitary circle so  $\mathbf{s}_i = (\cos(\theta_i), \sin(\theta_i))$ . In the *XY-model* the appearance of *spin-vortex* excitations lead to the this particular *phase transitions*.

Another important kind of *PTs* are quantum phase transitions. These happen at  $T = 0$  and are due to quantum fluctuations. An interesting example is the *Superfluid-Mott Insulator* phase transition in the *Bose-Hubbard model* [22, 23]. The model is defined by:

$$\hat{H}_{BH} = \int dr^3 \left[ -\frac{\hbar^2}{2m} \hat{\psi}^\dagger \nabla^2 \hat{\psi} + W(\mathbf{r}) \hat{\psi}^\dagger \hat{\psi} + \frac{U_0}{2} (\hat{\psi}^\dagger)^2 \hat{\psi}^2 \right]$$

where  $U_0$  is a constant energy,  $\hat{\psi}^\dagger$  and  $\hat{\psi}$  are the quantum field operator which create or annihilate a boson and  $W(\mathbf{r})$  is the harmonic plus the periodic confining potential which traps the bosons in different wells.

### 2.1.1 Phase transitions in *2d Potts model*

At  $T_c$ , in  $2d$ , the *Potts* model has a *paramagnetic-ferromagnetic* phase transition [1] which can be continuous or discontinuous depending on the parameter  $q$ : this is fundamental for this thesis. For  $q \leq 4$  there is a  $2^{nd}$  order or continuous phase transition. Instead, for  $q > 4$  the transition is a  $1^{st}$  order or discontinuous one. An important feature of  $1^{st}$  order phase transitions is that, at the critical point, the two different phases involved coexist in the so called *mixed phase region*. From the equilibrium statistical mechanics point of view, this means that the system is composed by a certain fraction of one phase and a complementary fraction of the other phase. Analyzing this phenomenon from the out of equilibrium<sup>13</sup> point of view, instead, we can say that we have a dynamical equilibrium between the two phases. This coexistence gives rise to an interesting phenomenon: the *metastability*. One particularly meaningful example of this phenomenon is the *disordered metastable state* found in the *2d ferromagnetic Potts* model. Another peculiarity of  $1^{st}$  order phase transitions is that, with the addition of *quenched disorder* the *FOT* becomes a  $2^{nd}$  order one [24]. *Quenched disorder* is that kind of disorder given by the randomness of some *quenched/frozen* observable. Due to the fact that they are *frozen*, these stochasticities, do not evolve with time. In the *Potts* case we can introduce *quenched disorder* by means of the couplings  $J_{ij}$ . Indeed, we can sample them from a certain probability distribution function. There are, so, random *ferromagnetic* or *antiferromagnetic* interactions for each spin couple<sup>14</sup>.

---

<sup>13</sup>Defined in *sec.(2.2.1)*.

<sup>14</sup>Evidenced by the site dependence of the coupling strength:  $J_{ij}$ .

## 2.2 A dynamical point of view

As said before, quenching the *2d ferromagnetic Potts* model to a sub-critical temperature, we made it undergoing a *ferromagnetic-paramagnetic* phase transition. Let us simulate it: we start from a disordered configuration ( $T \rightarrow \infty$ ) and then we update following the *heat bath* rules<sup>15</sup> with the new temperature. Time after time, we see gradually the appearance of some bigger and bigger clusters of spins with the same colour until we reach the equilibrium configuration. That, is usually<sup>16</sup>, made of big islands with flat and stable interfaces or, if the temperature is really close to 0, a completely ordered state made of spins with the same colour. In *fig.(2.3)* we show an example of evolution, by means of snapshots of the lattice at the initial and final time.

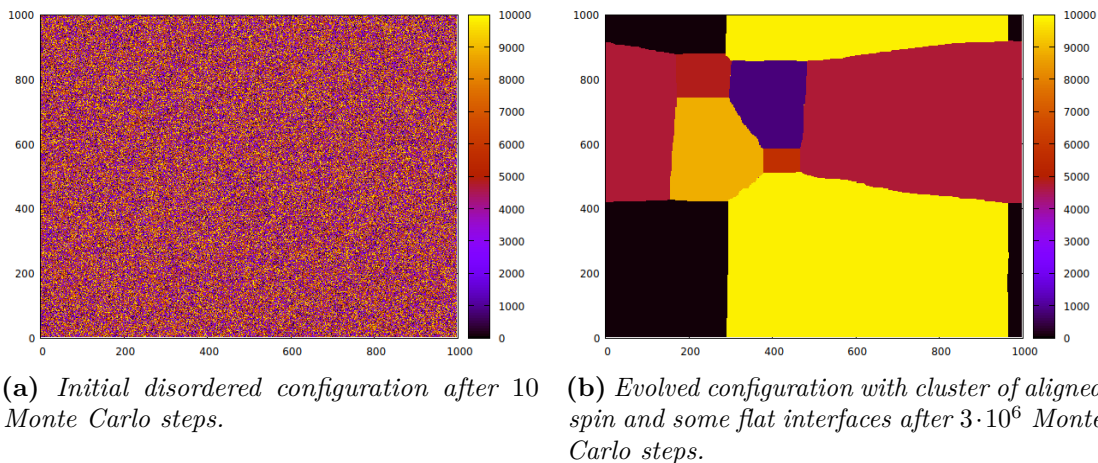


**Figure 2.3:** Example of initial and final configuration for a *Potts model* with  $q = 10^4$ ,  $T = 0.98T_c$  and  $L = 1000$ .

This is a dynamical process. We study how the equilibrium is reached, passing through the different dynamical behaviours<sup>17</sup> of this model. To explore all of them,  $T$  and  $q$  have to be varied. Understanding how these parameter influence the dynamics is the central topic of this thesis.

<sup>15</sup>Defined in chapter 3.

<sup>16</sup>It depends on  $q$  and  $T/T_c$  and It will be formalized in the next chapters.

<sup>17</sup>Analyzed in details in the following paragraph.

## 2.2.1 Out of equilibrium Statistical Physics

Passing rapidly from  $T \rightarrow \infty$  to  $T < T_c$  means that the system undergoes a "shock" and needs to stabilize. To do so, it reorganizes itself in order to minimize its *free energy* in the new phase. Since the quench is very rapid, the system can not equilibrate without exploring some *out of equilibrium steady states*<sup>18</sup>. This kind of phenomena are studied by a branch of statistical mechanics called *Out of equilibrium statistical physics*. There are different approaches to this kind of physics, we will deepen the numerical one, which is crucial to our goal.

### Monte Carlo-Markov chain approach

A *Markov process* is a, continuous or discrete, time dependent stochastic process. For the sake of simplicity, let us introduce it in the discrete formulation. The process is represented by a state variable:

$$x_t \text{ where } t \in \{1, \dots, T\} \text{ and } x_t \in \Omega \quad (2.6)$$

where  $\Omega$  is the space of all the possible configuration that can be explored by our stochastic process (*i.e.*  $\Omega = 2^N$  for the *Ising* model or  $\Omega = q^N$  for the *Potts* model). The main feature that discriminates the *Markov process* from the other stochastic processes, is the *memorylessness* or *Markovianity* *i.e.*

$$\begin{aligned} \mathbb{P}_{i,j} = \mathbb{P}_{i \rightarrow j} = \mathbb{P}(x_{t+1} = j | x_t = i, x_{t-1} = i_{t-1}, \dots, x_0 = i_0) = \mathbb{P}(x_{t+1} = j | x_t = i) \\ \forall t, i, j, i_{t-1}, \dots, i_0 \text{ allowed} \end{aligned} \quad (2.7)$$

This means that the probability to change from the current state  $x_t$ , to the subsequent one in time  $x_{t+1}$ , depends only on  $x_t$  (*i.e.* on the current state). Notice, also, that  $\mathbb{P}_{i,j}$  is a *pdf* on  $j$ . The  $\mathbb{P}_{i,j}$  probabilities can be grouped in a non negative matrix  $\hat{\mathcal{P}}$  whose rows sum up to one<sup>19</sup>.

$$\hat{\mathcal{P}} = \begin{pmatrix} \mathbb{P}_{1,1} & \mathbb{P}_{1,2} & \mathbb{P}_{1,3} & \dots & \mathbb{P}_{1,N} \\ \mathbb{P}_{2,1} & \mathbb{P}_{2,2} & \mathbb{P}_{2,3} & \dots & \mathbb{P}_{2,N} \\ \mathbb{P}_{3,1} & \mathbb{P}_{3,2} & \mathbb{P}_{3,3} & \dots & \mathbb{P}_{3,N} \\ \vdots & \vdots & \vdots & \ddots & \vdots \\ \mathbb{P}_{N,1} & \mathbb{P}_{N,2} & \mathbb{P}_{N,3} & \dots & \mathbb{P}_{N,N} \end{pmatrix} \quad (2.8)$$

---

<sup>18</sup>Doing a quasi-static transformation (*i.e.* changing very slowly the *control parameter*) the system finds its final configuration going through only *equilibrium* states and these phenomena are usually analyzed by equilibrium statistical mechanics and thermodynamics. We are, instead, doing a very rapid transformation, so *out of equilibrium physics* is needed.

<sup>19</sup> $\hat{\mathcal{P}}$  is a stochastic matrix.

$$\bullet \mathbb{P}_{i,j} > 0 \quad \forall i, j \quad (2.9)$$

$$\bullet \sum_j \mathbb{P}_{i,j} = 1 \quad \forall i \quad (2.10)$$

For a spin model like the Potts one we call  $\pi^{(t)}$  the time dependent<sup>20</sup> configuration probability.

At equilibrium, this is described by the *ensemble* physics:

$$\pi^{eq}(\{s_i\}) = \frac{1}{Z} e^{-\beta H_{Potts}(\{s_i\})} \text{ in the } \textit{canonical ensemble}. \quad (2.11)$$

*Markov chains* are crucial in the building of *Monte Carlo* numerical methods. In statistical physics, very few models are analytically solvable. The vast majority of them are simulated, with extremely meaningful results. As the name could suggest, these methods are strongly related to the use of *pseudo-random number* and thus they are useful to sample *pdf* like the one defining the *canonical ensemble*, being perfect for our aim. The *Monte Carlo Markov chain* samples the *canonical ensemble pdf* by means of an *ergodic*<sup>21</sup> *random walk* on the space of the possible configuration reachable by the system. These kind of *stochastic* processes follow some mathematical rules which characterize the dynamics and make the system reach the, theoretically predicted, equilibrium configuration. The simplest way to ensure convergence, of our numerical *MCMC* method with the equilibrium *Boltzmann* distribution is defining the dynamical rules in a way to fulfill a particular condition called *detailed balance condition* [25].

*Detailed balance condition:*

$$\pi^{eq}(\{s_i\}) \mathbb{P}_{\{s_i\} \rightarrow \{s'_i\}} = \pi^{eq}(\{s'_i\}) \mathbb{P}_{\{s'_i\} \rightarrow \{s_i\}} \quad (2.12)$$

Where:

- $\{s_i\}$  and  $\{s'_i\}$  are two spin configurations which have just one spin in a different configuration.
- $\mathbb{P}_{\{s_i\} \rightarrow \{s'_i\}}$  is the transition probability to go from the configuration  $\{s_i\}$  to  $\{s'_i\}$ .

---

<sup>20</sup>Time dependence because the dynamics will modify the set  $\{s_i\}$  at each update with  $i \in \{1, \dots, N\}$  and  $s_i \in \{1, \dots, q\} \in \mathbb{N}$ .

<sup>21</sup>Each possible configuration will be explored by the walker.

The *Potts* or the *Ising* model do not have a defined dynamics, so we need to explicit it in a way to fulfil (2.12) (for simplicity) and ensure the reaching of the right final state after the quench. We will use some microscopical rules which define the so called *Heat bath dynamics*<sup>22</sup> [26, 27] for the *MCMCs*. This inherits its name from the fact that it simulates the dynamics of a system coupled with a source of heat much bigger than the system itself: an *heat reservoir*. At each proper time unit, a spin is randomly chosen and eventually modified. For a system with  $N$  spins, one *Monte Carlo* step is made by  $N$  updates. Let us define rigorously the *heat bath rules*:

1. Chose randomly and uniformly a spin  $k$  between the  $N$  available.
2. Regardless of its current value, choose a new values  $s_k$  with a probability proportional to the Boltzmann weight. The values are drawn from a so called *heat bath*. We give the spin a value  $n$  lying between 1 and  $q$  with a probability

$$\mathbb{P}_{\{s_i\} \rightarrow \{s'_i\}} = \mathbb{P}_n(s_k = n) = \frac{e^{-\beta E_n}}{\sum_{m=1}^q e^{-\beta E_m}} \quad (2.13)$$

Where:

- $\{s'_i\} = \{s_1, \dots, s_k = n, \dots, s_N\}$ , the transition probability depends only on the state in which  $s_k = n$ ;
- $E_n = H_{Potts}(\{s_1, \dots, s_k = n, \dots, s_N\})$  is the energy of the system if the  $k_{th}$  spin has the value  $n \in \{1, \dots, q\} \in \mathbb{N}$ .

Notice that:

- The transition probabilities depends only on the final state.
- The algorithm is a single spin flip one. Indeed, at each update, only one spin has been changed.
- The probabilities add up to one and so a spin is modified for each step, even if it is possible to choose again the old colour<sup>23</sup>.

---

<sup>22</sup>With *heat bath* we avoid the problem of slowing down for large  $q$  found in the *Metropolis* algorithm (which is one of the most common algorithms). Indeed, the *heat bath* algorithm does not loose time looking for the right colour among the  $q$  ones. This, will be treated rigorously in *sec.(3.2)*.

<sup>23</sup>This corresponds to a "rejection" in *Monte Carlo* worlds. Though, this is incredibly improbable in the large  $q$  case except for some particular situations in which we have ordered and stable states.

- This dynamic is a non conservative one. Indeed, modifying the colour of the spins for each update, we necessarily modify the magnetization.

It can be proven that the *heat bath dynamics* fulfils the *detailed balance condition* and this ensures the convergence of the numerical method to the right equilibrium state.

- To move from a state in which  $s_k = n$  to a state with  $s_k = n'$  we have a probability  $\mathbb{P}_{n'}(s_k = n')$ .
- To move back to the state with  $s_k = n$  we have a probability  $\mathbb{P}_n(s_k = n)$ .

$$\pi^{eq}(\{s_1, \dots, s_k = n', \dots, s_N\})\mathbb{P}_n(s_k = n) = \pi^{eq}(\{s_1, \dots, s_k = n, \dots, s_N\})\mathbb{P}_{n'}(s_k = n')$$

$$\frac{e^{-\beta E'_n}}{Z} \frac{e^{-\beta E_n}}{\sum_{m=1}^q e^{-\beta E_m}} = \frac{e^{-\beta E_n}}{Z} \frac{e^{-\beta E'_n}}{\sum_{m=1}^q e^{-\beta E_m}}$$
(2.14)

### Continuous time Monte Carlo methods

There is another important feature to be added to our algorithm to avoid that the it gets too slow in some particular situations. We can, indeed, define the *Continuous time Monte Carlo* method [28, 29, 30]. This is extremely helpful to simulate systems at low temperatures. Indeed, once the system reaches one stable configuration, and  $T$  is very close to 0, the algorithm will evolve very slowly due to the fact that it rejects<sup>24</sup> almost every proposed spin-change. This because for  $T \rightarrow 0$  or  $\beta \rightarrow \infty$ , the Boltzmann factor  $e^{-\beta} \rightarrow 0$  and the algorithm, basically wastes time doing nothing while it tries to choose randomly how to update the configuration. After a large number of *Monte Carlo* steps the system could evolve, but it is rapidly attracted back by the starting stable state, in which it falls again. These states make the algorithm visit all the possible configuration of the system in an extremely slow way. This dynamical behaviour, is of course reasonable for a system cooled down to low temperatures. The important fact is that, simulating this, we do not want to loose an incredibly large amount of computer time. To makes things simpler and to speed up the algorithm, we can say that the system is going to spend a certain time<sup>25</sup> in the current stable state before moving to an excited one, skip all the useless time-steps and move straight to the time in which the excitation is reached. In this method, the time step changes depending on how long we need to wait before the system moves to the next state.

---

<sup>24</sup>With the *Heat bath* algorithm this means choosing again a spin with the same colour.

<sup>25</sup>Sampling it from a suitable *pdf*.

## 2.2.2 How to recognize the dynamical regimes: the growing length $R(t)$

A very important observable, that will help us in the purpose of understanding the dynamics of this model, is the growing length<sup>26</sup>  $R(t)$ . This is, on average, the linear typical size of a spin domain. We can measure it, in  $d$  dimensions, using the energy. By construction the energy is associated to the total interface between different clusters and the background.

This is done:

- Calling  $N_{diff}$  the number of couple of neighbouring spins not aligned.
- Considering the fact that these are placed on the interfaces between the  $N_{cluster}$  clusters of ordered phase and the "sea" made by the disordered phase.

We can say that:

$$\begin{aligned}
 N_{diff} &\propto N_{clusters} R(t)^{d-1} \text{ since the unaligned spins live on the clusters' surfaces} \\
 N_{clusters} &\propto \frac{N}{R(t)^d} \text{ since there are } N \text{ spins and a cluster has a typical size of } R(t)^d \\
 N_{diff} &\propto \frac{N}{R(t)} \\
 R(t) &\propto \frac{N}{N_{diff}}
 \end{aligned} \tag{2.15}$$

Now we can relate this with the quantity *excess of energy*:

$$E_{exc} = e(t; q, T/T_c) - e(t \rightarrow \infty; q, T/T_c) \geq 0 \tag{2.16}$$

Where:

- $e(t; q, T/T_c) = \frac{H_{Potts}(\{s_i^{(t)}\})}{N}$  is the density of energy related to the  $\{s_i\}$  configuration at time  $t$ .
- $e(t \rightarrow \infty; q, T/T_c) = e_{eq}(q, T/T_c)$  is the equilibrium energy per spin.

$E_{exc}$  is proportional to the surface tension created by the clusters interfaces which is proportional to  $N_{diff}$  which is, in turn, proportional to  $R(t)^{-1}$  and thus:

$$R(t) \propto E_{exc}^{-1} \tag{2.17}$$

---

<sup>26</sup>Time is measured in Monte Carlo steps units and we imply the  $q$  and  $T/T_c$  parametric dependence of  $R(t; q, T/T_c)$ .

Normalizing (the excess energy) we can write the definition of the growing length<sup>27</sup>:

$$R(t) = \frac{e(t \rightarrow \infty; q, T/T_c)}{e(t \rightarrow \infty; q, T/T_c) - e(t; q, T/T_c)} \quad (2.18)$$

For this kind of quenches, on the square lattice, we have that<sup>28</sup> :

$$\begin{aligned} e(t \rightarrow \infty; q, T/T_c) &\simeq -2, \text{ ordered phase.} \\ e(t = 0; q, T/T_c) &= 0, \text{ completely disordered phase.} \end{aligned} \quad (2.19)$$

Measuring  $R(t)$  we can understand which dynamical regimes are explored by the system. This very is useful for us to know when we are in the disordered *metastable* state and for how long the system is stuck there. Indeed in this regime we have straightforwardly that:

$$R(t) \simeq 1 \quad (2.20)$$

since in the disordered state  $e(t_{disordered}; q, T/T_c) \simeq 0$

It is also known that the *coarsening* regime<sup>29</sup> [31, 32] is characterized by:

$$R(t) \sim t^{1/2} \quad (2.21)$$

The *nucleation* phenomenon<sup>30</sup> [33] is instead depicted by a rapid increase of  $R(t)$ .

When  $R(t)$  is constant, but different from 1, for relatively long times, the system is trapped in a *blocked* state<sup>31</sup> [34].

The ordered phase, instead, is found when the linear size of the lattice is reached by  $R(t)$ .

In *fig.(2.4)*, we can clearly see the main dynamical regimes. A *metastable* state survives until  $t \simeq 100$ . At this time there is a rapid jump of  $R(t)$  from 0 to a value close to 20. This is the witness of the *nucleation* regime. The *coarsening* regime appears after *nucleation* and brings the system to a quite ordered configuration. At  $t \simeq 10^6$  the system is found in a *blocked-stripped*<sup>32</sup> state.

---

<sup>27</sup> $R(t)$  is meaningful until it is  $\leq L$ . So, it is bounded by 0 and  $L$ ,  $R(t) \in \{0, L\}$ .

<sup>28</sup>We put  $J = 1$ .

<sup>29</sup>See paragraph 2.3.3.

<sup>30</sup>See paragraph 2.3.2.

<sup>31</sup>See paragraph 2.3.4.

<sup>32</sup>A striped state is a kind of *blocked state*. Its name derives from the particular *striped* geometry of the lattice.

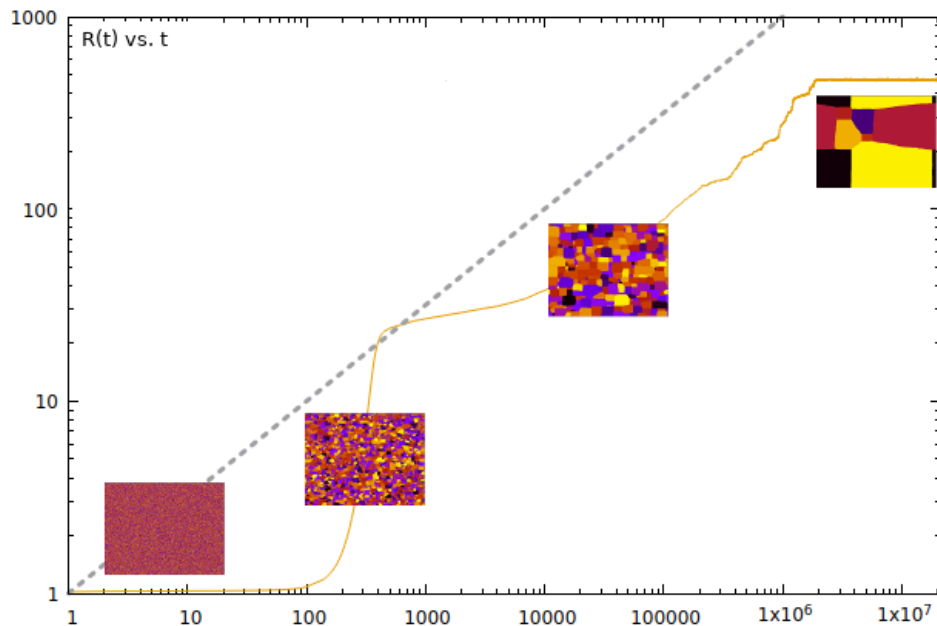


**Figure 2.4:** Example of  $R(t)$  for the *Potts* model defined on a square lattice:  $q = 10^4$ ,  $L = 1000$  with snapshot of the lattice to characterize the different regimes. The dotted line is  $t^{1/2}$ .

The growing length is also useful in the case in which  $q = 2$  for the geometrical analysis of spin-cluster at very low temperatures. Indeed it is possible to find, with finite probability some particularly interesting *striped*<sup>33</sup> states which eventually percolate [35].

## 2.3 Dynamical regimes

Before entering into details of the analysis of the dynamics let us give a small definition and description of the dynamical regimes.

<sup>33</sup>This name follows from the striped geometry of the clusters.

### 2.3.1 Metastable regime

Again, since we are considering two different phases separated from a *FOT* we know, that there will be a *mixed phase region* in the vicinity of  $T_c$ . This coexistence of ordered and disordered phase close to the critical point gives rise to *metastability*. Indeed quenching from high to low  $T$  (and conversely from low to high  $T$ )<sup>34</sup> we clearly see that a disordered state (ordered for the upper quench) survives for long times<sup>35</sup>. An example of *metastable* regime is showed in the following figure, by means of the plot of  $R(t)$  vs.  $t$  for  $q = 10^4$ ,  $L = 10^3$  and different temperatures.

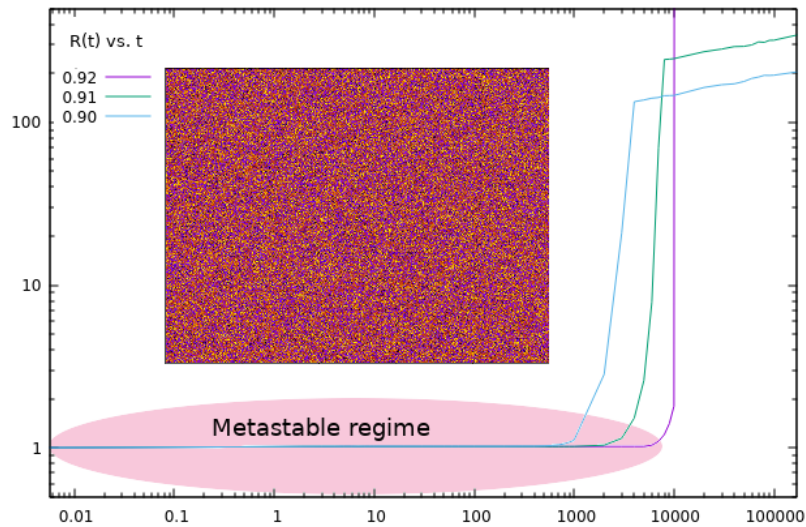


**Figure 2.5:** Generic disordered *metastable* state and  $R(t)$  vs.  $t$  for  $q = 10^4$  with  $L = 10^3$  at different temperatures given in the key.

To describe properly this phenomenon, it is very helpful to use the *Gibbs-Dhuen criterion* [36, Chapter 1]. Let us analyze this in general. To be in an equilibrium configuration it must hold that<sup>36</sup>:

*Gibbs-Dhuen criterion:*

$$\Delta U + W - T\Delta S \geq 0 \quad (2.22)$$

<sup>34</sup>High to low  $T \rightarrow$  lower quench. Low to high  $T \rightarrow$  upper quench.

<sup>35</sup>In particular cases, it can happen that this state will never be escaped.

<sup>36</sup> $U$  is the internal energy of the system,  $W$  is the work,  $S$  is the entropy.

where  $\Delta$  represents a variation of some thermodynamic quantities from the equilibrium state. Strictly speaking, this criterion is related to the fact that given a thermodynamic potential, suitable for the description of the phase transition, we have a stable configuration when this is minimum. The *Helmholtz free energy* for example:

$$\mathcal{F} = U - TS \tag{2.23}$$

is minimized at finite temperature maximizing the entropy and minimizing the internal energy. The minimum of the *free energy*, must be so for all the infinitesimal variation of each *phase space* variable. Let us write  $\Delta\mathcal{F}$  in series of infinitesimal variations, near an equilibrium point:

$$\Delta\mathcal{F} = \delta\mathcal{F} + \frac{1}{2}\delta^2\mathcal{F} + \frac{1}{3!}\delta^3\mathcal{F} + \frac{1}{4!}\delta^4\mathcal{F} + \dots \tag{2.24}$$

To be in the equilibrium configuration the condition:

$$\delta\mathcal{F} = 0 \tag{2.25}$$

is needed.

If in addition we have:

$$\delta^2\mathcal{F}, \delta^3\mathcal{F}, \delta^4\mathcal{F}, \dots > 0 \tag{2.26}$$

the equilibrium is stable *i.e.* we are in the absolute minimum of the *free energy*. If, instead, we have that:

$$\delta^2\mathcal{F} > 0 \text{ but } \delta^3\mathcal{F}, \delta^4\mathcal{F} \dots < 0 \tag{2.27}$$

the equilibrium is said to be *metastable*. This means that we are in a relative minimum and the absolute one could be reached with some thermal perturbation. A certain barrier must be stepped over to reach the stable equilibrium configuration and this can take extremely long times<sup>37</sup>.

If:

$$\delta^2\mathcal{F} < 0 \tag{2.28}$$

the equilibrium is said to be unstable *i.e.* we are in a maximum of the *free energy* and a very small perturbation can make the system collapse in a more stable state.

---

<sup>37</sup>Maybe infinite.

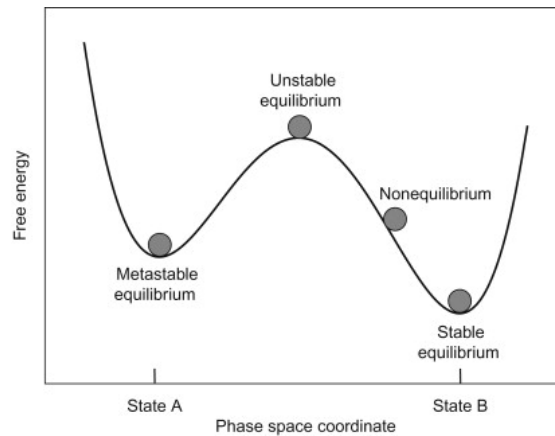


**Figure 2.6:** *Metastable, stable, unstable equilibrium.* Taken from [37].

The condition  $\delta^2\mathcal{F} = 0$  defines the *spinodal curve*. This curve tells us a particularly important information. Indeed, if we have a system prepared in an equilibrium state, which lies on the *spinodal curve*, and we apply to it a thermodynamic transformation, this, will pass from *metastability* to instability and we notice the emergence of a phase transition. For this reason, the *spinodal curve* gives the "*metastability limit of the equilibrium*" [36, Chapter 1].

### 2.3.2 Nucleation regime

The *nucleation* phenomenon is crucial in the description of the 1<sup>st</sup> order phase transitions. Indeed, it is one of the mechanisms useful to escape from the *metastable* state and reach eventually the equilibrium.

It consists of the emergence of some *nuclei*<sup>38</sup> of the new phase in the old one. These *nuclei* can shrink and disappear soon or, if some critical radius has been reached, grow and fill the "ocean" of the old phase with the new one. For the *Potts* model we have a *multi-nucleation* [33] phenomenon: indeed, we can clearly see the appearance of more than one phase, each one associated with one colour, as shown in *fig.(2.8)*.

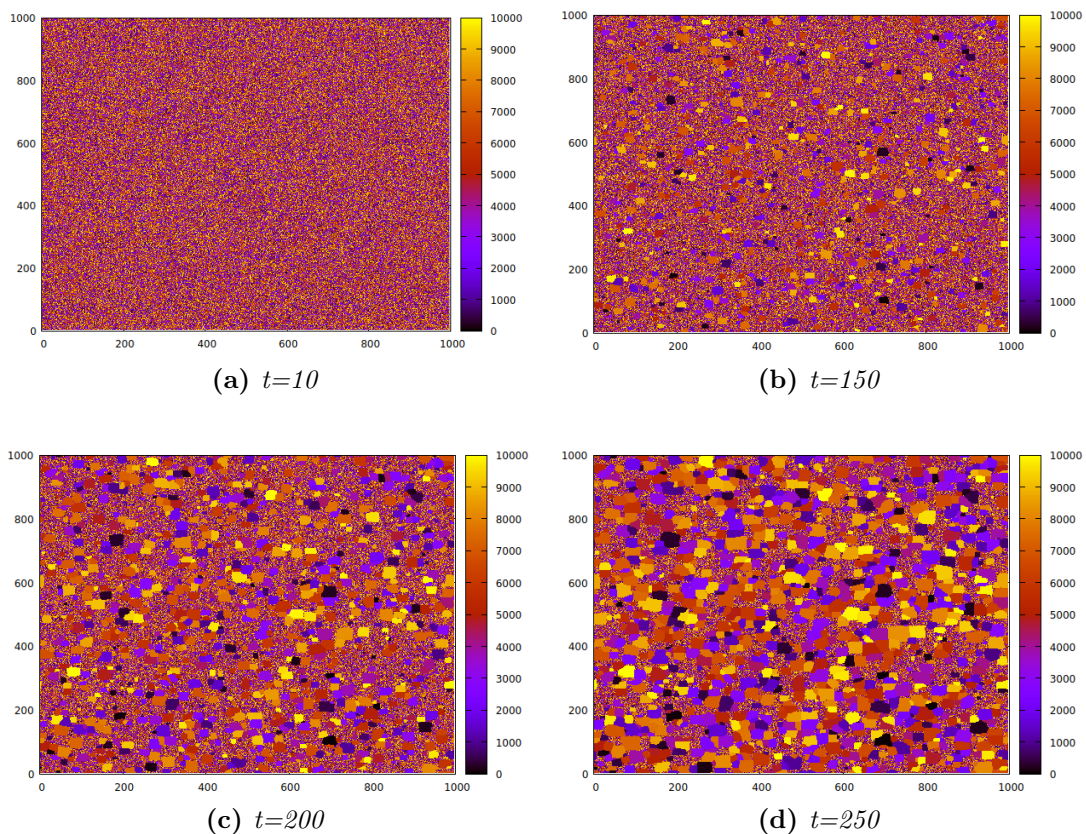


**Figure 2.7:** *Potts* model with  $q = 10^4$ ,  $T = 0.85T_c$ ,  $L = 1000$ .

From *fig.(2.8)*, where we show  $R(t)$  vs.  $t$ , we can see that the *nucleation*

<sup>38</sup>Thanks to some thermal fluctuation, for example.

phenomenon starts around  $t = 100$  and indeed, we have the appearance of the *nuclei*, evident in *fig.(2.7-b)*.

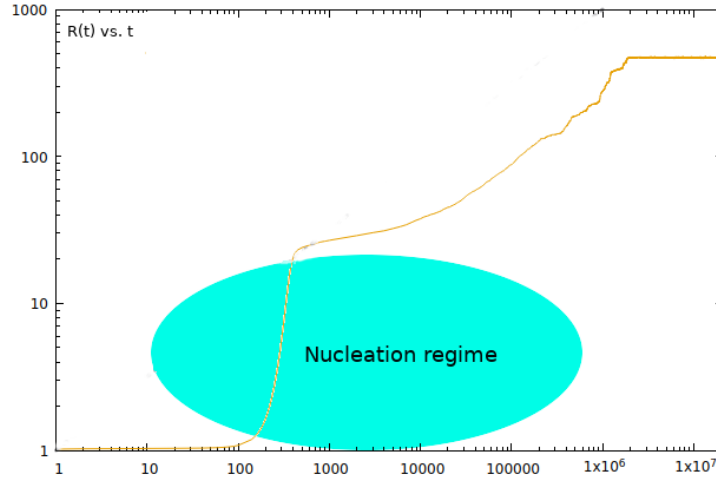


**Figure 2.8:**  $R(t)$  vs.  $t$  at  $T = 0.85T_c$  for a Potts model with  $q = 10^4$  and  $L = 10^3$ .

The critical radius is the one related to the droplet of the new phase who makes the system more stable (*i.e.* minimize the energy). In particular, some *volume vs surface* considerations have to be done to understand this mechanism. Indeed, let us say that we have the appearance of some droplets of ordered phase (all spin with the same colour) in the disordered configuration. These droplets excitations are favoured by the fact that the internal energy contribute lowers the total energy (volume contribute) but, between the droplets and the old phase, there are interfaces which are disadvantaged energetically (surface contribute). So, the competition between surface and volume contributes makes the *nuclei* shrink or grow and lets, eventually, the system escape from the *metastability*.

Let us deepen this argument in  $d$  dimensions, for a general lattice model with spins  $s_i$ . To do so we need some concepts about *field theories*.

### Statistical field theory: few concepts

If we are not interested in the single micro-state but we need to study in a broadest way the phenomenology of the model, then we can change approach and gain some meaningful insights.

We are interested in studying the *PT*, thus, we concentrate on the description of the system close to the *critical point*.

A very important variable, for our aim, is the *correlation length*  $\xi$  [38, Chapter 31],

[39]. This, is the typical length scale over which the correlation function<sup>39</sup>

$$C(\mathbf{r}) = \langle s_i s_j \rangle - \langle s_i \rangle \langle s_j \rangle \quad (2.29)$$

is different from zero<sup>40</sup>.

Close to the critical point the *correlation length*  $\xi$ , is huge<sup>41</sup>: in particular  $\xi \gg a$ , where  $a$  is the lattice spacing.

During a *PT* there are fluctuations of thermal quantities at each scale. This is due to the fact that the system is made of parts completely correlated at each length scale. This evidences a *statistical fractal* nature. The fact that close to criticality  $\xi \gg a$  makes possible to develop the following approach: indeed let us divide the lattice into boxes of linear size  $\lambda$  such that:

$$a \ll \lambda \ll L \quad (2.30)$$

and let us take the spatial average of observables defined on our lattice (*e.g.* the magnetization). These boxes are centred in some points  $\mathbf{x}$  at which we associate the value of the average operation. So, at each  $\mathbf{x}$  point there is a value of the new continuous *order parameter* which, by construction, is a smooth *field*  $\phi(\mathbf{x})$ . Indeed, choosing  $a \ll \lambda \ll L$  in a region in which  $\xi$  is big enough is sufficient to ensure the smoothness property of  $\phi(\mathbf{x})$ .

This operation is called *coarse graining*. With this approach we obtain informations about the system not from a microscopical point of view but from a coarser one.

Doing this, we have built a formulation of the statistical physics, close to the critical point, in which the *order parameter* is a continuous field with values on each point  $\mathbf{x}$ . We gain a continuous description of the lattice model: *Statistical field theory*. With this approach phase transitions, can be studied using some well developed *QFT* tools like the *Feynman Diagrams*.

Within this formulation, to analyze the *nucleation* phenomenon, we can use the *Ginzburg-Landau* potential. It has the following features:

- It is minimum at the thermodynamic equilibrium.

---

<sup>39</sup>The correlation function depends on  $\mathbf{r}$  which is the *cartesian* distance between the *i-th* and the *j-th* spins.

<sup>40</sup>In other words, is the length scale, characterizing the system, over which thermal fluctuations of the spin variables are correlated.

<sup>41</sup>Diverges exactly at the critical point in the thermodynamic limit for a *SOT*. Instead, on a finite lattice of linear size  $L$ ,  $\xi \sim L$  at  $T_c$ .

- Close to the transition it is assumed to be expandable analytically in power of the *order parameter* with temperature dependent coefficients<sup>42</sup>.

The *Ginzburg-Landau* theory is a *mean field* one so it is approximated. The *mean field* approximation is obtained by neglecting terms of second order in fluctuations of the spin variables. For example for the *Ising model*:

$$\begin{aligned} s_i s_j &= (s_i - \langle s_i \rangle)(s_j - \langle s_j \rangle) + \langle s_i \rangle s_j + \langle s_j \rangle s_i - \langle s_i \rangle \langle s_j \rangle \\ &\simeq \langle s_i \rangle s_j + \langle s_j \rangle s_i - \langle s_i \rangle \langle s_j \rangle \\ &= m(s_i + s_j) - m^2 \end{aligned} \quad (2.31)$$

and thus neglecting the constants we have:

$$H_{Ising} = -4Jm \sum_i s_i \quad (2.32)$$

which is, actually, an Hamiltonian describing an interaction between each spin and the *effective field*  $-4Jm$ .

Now let us come back to a general formulation. Let  $\phi(\mathbf{x})$  be the *coarse-grained order parameter* for our lattice model:

$$\phi(\mathbf{x}) = \frac{1}{\lambda^d} \sum_{i \in \lambda(\mathbf{x})} s_i \quad (2.33)$$

Where  $\lambda^d$  is the hypercube centered in  $\mathbf{x}$ .

And let  $\mathfrak{F}[\phi(\mathbf{x})]$  be the *Ginzburg Landau free energy*<sup>43</sup>:

$$\mathfrak{F}[\phi(\mathbf{x})] \simeq \int d^d \mathbf{x} \frac{1}{2} r(T) \phi^2(\mathbf{x}) + \frac{1}{2} c(T) (\nabla \phi(\mathbf{x}))^2 + \phi^4(\mathbf{x}) \quad (2.34)$$

$r(T)$  and  $c(T)$  characterize the model. They are theoretically unknown and approximated by means of an expansion with experimental coefficients.

Thanks to equation (2.34), we are ready to develop the *classical nucleation theory (CNT)*.

### Classical theory of *nucleation*

Let us say that we are in *state A* of the *free energy* plotted in *fig.(2.7)*: a *metastable* state. We want to analyze with the *CNT* formalism how and if this state is escaped.

---

<sup>42</sup>This is a wrong assumption so the Landau approximation is not completely exact but for the sake of describing the *PTs* this is sufficiently adequate.

<sup>43</sup> $\simeq$  because is a truncated expansion.

As said in the previous paragraph, the *metastable* state is in thermodynamic equilibrium. This, is true, until a big enough thermal fluctuation drives the system out of the potential well. At this point, the system becomes "aware" of the existence of a state with lower energy and the escaping process starts. To describe this process, with the *CNT*, some assumptions have to be done:

1. The fluctuations that make possible to abandon the *metastable* state have to be considered as equilibrium fluctuations close to the local minimum of the *free energy*<sup>44</sup>.
2. The droplets of the new phase are considered isolated and non-interacting, thus, we can treat them as fluctuations around the *metastable* equilibrium.
3. The droplets are compact and this means that their volume  $V$  scale as the linear size elevated to the spatial dimension:

$$V \sim L^d \tag{2.35}$$

4. There is a surface tension,  $\sigma$ , between the new and the old phase. This does not feel the influence of the final temperature of the quench.
5. The *free energy* density of the bulk of the droplets is the one of the stable phase.

With these we can calculate the *free energy* difference between the *metastable* state and the one with nucleating droplets:

$$\Delta\mathfrak{F} = -|\Delta f|r^d + \sigma r^{d-1} \tag{2.36}$$

Where  $\sigma$  is the surface tension,  $r$  is the droplet radius and  $\Delta f$  is the difference of the interior<sup>45</sup> *free energy* density between the *metastable* and the droplet state.

Again we notice that there is a competition between surface and volume contribution:

- The bulk term, proportional to the droplet volume, favourites the nucleation.
- The surface term, describing the interfaces between the new and the old phase, makes the droplet creation disadvantageous.

---

<sup>44</sup>This is correct if the state is escaped after a certain time needed to reach some *metastable* equilibrium.

<sup>45</sup>Inside the droplet.

$\Delta\mathfrak{F}$  change sign at the critical radius, indeed after  $r_c$  the *nucleation* process is favourable energetically:

$$r_c = \frac{d-1}{d} \frac{\sigma}{\Delta f} \quad (2.37)$$

and

$$\Delta\mathfrak{F}_c \propto \frac{\sigma}{\Delta f^{d-1}} \quad (2.38)$$

is the *free energy* cost needed to create a critical droplet. This, has  $r = r_c$  and has the same probability to grow and to shrink. Droplets with  $r > r_c$  will grow and help the system to escape from the *metastable state* while droplets with  $r < r_c$  will shrink and the system remains stuck.

The probability to find a droplet with  $r = r_c$  is proportional to the inverse of the time spent in the *metastable state*:

$$P_c \propto \tau^{-1} = \exp(\beta\Delta\mathfrak{F}_c) \quad (2.39)$$

This holds as long as the droplets are non interacting which, unluckily, is not always true. In that case, there are more refined methods like the *Becker-Doring* theory [40] that describe properly the situation.

### 2.3.3 Coarsening regime

Another fundamental dynamical regime, for the *Phase ordering kinetics* theory of spin system, is the *coarsening* one [31, 32]. In general, the class of phenomena in which there is a driven growth process of a new phase inside the old one are called *coarsening* phenomena. In the *Potts* case, *coarsening* is determined by a surface tension mechanism. When a subcritical quench has been done, the system is forced to start ordering<sup>46</sup>. When we have *coarsening*, the interior part of the new domains is thermodynamically at equilibrium. The dynamical game is all played by the interfaces between new and old phase. These are not always stable, indeed for a spin system we have that<sup>47</sup>:

- An interface is stable if is flat.
- An interface is unstable if a curvature is present.

The following figure, by means of a snapshot of the lattice, shows an example of flat and curve interfaces.

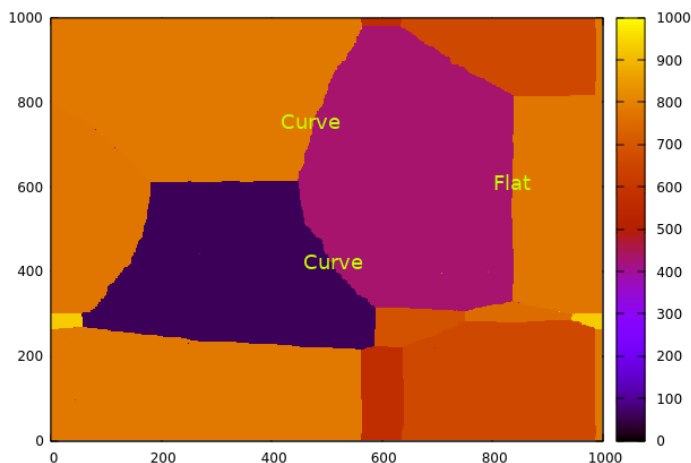


**Figure 2.9:** Example of flat and curve interfaces.

There will be a *curvature driven* process who leads to the "ordering" of some *paramagnetic* phase and stabilization of the system. During this process,  $R(t)$  grows until it becomes as big as the lattice side  $L$ .  $R(t) \simeq L$  is the witness of the fact that the system has reached the equilibrium.

<sup>46</sup>If it is not stuck in *metastable* states.

<sup>47</sup>In the next chapters this will be explained properly.

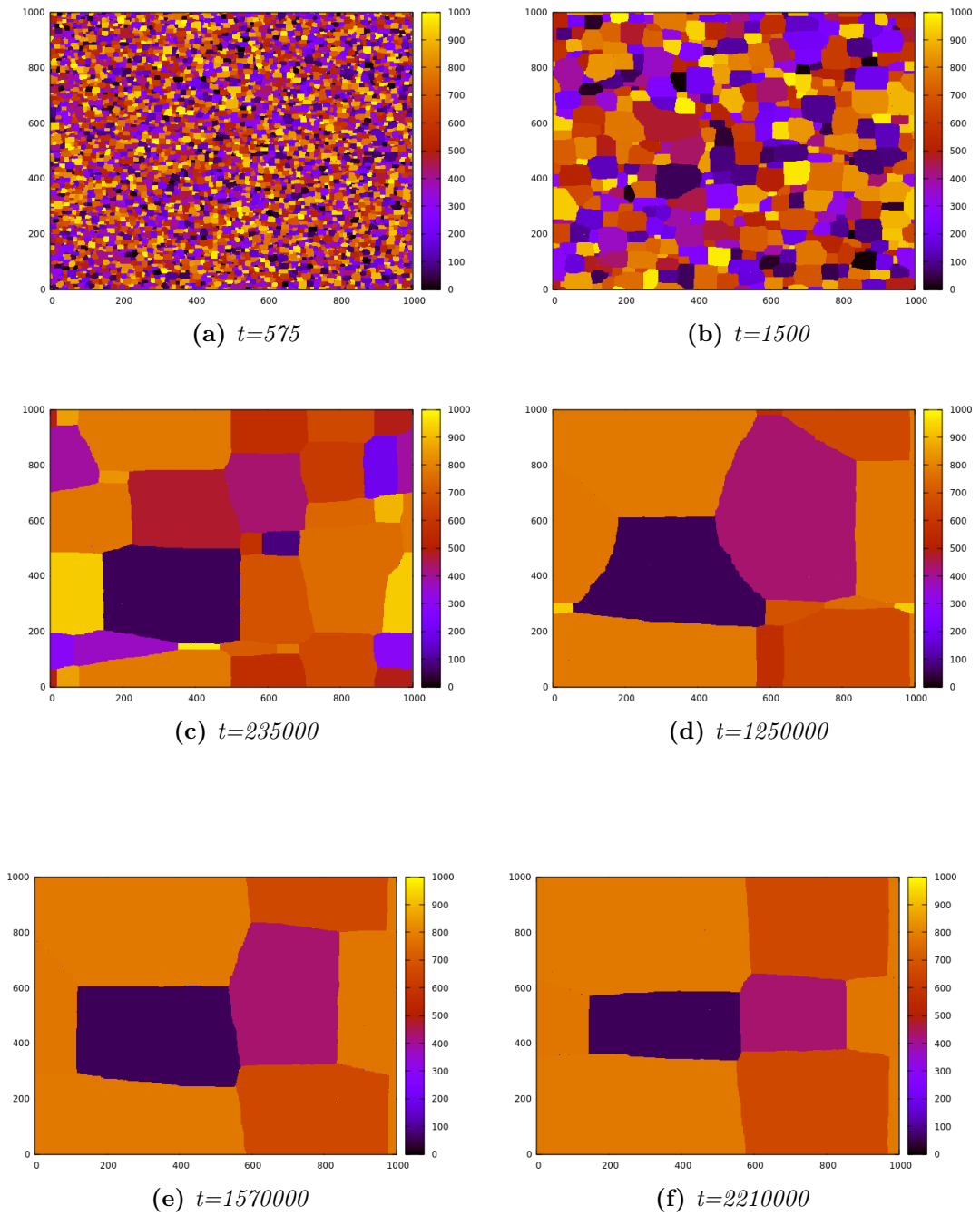


**Figure 2.10:** *Coarsening* of domains for a *Potts* model with  $q = 10^3$ ,  $T = 0.80T_c$ ,  $L = 1000$ .

*Fig.(2.10-a), fig.(2.10-b), fig.(2.10-c), fig.(2.10-d)* corresponds to the *coarsening* regime, as showed by the following figure.

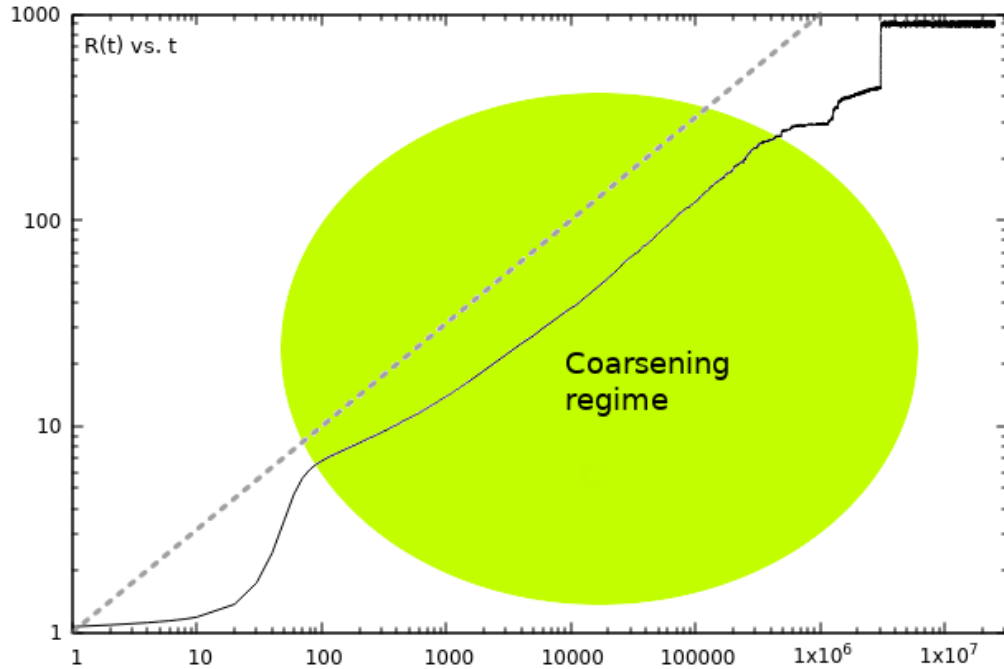


**Figure 2.11:**  $R(t)$  vs.  $t$  at  $T = 0.80T_c$  for a *Potts* model with  $q = 10^3$  and  $L = 1000$ .

## Dynamical scaling hypothesis

In the studying of *coarsening* dynamics, an important hypothesis has to be done. This is called *Dynamical scaling hypothesis* and it states that:

"A long time after the quench, if we study the system properties in the *scaling limit*<sup>48</sup>  $r \gg \xi$ , these can be described by an unique proper length scale:  $R(t)$ ".

$R(t)$  is *universal* in this regime and follows an algebraic law in  $t$ :  $R(t) \sim t^{1/z_d}$ , where  $z_d$  is called dynamical exponent and characterize the kind of dynamics<sup>49</sup> [41]. [32]. The exponent is universal and thus, independent of the parameters defining the model, which enter all in a prefactor. Also, measuring distances in  $R(t)$  units, we notice that the structures of spin clusters are statistically equivalent at different times. This holds if  $R(t)$  is smaller than the linear size  $L$  and, above all, for  $R(t)$  much greater than the lattice spacing  $a$ :

$$R(t) \ll L \tag{2.40}$$

$$R(t) \gg a \tag{2.41}$$

The growing length can be measured numerically<sup>50</sup> or analytically. For spins system like *Ising* or *Potts* and non conservative dynamics<sup>51</sup> we have that:

$$R(t; q, T/T_c) \simeq [a_q(T/T_c)t]^{1/2} \tag{2.42}$$

Where  $a_q(T/T_c)$  is the prefactor in the *Potts* model case. To make the notation not too heavy we imply the  $q, T/T_c$  dependence of the growing length, saying simply that:  $R(t) \sim t^{1/2}$ , in this regime.

---

<sup>48</sup> $r$  is a generic distance and  $\xi$  is the correlation length.

<sup>49</sup>*e.g.*  $z_d = 1/3$  for the *Ising* model with conservative *Kawasaki* dynamics

<sup>50</sup>By means of the relation with the interfaces energy (surface tension) for example

<sup>51</sup>A group of dynamics, like the *Glauber* [35] one, in which the *order parameter* is not conserved

### 2.3.4 Blocked states regime

*Blocked* states are really important for the study of the dynamics of the *Potts* model [42]. These states are *highly symmetric* ones corresponding to a relative minimum of the *free energy*. Of course, they "block" the dynamics and make the relaxation towards the ground state slower. These kinds of states are strictly related to flat interfaces, T-junctions<sup>52</sup> [34] and corners. Indeed when the system is in such configurations, the dynamics is slowed down because the spins on the flat part of the interface, on the corners or in T-junctions are aligned with the majority of their nearest neighbours. This is favourable energetically<sup>53</sup>. Thus, a rather big amount of time will be needed in order to find the right thermal fluctuation and manage to escape from one of these states. To recognize a *blocked* state, again, we use the *growing length*  $R(t)$ . Indeed when  $R(t)$  remains constant<sup>54</sup> for a wide amount of time we are in a blocked state. Such situation is shown in *fig.(2.13)* for  $q = 10^4$ ,  $L = 10^3$  and  $T = 0.4T_c$ .

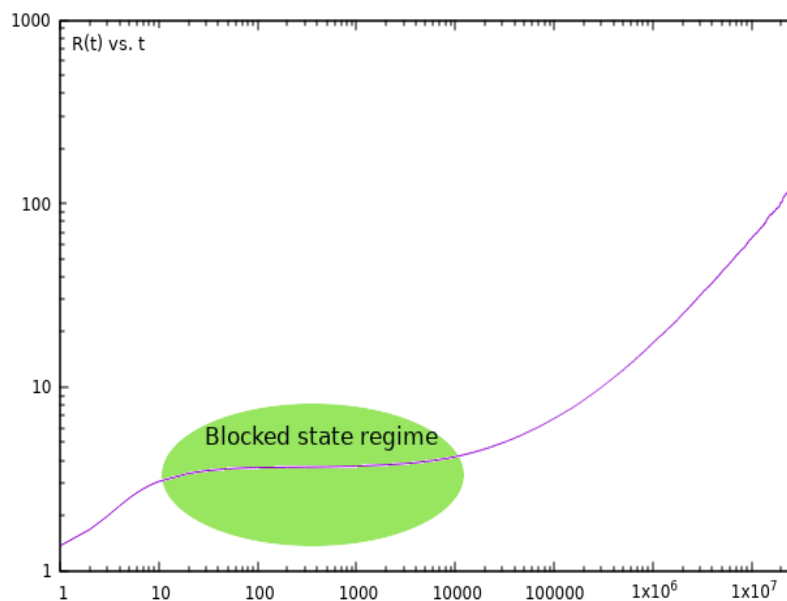


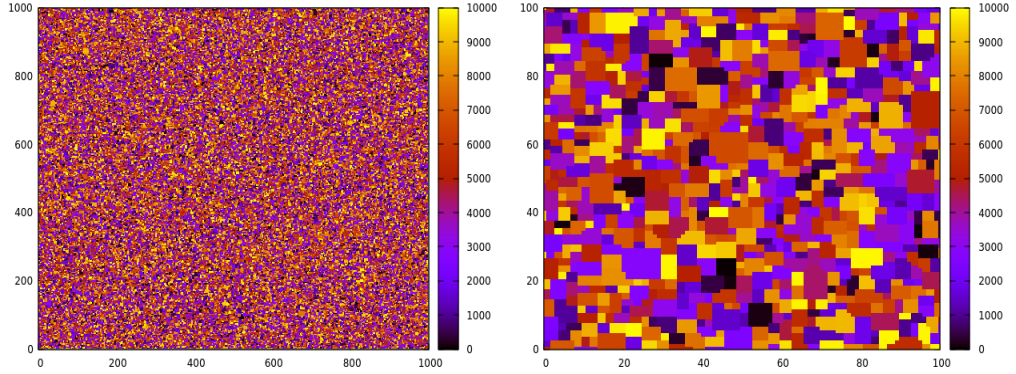
**Figure 2.12:**  $R(t)$  vs.  $t$  at  $T = 0.4T_c$  for a *Potts* model with  $q = 10^4$  and  $L=1000$ .

<sup>52</sup>They are called in this way because the interfaces of 3 different rectangle shaped spin clusters form a "T".

<sup>53</sup>This will be explained rigorously in the next *sec.(3.2)* and *sec.(3.5)*.

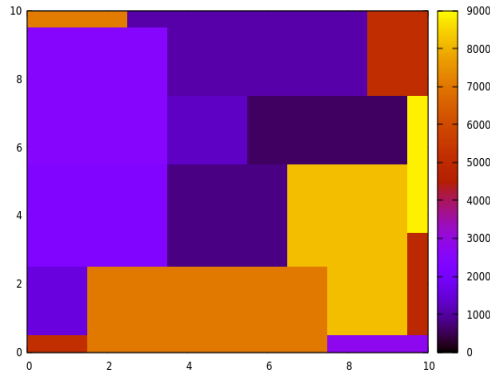
<sup>54</sup>Different from 1 or  $L$  which are related to other kinds of states.

*Fig.(2.13)* shows an example of *blocked state* configuration using snapshot. In particular, it is evident, by the magnified lattice, the presence of particular kinds of interfaces: T-junctions, flat interfaces and corners.



(a) *Blocked state at  $R(t) = 3.7$*

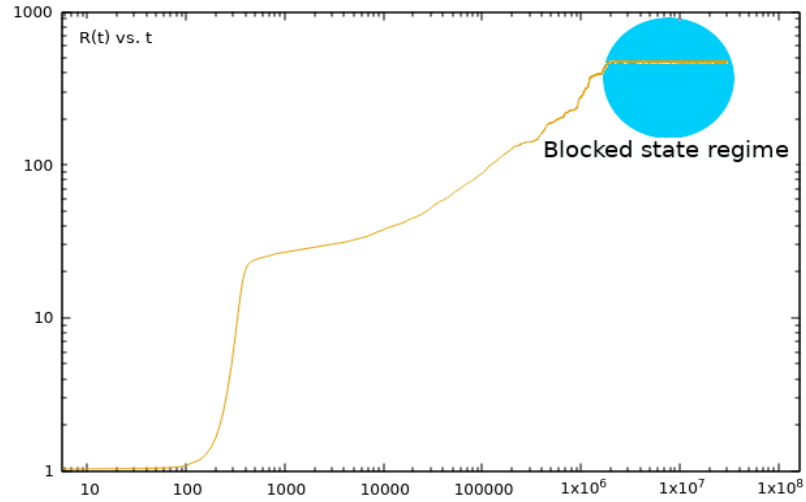
(b) *Blocked state at  $R(t) = 3.7$ ; zoomed indeed we can see only a  $100 \times 100$  section of the lattice.*



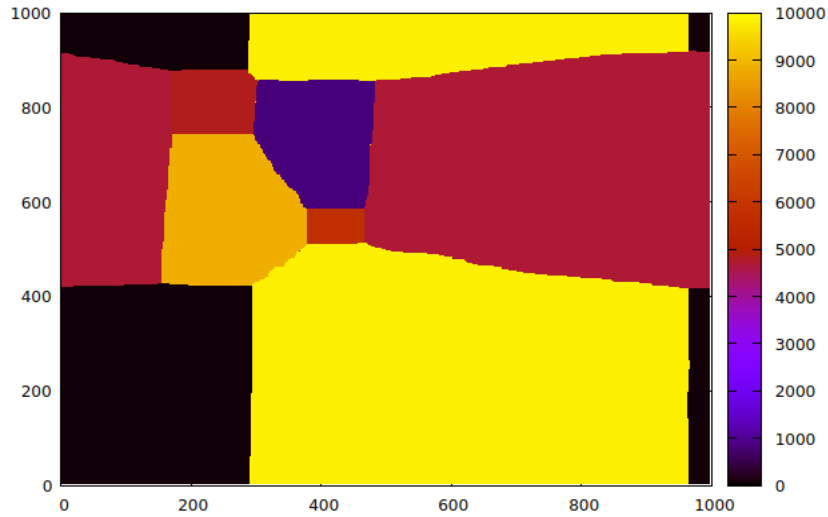
(c) *Blocked state at  $R(t) = 3.7$ ; zoomed indeed we can see only a  $10 \times 10$  section of the lattice.*

**Figure 2.13:** Snapshots of the lattice to see a *blocked state* for the *Potts* model at  $T = 0.40T_c$  with  $q = 10^4$ ,  $L = 1000$ . The last two figures have been zoomed to see better the interfaces. In *fig.(c)*, the presence of T-junctions, flat interfaces and corners it is evident.

In *fig.(2.14)*, another kind of *blocked* state is showed. This, is found at late time after *nucleation* and *coarsening*. For this reason, some relatively big domains appear and this, results in *blocked* states slightly different from the ones found at early times. Indeed, in this case we do not have highly symmetric small domains with flat interfaces, corner and T-junctions but relatively big ones.



(a)  $R(t)$  vs.  $t$  at  $T = 0.85T_c$  for a Potts model with  $q = 10^4$  and  $L = 1000$



(b) Blocked state for the Potts model with  $q = 10^4$ ,  $T = 0.85T_c$ ,  $L = 1000$  at  $t = 1.5M$ .

**Figure 2.14:** Another kind of *blocked-stripped* state.

## Chapter 3

# Theoretical consideration and numerical simulation of the bidimensional large $q$ states *Potts* model

### 3.1 Introduction

The vast majority of the work about the dynamics of the *Potts* model after subcritical quenches, focus on the ordering process. This, is developed in the *coarsening* regime which leads the system to one of the  $q$  possible ground states. The parameters, for the simulations of those works, are set in a way to avoid to freeze in the long lived *blocked* and *metastable* states and to concentrate on the ordering kinetics process [43], [42].

Our interest go further: we give the needed importance to the avoided regimes, in order to try to give a complete scenario of the dynamics for this model. Indeed, we want to deepen the *freezing* and *metastability* of the dynamics and also, understand how and when there is the (eventual) crossover with the usual *coarsening* regime.

To do so, at first, we have characterized the complete dynamical behaviour of the model after rapid quenches from  $T \rightarrow \infty$  to  $T < T_c$ . To pursuit our aim, many simulations at fixed (large)  $q$  with a variable  $T/T_c$  and viceversa with fixed  $T/T_c$  and varying the number of states  $q$  have been launched. Then, from the analysis of the various  $R(t)$  obtained, we have chosen the "zone" to be better investigated. This has been done setting, not only the parameters  $q$  and  $T/T_c$ , but also the temporal length of the simulation and the times at which we take snapshots. For example setting these parameters in a clever way we were able to take snapshots

in the vicinity of the jumps of  $R(t)$  to see the appearance of *nucleating* domains. Also, with other simulations and different settings we took some other snapshots in the *blocked* state to analyze the geometrical properties of spin clusters and so on...

Some bounds, delimiting the temperature region in which the *metastable* state are never escaped, have been found with a mixture of theoretical and numerical methods. In particular we concentrate on the analysis of the *heat bath* transition rules in some particular limits of the parameters  $q$  and  $T/T_c$ .

From the  $R(t)$  plots, we have noticed a particular feature of the dynamics. Studying the growing length in the regime  $T/T_c < 1/2$ , with a critic eye and with a smart rescaling of the times, we have found the main result of this work: a *universal* behaviour of the dynamics, in  $q$  and  $T/T_c$ , associated to a *blocked* state. Indeed, simulating *Potts*, for any  $q$  large enough ( $q \geq 10^3$ ) and for all the reduced temperatures in this regime, we obtain the very same dynamical behaviour for each one of them.

In the "work in progress" paper [2] the study of the dynamics has been done also on honeycomb and triangular lattices in order to check if the universality of the dynamics holds also on different lattice topologies<sup>1</sup>.

## 3.2 Heat bath dynamics for the Potts model

The *Metropolis* microscopic dynamics is usually used to simulate spin models. Let us rapidly define it:

1. Call:

$$e_i = \frac{H_{Potts}(\{s_1, \dots, s_i, \dots, s_N\})}{N} \quad (3.1)$$

the density of energy related to a particular spin configuration  $\{s_i\}$ .

2. Chose at random a spin  $s_i$  between the  $N = L^2$  ones available.
3. Try to change the value of the selected spin choosing randomly between the  $q - 1$  left and calculate the new local energy  $e'_i$

$$e'_i = \frac{H_{Potts}(\{s_1, \dots, s'_i \neq s_i, \dots, s_N\})}{N} \quad (3.2)$$

4. The move is accepted if the new local energy  $e'_i$  is lower than the old one  $e_i$ :

$$e'_i < e_i$$

---

<sup>1</sup>We found that the dynamics on the honeycomb and on the square lattices have the same behaviour, while the triangular lattice develops different dynamical properties.

5. Otherwise it is accepted with probability

$$\mathbb{P}_{Metropolis} \propto e^{-\beta(e'_i - e_i)} \quad (3.3)$$

This is very slow in the large  $q$  case. It happens that, at very low temperatures<sup>2</sup>, the algorithm wastes time trying to choose randomly a new  $q$  value to update the configuration. For these temperatures, indeed, the algorithm accepts basically only configurations with lower energy *wrt* the starting one, all the others are rejected. This happens because the *Boltzmann* factor is very small:

$$e^{-\beta(e'_i - e_i)} \ll 1 \quad (3.4)$$

It is slow to find among the  $q \gg 1$  values the one which makes the energy decrease and, consequently, the *acceptance ratio* is very close to 0 too. So, there are many *Monte Carlo* steps in which basically the algorithm does nothing.

Luckily, another kind of microscopic dynamics is available. This speeds up the algorithm and allows, also, a detailed analytical treatment: the *heat bath* dynamics [26, 27]. Let us analyze, in details, this stochastic dynamics for the *large  $q$ -Potts* model. We recall the algorithm, already written in *chapter (2)*:

1. Pick a random spin  $s_k$  uniformly between the  $N$  ones lying on the lattice.
2. Extract a new value  $n \in \{1, \dots, q\}$ , for the  $k_{th}$  spin, from the *heat bath* and give it to this spin with a probability:

$$\begin{aligned} \mathbb{P}_n(s_k = n) &= \frac{e^{-\beta e_n}}{\sum_{m=1}^q e^{-\beta e_m}} \\ &= \frac{w_k(s_k = n)}{\sum_{m=1}^q w_k(s_k = m)} \end{aligned} \quad (3.5)$$

which depends only on the target state.

We have used:

- $e_n = \frac{H_{Potts}(\{s_1, s_2, \dots, s_k = n, \dots, s_N\})}{N} = \frac{E_n}{N}$ , the energy per spin if the  $k_{th}$  spin has value  $n$  *i.e.*  $s_k = n$  with  $n \in \{1, \dots, q\}$ .
- $w_k(s_k = n) = e^{-\beta e_n}$ , the weight associated to the chosen configuration.
- $\sum_{m=1}^q w_k(s_k = m)$ , the normalization factor.

---

<sup>2</sup>Like the one we have used in the simulations.

At this point, considering that our  $k_{th}$  spin is surrounded by other 4 spins<sup>3</sup>, we are ready to write a small example on how to calculate the transition probabilities for the updates, as it was done recently in [44]. Let us say that our spin  $k$  has value 1:

$$s_k = 1$$

and its neighbouring spins are equal to:

$$s_k^{nord} = 1$$

$$s_k^{sud} = 2$$

$$s_k^{est} = 1$$

$$s_k^{ovest} = 3$$

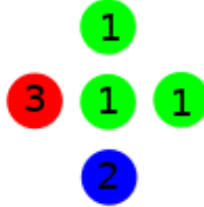


**Figure 3.1:** Example of spins configuration.

To calculate the transition probabilities for the  $k_{th}$  spin, the weights, written in units in which  $J = 1$ , are very useful:

$$w_k(s_k) = \exp\left(\beta \sum_{(i,j) \in \mathcal{N}(k)} \delta_{s_i, s_j}\right)$$

where  $\mathcal{N}(k)$  means that the sum is restricted to the neighbours of the  $k_{th}$  spin.

$$w_k(s_k = 1) = e^{2\beta}$$

$$w_k(s_k = 2) = e^{\beta}$$

$$w_k(s_k = 3) = e^{\beta}$$

$$w_k(s_k = j) = 1 \text{ with } j \in \{1, \dots, q\} \setminus \{1, 2, 3\}, \text{ there is so a } q - 3 \text{ degeneracy.}$$

---

<sup>3</sup>In the chosen topology: square lattice with coordination number equal to 4.

Thus, to obtain the transition probabilities for the central spin, we normalize the weights and we get:

$$\begin{aligned}
 T_{1 \rightarrow 1} &= \frac{e^{2\beta}}{e^{2\beta} + 2e^\beta + q - 3} \\
 T_{1 \rightarrow 2} &= \frac{e^\beta}{e^{2\beta} + 2e^\beta + q - 3} \\
 T_{1 \rightarrow 3} &= \frac{e^\beta}{e^{2\beta} + 2e^\beta + q - 3} \\
 T_{1 \rightarrow j} &= \frac{1}{e^{2\beta} + 2e^\beta + q - 3}
 \end{aligned}
 \tag{3.6}$$

For all  $q \geq 5$  it is easy to enumerate all the local configurations<sup>4</sup> and all the update probabilities for the central spin. To do so, we count how many neighbouring spins have the same value as the central one and we call this number  $n_1$ . Then, we call  $n_2$  the number of the most present spin value (different from the central one) among the neighbours of the central spin,  $n_3$  the number of the 2<sup>nd</sup> most present spin value (different from the central one) among the neighbours of the central spin, and so on... It is easy to notice that there are only 12 local configurations<sup>5</sup> [44]:

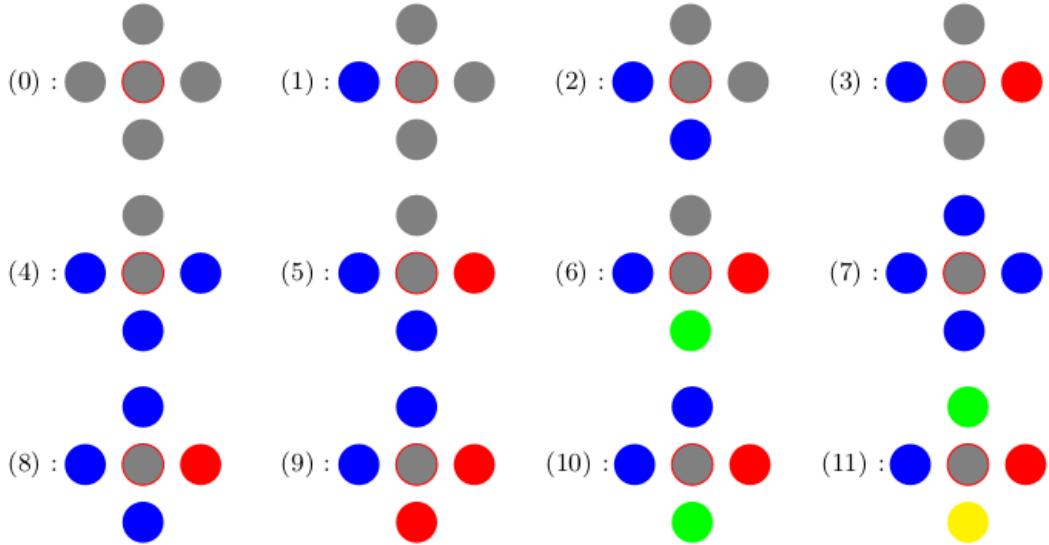


**Figure 3.2:** All the 12 possible local configurations, taken from [44].

<sup>4</sup>These are called vertex and are made of a central spin and its 4 nearest neighbours (in the square lattice).

<sup>5</sup>Each one with its degeneracy.

Here we list all the  $n_i$  different from zero and all the reachable configurations, starting from each kind of vertex:

- (0) has  $n_1 = 4$  and can go in  $\rightarrow (0); (7)$
- (1) has  $n_1 = 3, n_2 = 1$  and can go in  $\rightarrow (1); (4); (8)$
- (2) has  $n_1 = 2, n_2 = 2$  and can go in  $\rightarrow (2); (2); (9)$
- (3) has  $n_1 = 2, n_2 = 1, n_3 = 1$  and can go in  $\rightarrow (3); (5); (10)$
- (4) has  $n_1 = 1, n_2 = 3$  and can go in  $\rightarrow (4); (1); (8)$
- (5) has  $n_1 = 1, n_2 = 2, n_3 = 1$  and can go in  $\rightarrow (5); (3); (10)$
- (6) has  $n_1 = 1, n_2 = 1, n_3 = 1, n_4 = 1$  and can go in  $\rightarrow (6); (11)$
- (7) has  $n_1 = 0, n_2 = 4$  and can go in  $\rightarrow (4); (1); (8)$
- (8) has  $n_1 = 0, n_2 = 3, n_3 = 1$  and can go in  $\rightarrow (8); (1); (4)$
- (9) has  $n_1 = 0, n_2 = 2, n_3 = 2$  and can go in  $\rightarrow (9); (2)$
- (10) has  $n_1 = 0, n_2 = 2, n_3 = 1, n_4 = 1$  and can go in  $\rightarrow (10); (3); (5)$
- (11) has  $n_1 = 0, n_2 = 1, n_3 = 1, n_4 = 1, n_5 = 1$  and can go in  $\rightarrow (11); (6)$

- The (11) configuration is called *sand* and represents the disordered state
- the (0) configuration is the ordered state.

After this reasoning, we can use the fact that the (1) configuration ( $n_1 = 3$  and  $n_2 = 1$ ) is present in a flat interface.

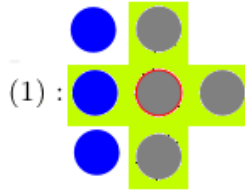


**Figure 3.3:** Flat interface configuration, the spins with a yellow background corresponds to a (1) vertex.

Indeed, we can understand how and why this particular geometry influences the dynamics and justify the assumption done in the previous chapters. To do so, let us calculate the transition probabilities from this configuration. With a single spin flip, from (1), we can stay in (1) or we can go in (4) and in (8). We can, thus,

write the configuration transition probabilities:

$$\begin{aligned}
 P_{1 \rightarrow 1} &= \frac{e^{3\beta}}{e^{3\beta} + e^\beta + q - 2} \\
 P_{1 \rightarrow 4} &= \frac{e^\beta}{e^{3\beta} + e^\beta + q - 2} \\
 P_{1 \rightarrow 8} &= \frac{q - 2}{e^{3\beta} + e^\beta + q - 2}
 \end{aligned} \tag{3.7}$$

Now, let us consider the probability  $P_{1 \rightarrow 4}$  (which is the probability to broke the interface with a "tip") in the large  $q$  limit. Before doing this let us notice that in this limit<sup>6</sup>:

$$\begin{aligned}
 \lim_{q \gg 1} e^\beta &= \lim_{q \gg 1} e^{\frac{1}{T}} \\
 &= \lim_{q \gg 1} e^{\beta_c T_c / T} \\
 &= \lim_{q \gg 1} e^{\frac{T_c}{T} \ln(1 + \sqrt{q})} \\
 &= \lim_{q \gg 1} (1 + \sqrt{q})^{T_c / T} \\
 &\simeq q^{\frac{T_c}{2T}}
 \end{aligned} \tag{3.8}$$

and thus:

$$\begin{aligned}
 \lim_{q \gg 1} P_{1 \rightarrow 4} &= \lim_{q \gg 1} \frac{e^\beta}{e^{3\beta} + e^\beta + q - 2} \\
 &\simeq \frac{q^{\frac{T_c}{2T}}}{q^{\frac{3T_c}{2T}} + q^{\frac{T_c}{2T}} + q - 2} \\
 &\simeq \frac{1}{q^{\frac{T_c}{T}} + 1 + q^{1 - \frac{T_c}{2T}}} \\
 &\rightarrow 0 \quad \forall T \leq T_c
 \end{aligned}$$

---

<sup>6</sup>We put  $k_B = 1$ .

In the same way, the probability to remain in the (1) configuration,  $P_{1 \rightarrow 1}$  in the large  $q$  limit tends to:

$$\begin{aligned} \lim_{q \gg 1} P_{1 \rightarrow 1} &= \lim_{q \gg 1} \frac{e^{3\beta}}{e^{3\beta} + e^\beta + q - 2} \\ &\simeq \frac{q^{\frac{3T_c}{2T}}}{q^{\frac{3T_c}{2T}} + q^{\frac{T_c}{2T}} + q - 2} \\ &\simeq \frac{1}{1 + q^{-\frac{T_c}{T}} + q^{1 - \frac{3T_c}{2T}}} \\ &\rightarrow 1 \quad \forall T \leq T_c \end{aligned}$$

For normalization, the probability<sup>7</sup>,  $P_{1 \rightarrow 8} \rightarrow 0$  for  $q \gg 1$ . Resuming:

$$\begin{aligned} \lim_{q \gg 1} P_{1 \rightarrow 1} &\simeq 1 \\ \lim_{q \gg 1} P_{1 \rightarrow 4} &\simeq 0 \\ \lim_{q \gg 1} P_{1 \rightarrow 8} &\simeq 0 \end{aligned} \tag{3.9}$$

In conclusion we can say that the "breaking-interfaces" updates are very improbable in the large  $q$  limit<sup>8</sup>!

---

<sup>7</sup>This is the probability to broke the interface with a tip creating an (8) vertex.

<sup>8</sup>Impossible for  $q$  infinite, of course.

Now we list all the possible configuration transition probabilities:

$$\begin{aligned}
 P_{0 \rightarrow 0} &= \frac{e^{4\beta}}{e^{4\beta} + q - 1} & P_{0 \rightarrow 7} &= \frac{q - 1}{e^{4\beta} + q - 1} \\
 P_{1 \rightarrow 1} &= \frac{e^{3\beta}}{e^{3\beta} + e^\beta + q - 2} & P_{1 \rightarrow 4} &= \frac{e^\beta}{e^{3\beta} + e^\beta + q - 2} & P_{1 \rightarrow 8} &= \frac{q - 2}{e^{3\beta} + e^\beta + q - 2} \\
 P_{2 \rightarrow 2} &= \frac{2e^{2\beta}}{2e^{2\beta} + q - 2} & P_{2 \rightarrow 9} &= \frac{q - 2}{2e^{2\beta} + q - 2} \\
 P_{3 \rightarrow 3} &= \frac{e^{2\beta}}{e^{2\beta} + 2e^\beta + q - 3} & P_{3 \rightarrow 5} &= \frac{2e^\beta}{e^{2\beta} + 2e^\beta + q - 3} & P_{3 \rightarrow 10} &= \frac{q - 3}{e^{2\beta} + 2e^\beta + q - 3} \\
 P_{4 \rightarrow 4} &= \frac{e^\beta}{e^\beta + e^{3\beta} + q - 2} & P_{4 \rightarrow 1} &= \frac{e^{3\beta}}{e^\beta + e^{3\beta} + q - 2} & P_{4 \rightarrow 8} &= \frac{q - 2}{e^\beta + e^{3\beta} + q - 2} \\
 P_{5 \rightarrow 5} &= \frac{2e^\beta}{2e^\beta + e^{2\beta} + q - 3} & P_{5 \rightarrow 3} &= \frac{e^{2\beta}}{2e^\beta + e^{2\beta} + q - 3} & P_{5 \rightarrow 10} &= \frac{q - 3}{2e^{2\beta} + e^{2\beta} + q - 3} \\
 P_{6 \rightarrow 6} &= \frac{4e^\beta}{4e^\beta + q - 4} & P_{6 \rightarrow 11} &= \frac{q - 4}{4e^\beta + q - 4} \\
 P_{7 \rightarrow 0} &= \frac{e^{4\beta}}{e^{4\beta} + q - 1} & P_{7 \rightarrow 7} &= \frac{q - 1}{e^{4\beta} + q - 1} \\
 P_{8 \rightarrow 8} &= \frac{q - 2}{e^{3\beta} + e^\beta + q - 2} & P_{8 \rightarrow 1} &= \frac{e^{3\beta}}{e^{3\beta} + e^\beta + q - 2} & P_{8 \rightarrow 4} &= \frac{e^\beta}{e^{3\beta} + e^\beta + q - 2} \\
 P_{9 \rightarrow 9} &= \frac{q - 2}{2e^{2\beta} + q - 2} & P_{9 \rightarrow 2} &= \frac{2e^{2\beta}}{2e^{2\beta} + q - 2} \\
 P_{10 \rightarrow 10} &= \frac{q - 3}{e^{2\beta} + 2e^\beta + q - 3} & P_{10 \rightarrow 3} &= \frac{e^{2\beta}}{e^{2\beta} + 2e^\beta + q - 3} & P_{10 \rightarrow 5} &= \frac{2e^{2\beta}}{e^{2\beta} + 2e^\beta + q - 3} \\
 P_{11 \rightarrow 11} &= \frac{q - 4}{4e^\beta + q - 4} & P_{11 \rightarrow 6} &= \frac{4e^\beta}{4e^\beta + q - 4}
 \end{aligned}$$

We can notice, that these probabilities are independent from the system size  $L$ . Also, we can highlight the fact that basically  $P_{i \rightarrow j}$  and  $T_{a \rightarrow b}$  are the same. The only difference, is the fact that  $P_{i \rightarrow j}$  refers to the vertices configuration transitions while  $T_{a \rightarrow b}$  refers to the single central spin transition.

Those probabilities become much more simple if we pass to the infinite  $q$  limit. Indeed thanks to the fact that  $e^\beta \simeq q^{\frac{T_c}{2T}}$  we have<sup>9</sup>:

$$\begin{aligned}
 P_{0 \rightarrow 0} &= 1 & P_{0 \rightarrow 7} &= 0 \\
 P_{1 \rightarrow 1} &= 1 & P_{1 \rightarrow 4} &= 0 & P_{1 \rightarrow 8} &= 0 \\
 P_{2 \rightarrow 2} &= 1 & P_{2 \rightarrow 9} &= 0 \\
 P_{3 \rightarrow 3} &= 1 & P_{3 \rightarrow 5} &= 0 & P_{3 \rightarrow 10} &= 0 \\
 P_{4 \rightarrow 4} &= 0 & P_{4 \rightarrow 1} &= 1 & P_{4 \rightarrow 8} &= 0 \\
 P_{5 \rightarrow 5} &= 0 & P_{5 \rightarrow 3} &= 1 & P_{5 \rightarrow 10} &= 0 \\
 P_{6 \rightarrow 6} &= 1; 4/5; 0 & P_{6 \rightarrow 11} &= 0; 1/5; 1 \\
 P_{7 \rightarrow 0} &= 1 & P_{7 \rightarrow 7} &= 0 \\
 P_{8 \rightarrow 8} &= 0 & P_{8 \rightarrow 1} &= 1 & P_{8 \rightarrow 4} &= 0 \\
 P_{9 \rightarrow 9} &= 0 & P_{9 \rightarrow 2} &= 1 \\
 P_{10 \rightarrow 10} &= 0 & P_{10 \rightarrow 3} &= 0 & P_{10 \rightarrow 5} &= 1 \\
 P_{11 \rightarrow 11} &= 0; 1/5; 1 & P_{11 \rightarrow 6} &= 1; 4/5; 0
 \end{aligned}$$

The initial disordered state is made of only (11) vertices, which are stable for  $T > T_c/2$ :  $P_{11 \rightarrow 11} = 1$  and  $P_{11 \rightarrow 6} = 0$ . The system will, thus, remain disordered forever in this limit. Instead, if  $T < T_c/2$  the (11) states change with probability  $P_{11 \rightarrow 6} = 1$  into a (6) ones. In this situation, it could happen that a spin, already connected to another spin and forming a (6) state, becomes a (3) one. There will need only few iterations to make the system made of only (0), (1), (2) and (3) *quasi*-stable states. These, inherits this name because they evolve only if a neighbour is flipped. The dynamics is similar for  $T = T_c/2$  but a little bit slower. Indeed a (6) state, which is "more ordered" than an (11), could become an (11) with finite probability:  $P_{6 \rightarrow 6} = 4/5$  making the ordering process less efficient.

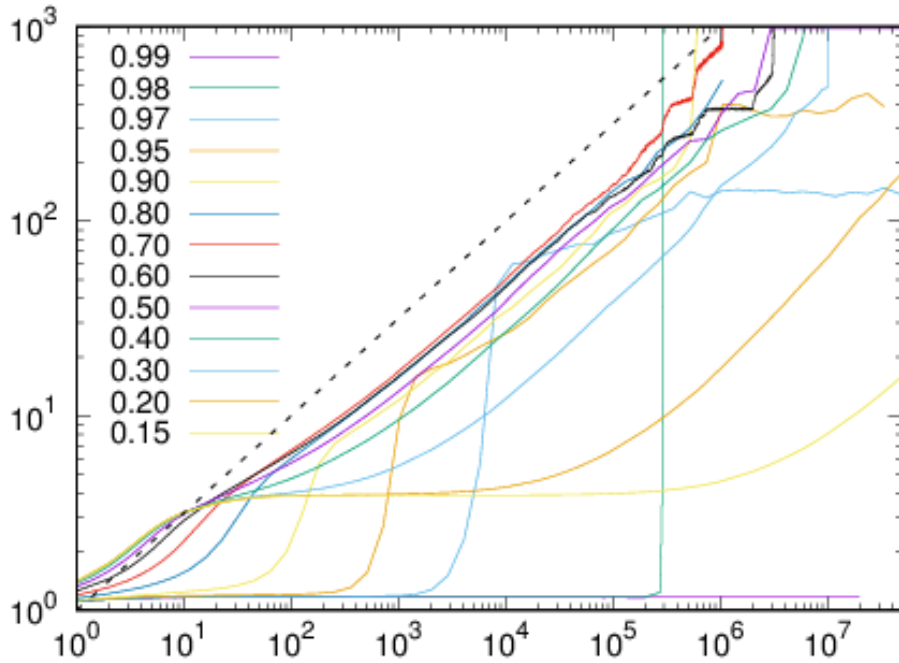
---

<sup>9</sup>When there are 3 values it means that the first value is referred to  $T < T_c/2$ , the second one to  $T = T_c/2$ , the third one to  $T_c/2 < T < T_c$ . When there is only one value it means that it is the same for each case.

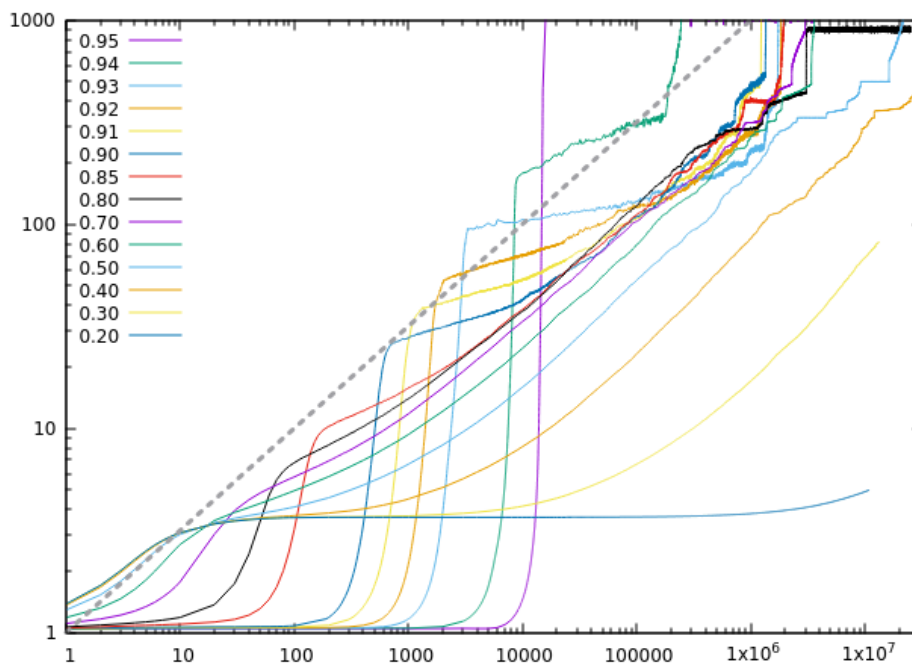
### 3.3 Characterization of the dynamics

Before concentrating in the *metastable* and *blocked* regimes, let us characterize in general the dynamics of the *Potts* model, thanks to the analysis of  $R(t)$  vs.  $t$  as could be seen from *fig.(3.14)*. We analyze and plot the growing length for different values of  $q$  (large but finite) and  $T/T_c$ , on a square lattice with side  $L = 1000$ . We use the notion explained in *chapter (2)* to read the following plots:

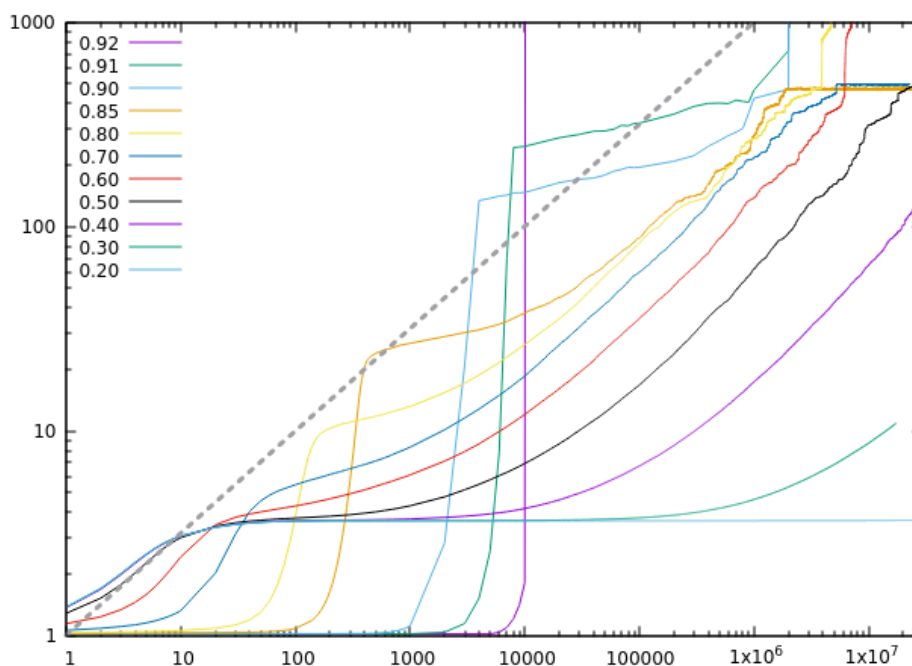
- $R(t) \simeq 1 \rightarrow$  disordered state.
- $R(t) = R \neq 1$  for relatively long times  $\rightarrow$  blocked state.
- $R(t) \simeq L \rightarrow$  ordered state.
- $R(t) \sim t^{1/2} \rightarrow$  coarsening regime.
- $R(t)$  jumps abruptly  $\rightarrow$  nucleation regime.



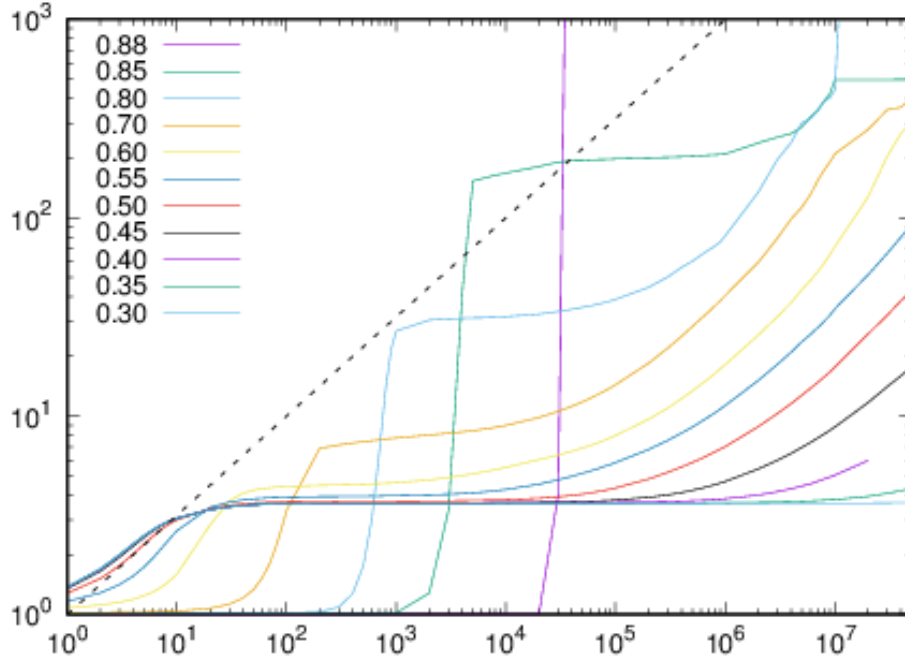
(a)  $R(t)$  vs.  $t$  for  $q=100$



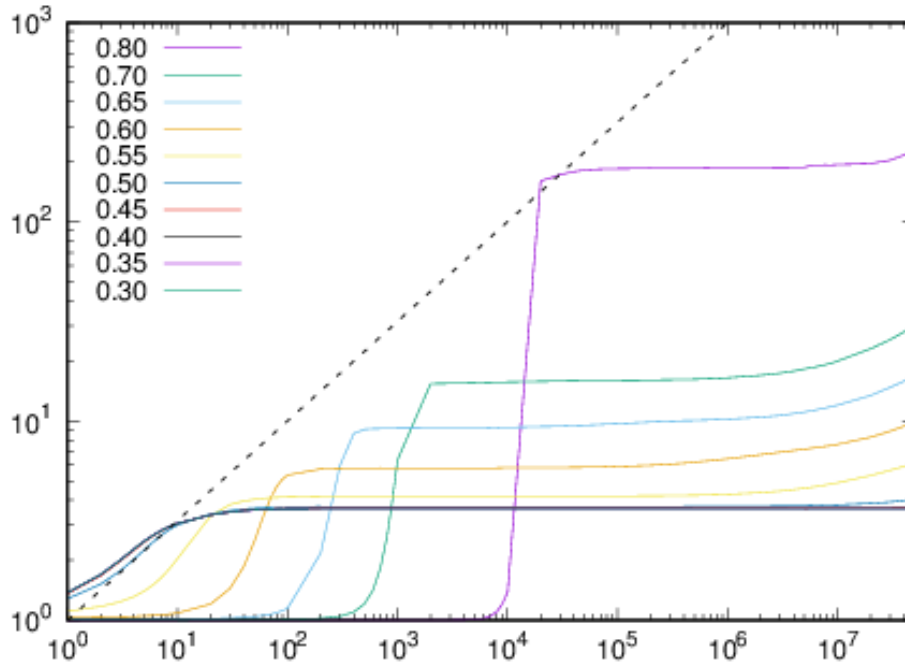
(b)  $R(t)$  vs.  $t$  for  $q=10^3$



(c)  $R(t)$  vs.  $t$  for  $q=10^4$



(d)  $R(t)$  vs.  $t$  for  $q=10^6$



(e)  $R(t)$  vs.  $t$  for  $q=10^9$

**Figure 3.4:**  $R(t)$  vs.  $t$  for  $L = 10^3$  at fixed (large)  $q$  increasing from top to bottom at different reduced temperatures  $T/T_c$ , given in the keys, for the characterization of the dynamics.

From *fig*(3.4) we can say that for the *Potts* model defined on the square lattice we have:

- For  $T/T_c \leq 1/2$  a *blocked* state with constant<sup>10</sup>  $R(t) = R \simeq 3.7$ . This state is escaped after a time  $t_b$  which becomes bigger as the ratio  $T/T_c$  becomes smaller. Once escaped the system equilibrates by means of *coarsening* of domains.
- For  $T/T_c > 1/2$  there is a *metastable* state, with  $R(t) = R = 1$ , which is escaped after a time  $t_e$  increasing with  $T/T_c$ . Later on when  $t > t_e$  there is a rapid jump towards a value  $R_m$  which grows in a similar way as  $t_e$ . Then  $R(t)$  grows slowly, for relatively small  $q$ , until the *coarsening* regime is finally reached. For very big  $q$  there is a plateau which substitutes the slow growth before the crossover with *coarsening* regime.

By now, we have noticed that the dynamics for this model can be divided into two regimes:  $T \leq T_c/2$  and  $T > T_c/2$ . This is related to the fact that for subcritical quenches the transition probability<sup>11</sup>  $P_{11 \rightarrow 6}$  in the infinite  $q$  limit is equal to 0 until  $T = T_c/2$  is reached. Here it has a jump to a value equal to  $4/5$  and then becomes equal to 1 for  $T < T_c/2$ . For finite, but large  $q$  values<sup>12</sup>, the probabilities are very close to the asymptotic ones. This is, of course, reflected in the  $R(t)$  behaviour highlighting very different dynamical behaviours on the right and on the left of  $T_c/2$  in this case too. Since the (11) states are the most<sup>13</sup> present in the starting configuration [44] this phenomenon strongly influences the dynamics. A better explanation can be found in *sec.*(3.4)

---

<sup>10</sup>This will be analyzed better in the section concerning the universality of the dynamics: *sec.*(3.6).

<sup>11</sup>As could be seen in *sec.*(3.2).

<sup>12</sup>as the one we have used in these simulation

<sup>13</sup>Unique in the infinite  $q$  limit.

### 3.4 *Metastability* and dynamics for $T > T_c/2$ with the *heat bath* rules

As stressed in the previous sections, the fact that there is a *FOT* between an ordered and a disordered phase, at  $T_c$ , makes possible the existence of *metastable* states. Indeed, due to this phenomenon, it is not ensured that starting from a disordered configuration and quenching sub-critically we would see, after some short or long transient, an ordered state. The same holds for the other kind of quenches *i.e.* starting from an ordered configuration and driving the system abruptly to supercritical temperatures. Again, in this case, the dynamics does not always bring the system into a disordered final state because an ordered *metastable* state could stop the disordering process.

This phenomenon seems to contradict thermodynamics and what we have previously written about  $PT$  and  $T_c$ . Indeed, in thermodynamics it is found analytically a  $T_c$  at which a transition happens leading the system to an uniform ordered phase. This is not happening when the system falls in a *metastable*<sup>14</sup> and it is not able to escape it. When we add dynamics to our models<sup>15</sup> we should be careful about *ergodicity*. Indeed, equilibrium statistical physics is constructed on the *ergodic hypothesis*:

$$\langle O \rangle = \frac{1}{2\tau} \int_{t-\tau}^{t+\tau} dt' O(t') \text{ with } t_0 \ll \tau \ll t \quad (3.10)$$

Where  $O$  is a generic observable,  $\langle \cdot \rangle$  is the statistical average over *ensambles*,  $t_0$  is the proper, microscopic time of the dynamics<sup>16</sup>,  $t$  is a time generic value and  $\tau$  is the time interval over which we average.

With dynamics we have a phenomenon called *ergodicity breaking* [16, 45]. Indeed, the time interval  $\tau$ , is big but is not infinite. So the statistical and time average can not be equal. This, because the system does not have enough time to visit all the possible available configuration. To obtain an equality we need to send  $\tau$  to infinity so the system manage to span all its *phase-space*. Another thing we can do to not broke the *ergodicity* is that we have to average (statistically) only on configurations that can explored by the system in that particular finite time interval  $\tau$ . It is easy to understand this, in the *2d-Ising* case.

If we "prepare" an *Ising* configuration at equilibrium in its ground state we notice that:

---

<sup>14</sup>Called also glassy state, even if there is not disorder in the model.

<sup>15</sup>*Ising* and *Potts* do not have a proper incorporate dynamics.

<sup>16</sup>*i.e.* the time needed to flip a spin.

- Calculating the statistical average of the magnetization we obtain<sup>17</sup>  $m = 0$ .
- Doing a temporal average, instead, we obtain  $m_t = 1$  or  $m_t = -1$  depending on which ground the system is into.

This is because we have not given enough time to the system to experience a, very unlikely but still possible complete spin flip.

Indeed, thermodynamics is obtained from *Statistical physics* doing the *ergodic* limit ( $\tau \rightarrow \infty$ ) before the thermodynamic one which is not done in our case [45].

### 3.4.1 Infinite $q$ case

Let us explain what happens to the system in the limit in which  $q \rightarrow \infty$  for a subcritical quench<sup>18</sup>. In this limit the critical temperature for the square lattice is:

$$T_c \simeq \frac{2J}{\ln(q)}$$

This can be expressed also as<sup>19</sup>:

$$q^{1/2} \simeq e^{J\beta_c} \quad (3.11)$$

For these kinds of quenches the initial state is chosen to be a fully disordered one. Since  $q \rightarrow \infty$  there are infinitely many colours, so, we can safely say that each spin is chromatically different from any other one at  $t = 0$ . Given the *Potts* Hamiltonian, is easy to notice that:

$$E(t = 0; q \rightarrow \infty, T/T_c) = E = (t_{disordered}; q \rightarrow \infty, T/T_c) = E_{disordered} = 0 \quad (3.12)$$

This state is found with a probability:

$$P_{disordered} = \frac{1}{Z} e^{-\beta E_{disordered}} = \frac{1}{Z} \quad (3.13)$$

When we bring the system out of equilibrium the *heat bath* dynamics starts its work. One of the  $N$  available spins tries to align with one of its 4 neighbours and with probability:

$$P_{excitation} = \frac{1}{Z} \frac{e^{-\beta E_{excitation}}}{q} = \frac{1}{qZ} e^{\beta J} \quad (3.14)$$

---

<sup>17</sup>Spin up and down are equiprobable and we sum over all the configurations.

<sup>18</sup>An analogous reasoning holds for the supercritical quench.

<sup>19</sup>We put  $k_B = 1$ .

it manages to do it<sup>20</sup>

To make the ordering phenomenon starts it must hold that:

$$\frac{P_{excitation}}{P_{disordered}} \geq 1 \quad (3.15)$$

$$\frac{e^{\beta J}}{q} \geq 1$$

This implies:

$$e^{\beta J} \geq q \simeq e^{2\beta_c J} \quad (3.16)$$

where in the last step we have used the approximation of  $T_c$  in the infinite  $q$  limit. This inequality holds for:

$$\beta \geq 2\beta_c \text{ or } T \leq T_c/2 \quad (3.17)$$

For subcritical quenches at  $T > T_c/2$  and  $q \rightarrow \infty$  we can safely say that there the disordered *metastable* state is never escaped and the system is frozen<sup>21</sup>.

Another way to see this aspect is considering the transition probabilities [44] in the infinite  $q$  limit. Emphasizing again what it is written at the end of *sec.*(3.2), we have that in the starting disordered configuration the vast majority<sup>22</sup> of the spins are in the (11) state. From the (11) state it is possible to stay in (11) or to go into the (6) state with probability:

$$\begin{aligned} P_{11 \rightarrow 6} &= \frac{4e^\beta}{4e^\beta + q - 4} \\ &\simeq \frac{4q^{T_c/2T}}{4q^{T_c/2T} + 1} \text{ for } q \rightarrow \infty \\ &= \frac{1}{1 + \frac{1}{4}q^{1-T_c/(2T)}} \end{aligned} \quad (3.18)$$

underlining again the important role played by  $T_c/2$ . We know that:

$$P_{11 \rightarrow 6} = 1 \text{ at } T < T_c/2; \ 4/5 \text{ at } T = T_c/2; \ 0 \text{ at } T > T_c/2$$

This means that with  $q \rightarrow \infty$ :

---

<sup>20</sup>The excited state has energy  $E_{excitation} = -J$ .

<sup>21</sup>In a subcritical quench the other bound is always given by  $T \leq T_c$ .

<sup>22</sup>A more precise "count" is done in [44].

- For  $T < T_c/2$  the (11) state will for sure transform into a "more ordered" (6) one and there is no *metastability*.
- For  $T = T_c/2$  the (11) state will transform into a "more ordered" (6) one with an high probability, thus the disordered *metastable* state can be escaped.
- For  $T > T_c/2$  the (11) state will never transform into a "more ordered" (6) one. The disordered *metastable* state is never escaped.

One important result of this work is that we have found a finite interval of temperatures  $T_c/2 < T \leq T_c$  in which for infinite  $q$  the model is always found in the disordered *metastable* state.

### 3.4.2 Finite but large $q$ case

For finite, but large<sup>23</sup> enough,  $q$  the scenario is not so different [44]. Of course we do not see the abrupt change of behaviour at  $T = T_c/2$  and the system can be found in an ordered state even after a quench at  $T > T_c/2$ . What is still true is the fact that the *metastable* states can be found only in the region in which  $T > T_c/2$ . For finite  $q$  and for subcritical quenches the *metastable* states are escaped, at a  $q$  dependent time:  $t_e(q)$ , up to a certain  $q$  dependent temperature  $T_m(q)$ . For quenches at  $T > T_m(q)$  it follows that  $t_e(q) \rightarrow \infty$  and the *metastable* state is never escaped. It is convenient to parametrize  $t_e(q)$  in function of  $T/T_c$ :

$$t_e(q) = T/T_c \tag{3.19}$$

Thus, for  $T/T_c > t_e(q)$  corresponds to the situation in which the system get rid of *metastability* and does not manage to get to the ordered phase. For example  $t_e(q = 10^3) \simeq 0.98$  [44], it means that:

- For  $T/T_c < 0.98$   $t_e$  is finite and the ordering dynamics can start for  $t > t_e$ ;
- For  $T/T_c \geq 0.98$  the ordering dynamics is never activated and the system is *metastable* forever.

It can be seen that, bigger is  $q$  smaller is the temperature ratio at which we observe the *metastability* phenomenon forever. This ratio, would eventually reach 0.5 in the infinite  $q$  limit [44]:

$$\lim_{q \rightarrow \infty} t_e(q) \rightarrow 0.5 \tag{3.20}$$

---

<sup>23</sup> $q \geq 10^3$ .

Here, we show two examples of the evolution of the system by means of some snapshot of the lattice. We are in the  $T > T_c/2$  regime, after a subcritical quench. Due to the finiteness of  $q$  and since  $T/T_c \leq t_e(q)$  the system manages to escape from a relatively long disordered *metastable* state, in both cases.

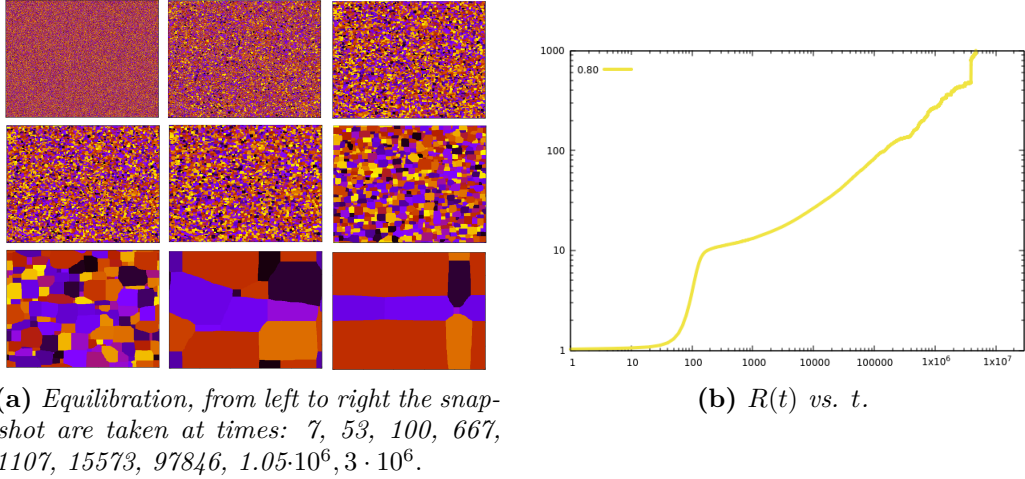


**Figure 3.5:** Snapshots of the lattice for  $T = 0.80T_c$ ,  $q = 10^4$  and  $L = 10^3$  at various times and  $R(t)$  vs.  $t$  to see the escaping from the *metastable* state.

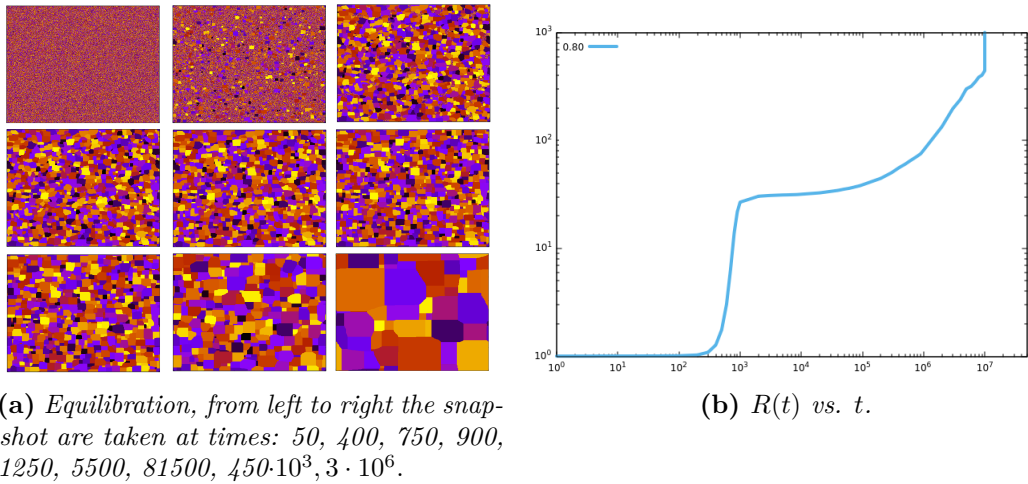


**Figure 3.6:** Snapshots of the lattice for  $T = 0.80T_c$ ,  $q = 10^6$  and  $L = 10^3$  at various times and  $R(t)$  vs.  $t$  to see the escaping from the *metastable* state.

### 3.4.3 More precise characterization of the dynamics in the $T > T_c/2$ regime

Giving more details on what is already written in *sec.(3.3)* we can say that, the dynamics in the  $T > T_c/2$  regime is strongly characterized by the presence of a *metastable* state.

This, for finite  $q$ , is escaped at a time  $t_e(q)$  which increases with  $q$  and with  $T/T_c$ . At a particular temperature  $T_m(q) > T_c/2$ , which decreases with  $q$  and reaches  $T_c/2$  in the infinite  $q$  limit, the *metastable* state is never escaped since  $t_e(q) \rightarrow \infty$ . In the finite  $q$  case, we do not know if the *metastable* state will survive the to thermodynamic limit  $N = L^2 \rightarrow \infty$ . From the simulations, a small lattice size dependency is detected, but we still have to investigate this aspect.

For very big  $q$ , when  $t > t_e(q)$ ,  $R(t)$  jumps, thanks to the *nucleation* phenomenon, on a plateau. The value of this plateau increases with  $q$  and  $T/T_c$ . The growing length spends a certain time there before crossing over with the *coarsening* regime characterized by  $R(t) \sim t^{1/2}$ . For relatively small  $q$  the behaviour of  $R(t)$  is the same as the very big  $q$  case. The unique difference is that the plateau is substituted by a slow growth which ends in the usual *coarsening* regime.

## 3.5 Equilibration for $T \leq T_c/2$

After the reasoning about *metastability*, we know that in the  $T/T_c < 1/2$  regime the ordering process is not troubled by a disordered *metastable* state. Thus, an ordering process will surely start. In any case, this does not ensure the reaching of a uniform phase. Indeed, we should consider also the fact that dynamics can freeze into *blocked* state with a particular shape.

### 3.5.1 Geometry of the clusters for infinite $q$

In this regime, each spin tries to align with one of its neighbours creating a bond. After a certain number of *Monte Carlo* steps<sup>24</sup> some spin creates one or more bonds with some of its neighbours. At the next step these bounds can be broken if one of the bonded spin changes its value to create a link with another of its neighbours in order to have a more stable configuration (for example a configuration in which it has two neighbours with the same colour rather than one). In this way, after a certain time, the dynamics creates some spin clusters with a particular shape.

---

<sup>24</sup>For a lattice with  $N$  spins one *Monte Carlo* step corresponds to the  $N$  attempt of updating the spins.

Geometrically speaking, we can say that the spins living on the interfaces between different clusters can be divided into two groups:

- The spins living on the flat part of the interface.
- The spins living on the corner between the interfaces.

We can notice that the "corner spins" have 2 neighbours with the same colour, while the "flat" ones have 3 aligned neighbours. This simple argument, in addition to what is written in *sec.(3.2)* about the stability of the flat interfaces explains why we see in the snapshots clusters with a squared or rectangular geometry.

In particular, in the infinite  $q$  limit, the probabilities<sup>25</sup>  $P_{1 \rightarrow 1}$  and  $P_{2 \rightarrow 2}$ , *i.e.* the probabilities to remain respectively in a flat and in a corner configuration, are equal to 1. This means that these configurations are completely stable and the uniform phase is never reached in this limit.

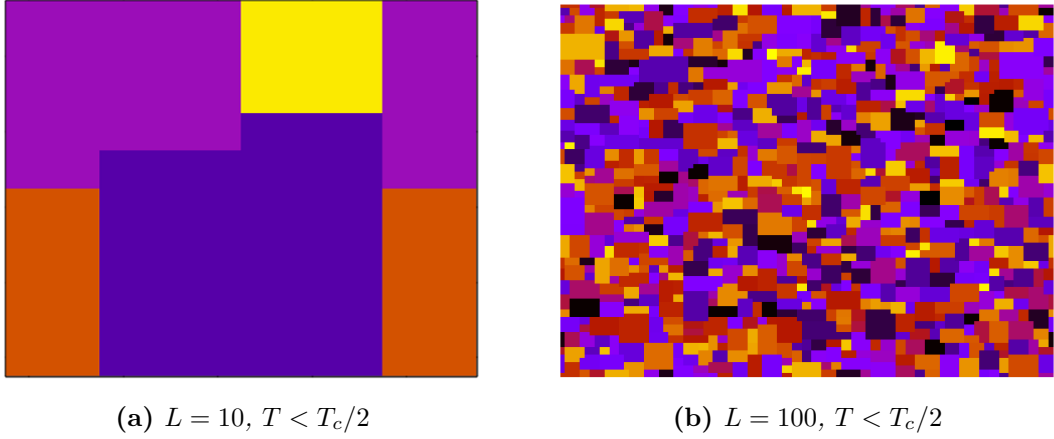


**Figure 3.7:** Snapshot of the lattice after equilibration with  $q \rightarrow \infty$  at  $T < T_c/2$  with  $L = 10$  for *fig.(a)* and at  $T < T_c/2$  with  $L = 100$  for *fig.(b)* to show the squared/rectangular shaped clusters.

---

<sup>25</sup>See *sec.(3.2)*.

### 3.5.2 Dynamics at finite $T \leq T_c/2$ with infinite $q$ and at finite $q$ but zero temperature: the *blocked* states

From *fig.*(3.8), it can be easily extrapolated an important feature of the dynamics of the *Potts* model.

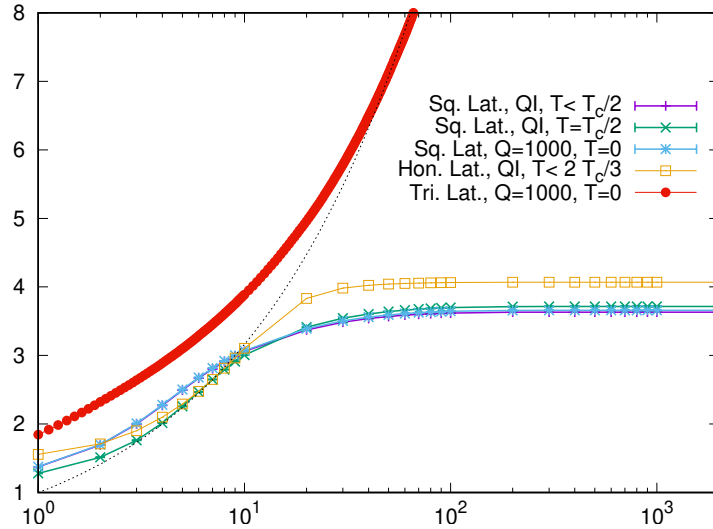


**Figure 3.8:**  $R(t)$  vs.  $t$  in lattices with  $L = 10^3$  to show the similitude between the dynamics with infinite  $q$  and finite  $T \leq T_c/2$  and the dynamics with finite  $q$  and zero temperature.  $R(t)$  is averaged over 10 samples. We plot also curves related to the honeycomb and triangular lattices.

Indeed, the dynamics, with the *heat bath* microscopic rules, is characterized by the fact that the simulations made with infinite  $q$  at finite temperature  $T \leq T_c/2$  result very similar to the ones done with finite (but large)  $q$  and zero temperature. As could be seen in *fig.*(3.7), the dynamics of the *Potts* model with infinite  $q$  and  $T \leq T_c/2$  is characterized by *blocked* states made of rectangular shaped clusters. *fig.*(3.8) ensures that the very same *blocked* states are found simulating the model at zero temperature with a large enough<sup>26</sup> but finite  $q$ . These *blocked* states are characterized by a constant growing length:

$$R(t) = R_b \simeq 3.7 \quad (3.21)$$

We can explain analytically, by means of the *heat bath* transition rules, why this similitude appears. Indeed, it is easily noticeable the fact that the transition

<sup>26</sup>We observe that for  $q < 100$  the two curves do not collapse on themselves anymore.

probabilities in the infinite  $q$  limit written in *sec.(3.2)* do not change if we keep  $q$  finite and we let  $\beta$  going to infinity ( $T$  going to 0). The only difference is that in the zero temperature case, since  $q$  is finite, the initial configuration is not made of only (11) state. This difference vanishes for  $q > 10^3$ , indeed, we see that only a negligible fraction of the spins is in  $(i) \neq (11)$ , making the two dynamics extremely similar.

Even if this go beyond the aim of this thesis, in *fig.(3.8)* we plot the behaviour of the growing length in the honeycomb and triangular lattice too. We can notice that in the honeycomb case, the dynamics is similar to the one found on a square lattice. The only difference is that the plateau, at which  $R(t)$  remains constant, is slightly bigger. Regarding the triangular lattice, instead, the dynamics is completely different. Indeed, we do not observe the presence of a *blocked* state. We can claim that this behaviour is linked with the *coordination number* of the lattices:

- $n_c^{honeycomb} = 3$
- $n_c^{triangular} = 6$

This topic will be deepened in the "work in progress" paper [2].

### 3.6 Dynamics in the $T/T_c \leq 1/2$ regime: the *universal behaviour*

In this section we argue the existence of a very important feature of the dynamics of the bidimensional *Potts* model with many states,  $q > 10^3$ , in the low temperature regime  $T \leq T_c/2$ . As always, the growing length  $R(t)$  is crucial to reach the goal of the analysis. In the general characterization of the dynamics (*sec.*(3.3), *fig.*(3.4)) we have seen that the dynamics is characterized by *blocked* state at constant  $R(t) = R_b \simeq 3.7$ . The system is frozen in this state for a certain time  $t_b$  as far as the crossover with the *coarsening* regime is reached. This, happens when the constant trend connects with the power law  $t^{1/2}$  [31]. The model remains frozen for a time  $t_b$  that increase as we decrease the ratio  $T/T_c$ . The reached *blocked* state represents the physics at zero temperature with finite  $q$  or infinite  $q$  and finite  $T$ , as explained in *sec.*(3.5.2). At this point, to better appreciate the dynamical behaviour in this regime, the  $R(t)$  data, are plotted again versus a rescaled time:

$$t/t_s(q, T/T_c) = a_q(T/T_c)t \quad (3.22)$$

Where  $a_q(T/T_c)$  is the prefactor associated to the growing length. In particular, the rescaling has been done using the time needed to reach the middle of the plateau at  $R(t) \simeq 3.7$  at  $T = 0.6T_c$  as reference<sup>27</sup>:

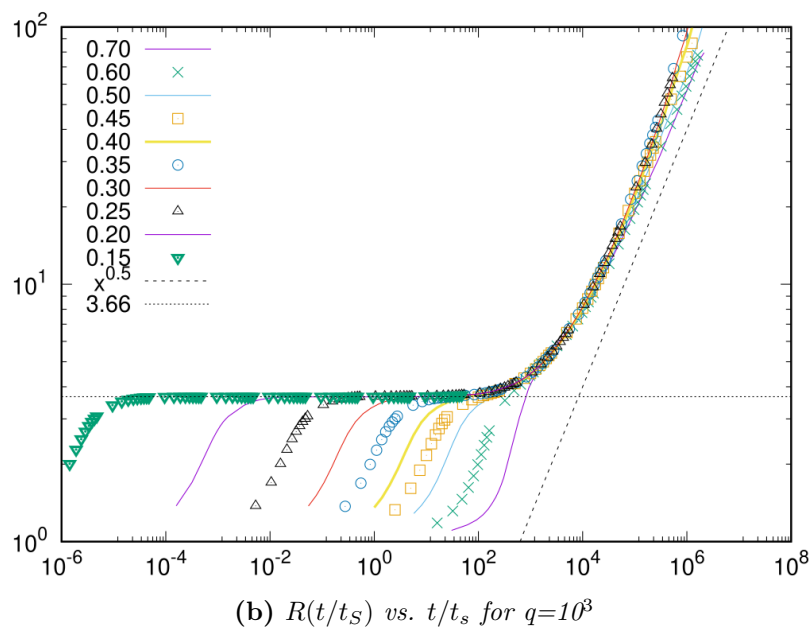
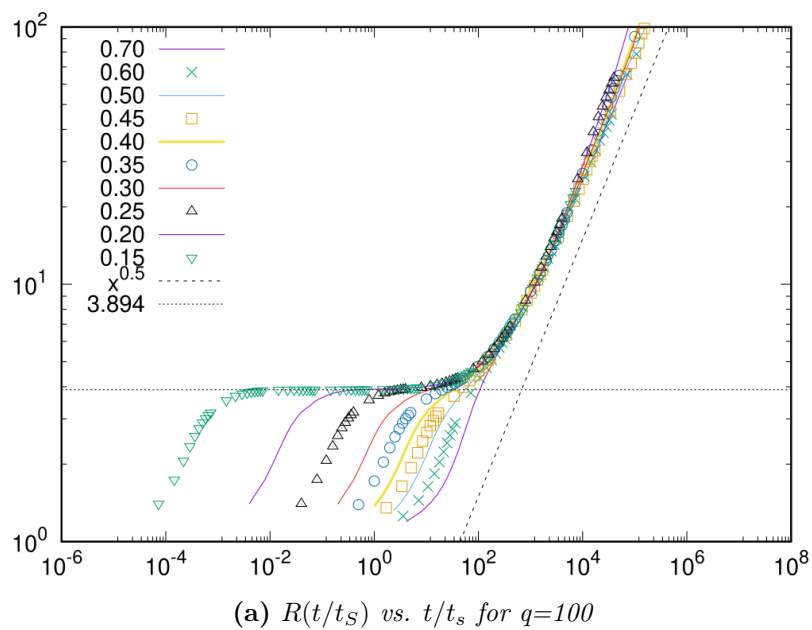
$$t_s(q, T/T_c = 0.6) = a_q^{-1}(T/T_c = 0.6) \quad (3.23)$$

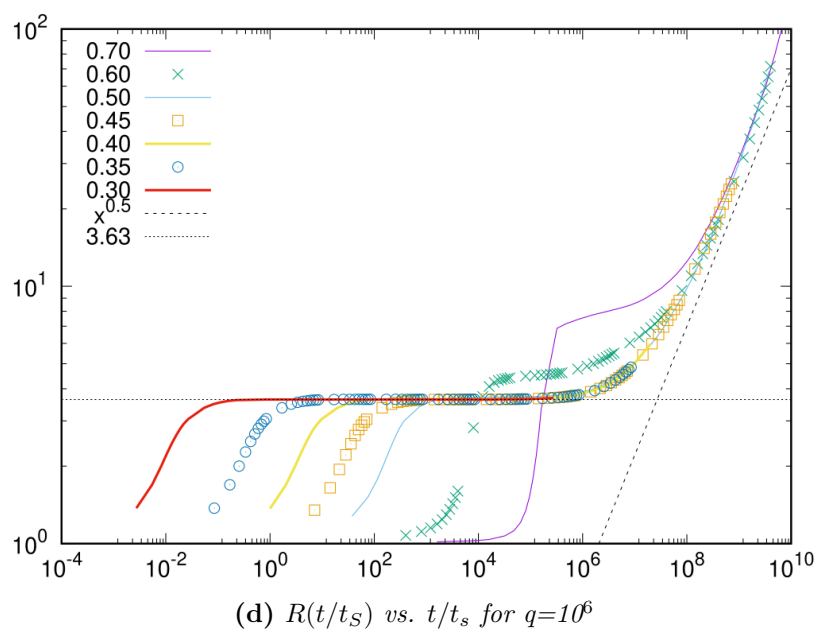
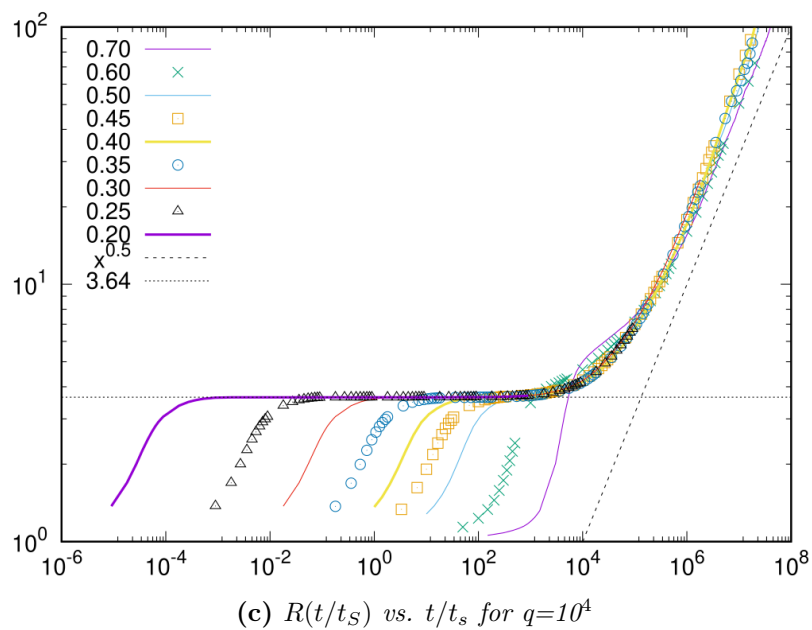
In the following plots we give a new version of the  $R(t)$  vs.  $t$  plot:

$$\begin{aligned} &R(a_q(T/T_c)t) \text{ vs. } a_q(T/T_c)t \text{ or} \\ &R(t/t_s(q, T/T_c)) \text{ vs. } t/t_s(q, T/T_c) \end{aligned}$$

---

<sup>27</sup>The choice of this value has been done simply because after some trials it does the required job.





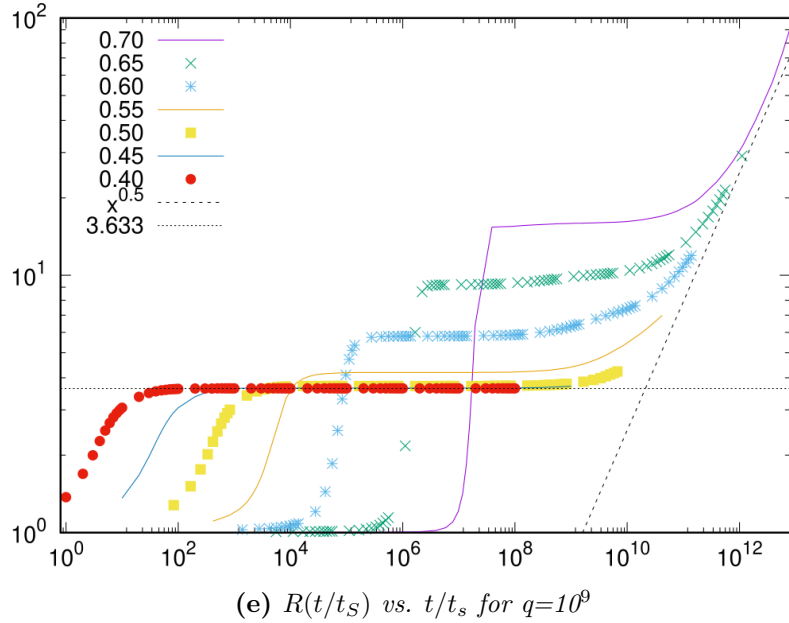


**Figure 3.9:**  $R(t/t_s)$  vs.  $t/t_s$  for  $L = 10^3$  at fixed (large)  $q$ , increasing from top to bottom and specified in the caption. The different final temperatures of the quenches are given in the keys. A dotted line in correspondence of the plateau has been plotted in addition to the usual one representing  $t^{1/2}$ .

From *fig.(3.9)* it is evident<sup>28</sup> (and we stress it again) that, the division of the dynamics into two region, one on the right and one on the left of  $T_c/2$ , is needed to characterize in a meaningful way the dynamics. Indeed, on the left of  $T_c/2$  we can see how the curves collapse perfectly on themselves, evidencing the fact that the dynamics is the same for each value of  $T$  in this range. In particular, after reaching all the same plateau, the curves have an inflection point at the very same rescaled time  $t_b/t_s(q, T/T_c)$  which connects the *blocked* state regime to the *coarsening* one. This means that we can declare that the *blocked* state is escaped in a *universal* way at the same rescaled time. To be precise, in the regime  $T \leq T_c/2$ , with  $q$  large enough, and after a short transient needed to reach the *blocked state*, we can claim the existence of a particular function  $a_q(T/T_c)$  such that<sup>29</sup>:

$$R(t; T/T_c, q) = f(a_q(T/T_c)t) = f(t/t_s(q, T/T_c)) \quad (3.24)$$

<sup>28</sup>In particular for extremely large  $q$  values.

<sup>29</sup>Of course the time scale is arbitrary, since we have done a particular choice for the rescaling of the times.

with  $f(x)$  an universal function:

$$f(x) \simeq \begin{cases} 3.7, & \text{for } x \ll 1 \\ x^{1/2}, & \text{for } x \gg 1 \end{cases} \quad (3.25)$$

To highlight the *universal* behaviour of the dynamics, we have simulated the model at fixed  $T/T_c$  varying  $q$ . The following plots<sup>30</sup> represent a rescaled version<sup>31</sup> of  $R(t)$  vs.  $t$  at fixed  $T/T_c$  for different  $q$  values, given in the keys. Moreover the following growing lengths have been averaged over 10 samples, thus we add error bars to the plots:

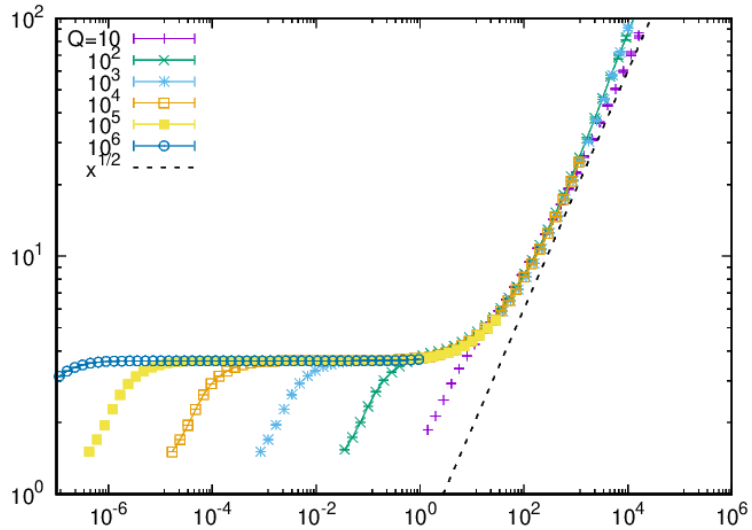
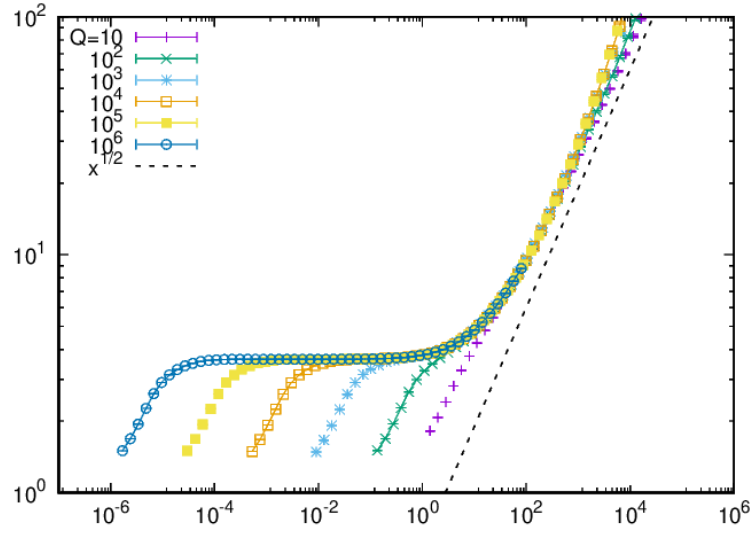


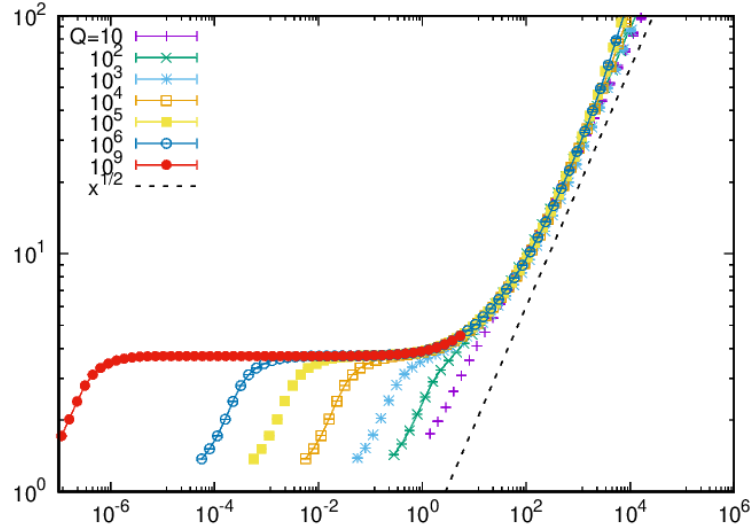
**Figure 3.10:**  $T/T_c = 0.30$

<sup>30</sup>In the usual temperatures regime, of course.

<sup>31</sup>The rescaling is done again using a generic value as reference in order to make the curve collapse on themselves.



(a)  $T/T_c = 0.40$



(b)  $T/T_c = 0.50$

**Figure 3.11:**  $R(t/t_s)$  vs.  $t/t_s$ , for  $L = 10^3$  at fixed  $T/T_c$  equal to 0.30,0.40,0.50 (from top to bottom) for different  $q$ , averaged over 10 samples.

We see, again, the same dynamical behaviour, confirming our claim about universality. From this plots we can see also the fact that the universality is no more valid for value of  $R(t)$  greater than  $10^2$ . This is explained by the fact that after a long time, when  $R(t)$  is close to  $L$  and the equilibration is quite complete, in some sample could happen that there are clusters which are completely stable. This affects the average value of  $R(t)$ , as showed in the figure, and justifies the

deviation from the common behaviour.

A final plot, showing the behaviour both with fixed and large  $q$  varying  $T/T_c$  in the usual regime and with fixed  $T/T_c \leq 0.5$  varying  $q$  (with  $q > 10^3$ ) confirms in an evident way our claim.

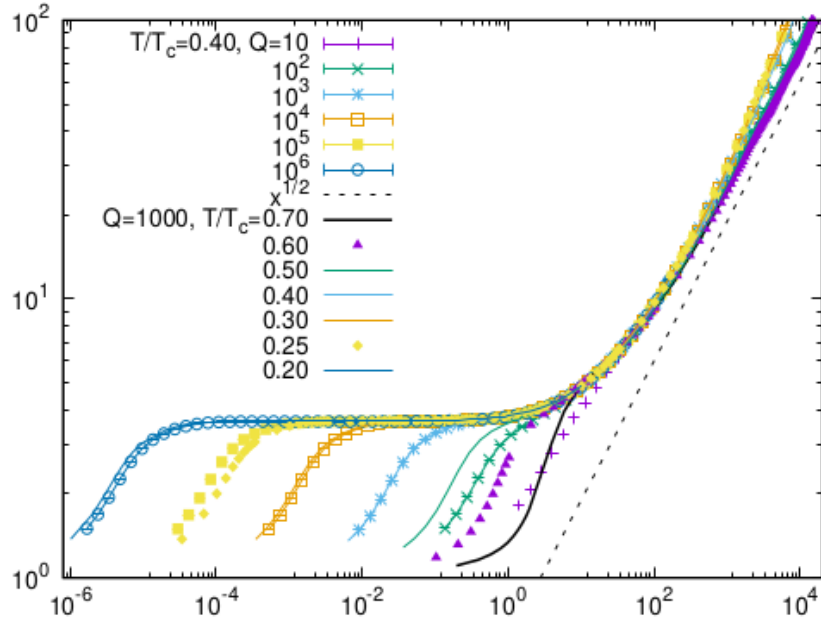


**Figure 3.12:** Universal behaviour for  $L = 10^3$  both in  $q$  and  $T/T_c$ , the legend gives information about the various values of  $q$  and  $T/T_c$  used in the simulations.

The only thing left to do, is to determine the parameter dependence of the rescaling factor  $t_s(q, T/T_c) = a_q^{-1}(T/T_c)$ . To do so, we need to introduce the characteristic time:

$$t_{R(t)=R^*} \text{ time needed for the system to reach } R(t) = R^*. \quad (3.26)$$

We have computed this quantity for  $R^* = 5, 20, 40, 80$  at fixed  $q = 10^2, 10^3, 10^4, 10^5$  in function of  $T/T_c$ , as can be seen in the following plots:

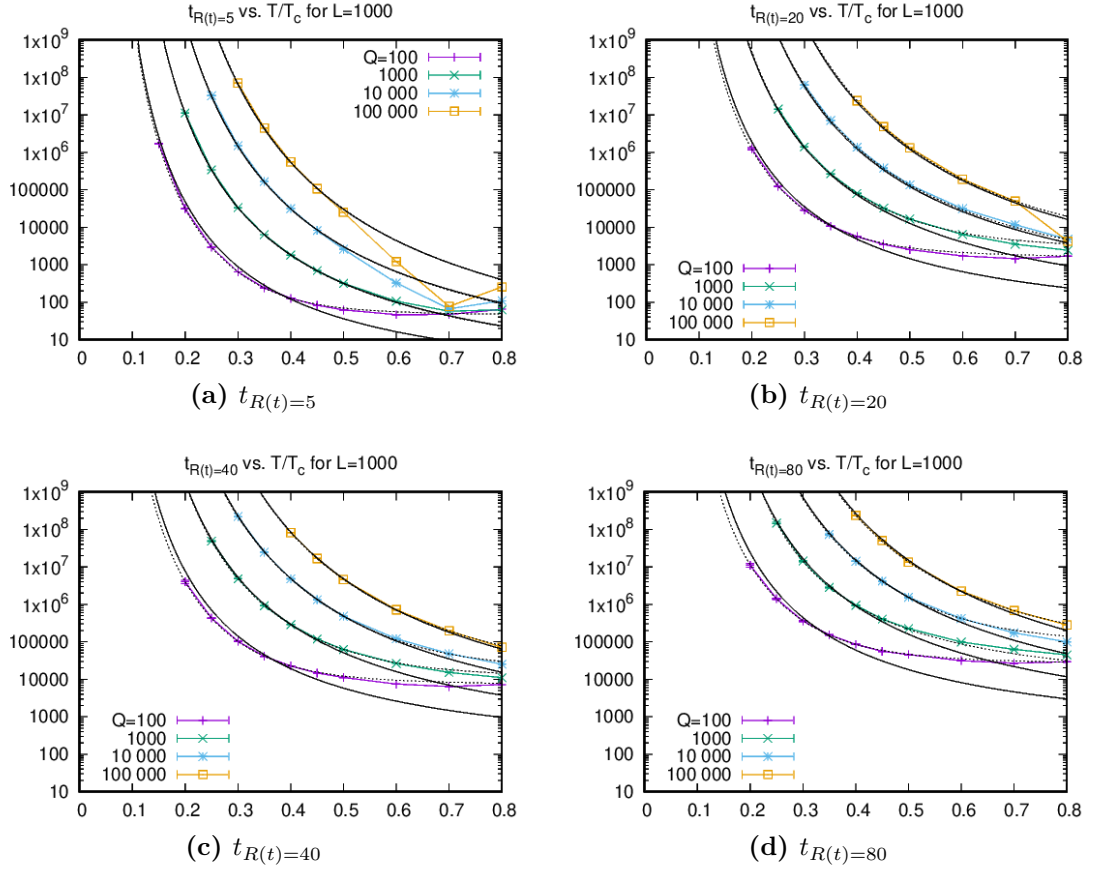


**Figure 3.13:**  $t_{R(t)=R^*}$  vs.  $T/T_c$  for  $L = 10^3$  at fixed  $q$ , given in the legend, averaged over 10 samples.

From the figure, we can see that these characteristic times diverge for very low reduced temperatures. The dotted line in the plots represents the best fit<sup>32</sup> of this time in the form<sup>33</sup>:

$$t_{R(t)} = ae^{b(T/T_c)^c} + d \quad (3.27)$$

where  $a, b, c, d$  are the parameters to be determined by the fitting. In each case we found that  $c \simeq -1$ . At this point, the fit has been done again. But now, we insert  $c = -1$  and we neglect  $d$  which is needed only for large  $T/T_c$  which are not considered in this case:

$$t_{R(t)} = ae^{b(T_c/T)} \quad (3.28)$$

<sup>32</sup>Very good results are obtained for small  $T/T_c$ .

<sup>33</sup>We put  $J = 1$ .

From this new fit we found that:

- $bT_c \simeq 1$  for each  $R^*$
- $a = 0.3$  for  $R = 5$
- $a = 12$  for  $R = 20$
- $a = 48$  for  $R = 40$
- $a = 150$  for  $R = 80$

Thus, the functional form of the characteristic time becomes simply:

$$t_{R(t)=R^*} = ae^{1/T} \text{ in units in which } J = 1, k_B = 1. \quad (3.29)$$

We can also repeat the fitting operation keeping  $T/T_c$  fixed and considering the characteristic time as a function of  $q$ :

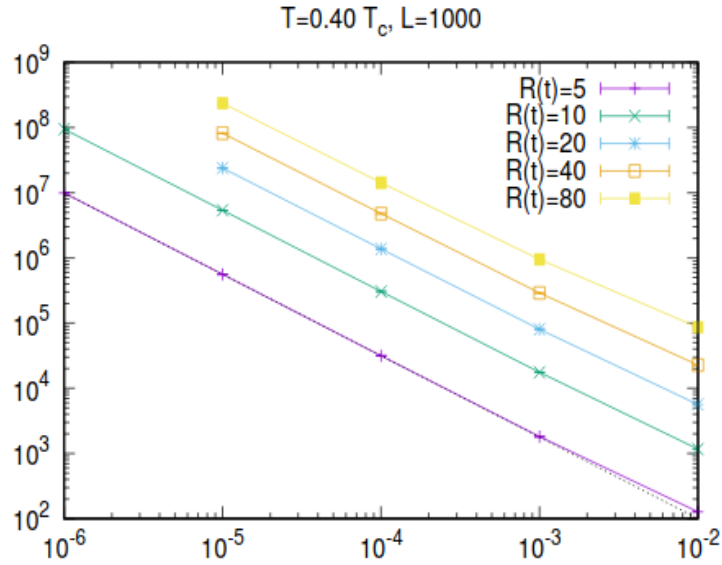


**Figure 3.14:**  $t_{R(t)=5}$  vs.  $q^{-1}$  for  $L = 10^3$  at  $T/T_c = 0.40$  averaged over 10 samples.

For  $R^* = 5$  and  $T/T_c = 0.4$  we found a power law behaviour with exponent 1.25:

$$t_{R(t)=R^*} \simeq 0.3q^{1.25} \quad (3.30)$$

which is basically equal to what we have found for the other kind of fitting at  $R^* = 5$  and  $T/T_c = 0.40$ , indeed:

$$\begin{aligned}
 0.3e^{1/T} &= 0.3e^{T_c/T\beta_c} \\
 &= 0.3e^{T_c/(T\log(1+\sqrt{q}))} \\
 &\simeq 0.3q^{T_c/2T} \text{ in the large } q \text{ limit.} \\
 &= 0.3q^{1/0.8} \\
 &= 0.3q^{1.25}
 \end{aligned} \tag{3.31}$$

To resume and to emphasize the main result of this work let us write, in a compact way, how the dynamics behaves. We have found a universal behaviour of the dynamics of the  $2d$ -Potts model both in  $q$  and in  $T/T_c$  in the  $T \leq T_c/2$  regime and for  $q \geq 10^3$ :

- After a short transient the system falls into a *blocked* state with  $R(t) = R_b \simeq 3.7$ .
- Then after a time  $a_q(T/T_c)t = t_b = e^{1/T}$  this is escaped in a universal way.
- The equilibrium is reached by means of the usual *coarsening* regime, which starts after the inflection point at  $t_b = e^{1/T}$ .

In formula, with the help of the universal function  $f(x)$ , we have:

$$R(t; T/T_c, q) \simeq f(e^{-1/T}t) \text{ with } f(x) \simeq \begin{cases} 3.7, & \text{for } x \ll 1 \\ x^{1/2}, & \text{for } x \gg 1 \end{cases} \tag{3.32}$$

### 3.7 Snapshots and geometrical properties of the clusters

We show some snapshots of the system (*fig.(3.15-3.17)*) to underline the fact that, at fixed  $R(t)$ , the model exhibits very similar geometrical properties. We have worked with  $L = 10^2$  and  $q = 10^2, 10^3, 10^4$ . For each  $q$  value, we took a snapshot when  $R(t) = 5, 10, 20, 40, 80$  as it is shown in the figure (from left to right). From top to bottom, instead, we have the snapshots at different temperatures. To be more precise we add also two tables. The *tab.(3.1)* shows, for  $q = 10^2$  and  $L = 10^2$  (upper part) and  $q = 10^2$  and  $L = 10^3$  (lower part), the characteristic time related to  $R(t) = 5$  and also the number of clusters  $N_{cl}$ , the number of clusters in which there is only a single spin  $N(1)$ , the area of the largest cluster  $max_A$ , the number of clusters containing more than 10 spins  $N(A > 10)$  and the number of colours related to this characteristic time. The *tab.(3.2)* reports the same measurement but for  $q = 10^4$  and  $L = 10^2$  (upper part) and  $q = 10^4$  and  $L = 10^3$  (lower part).

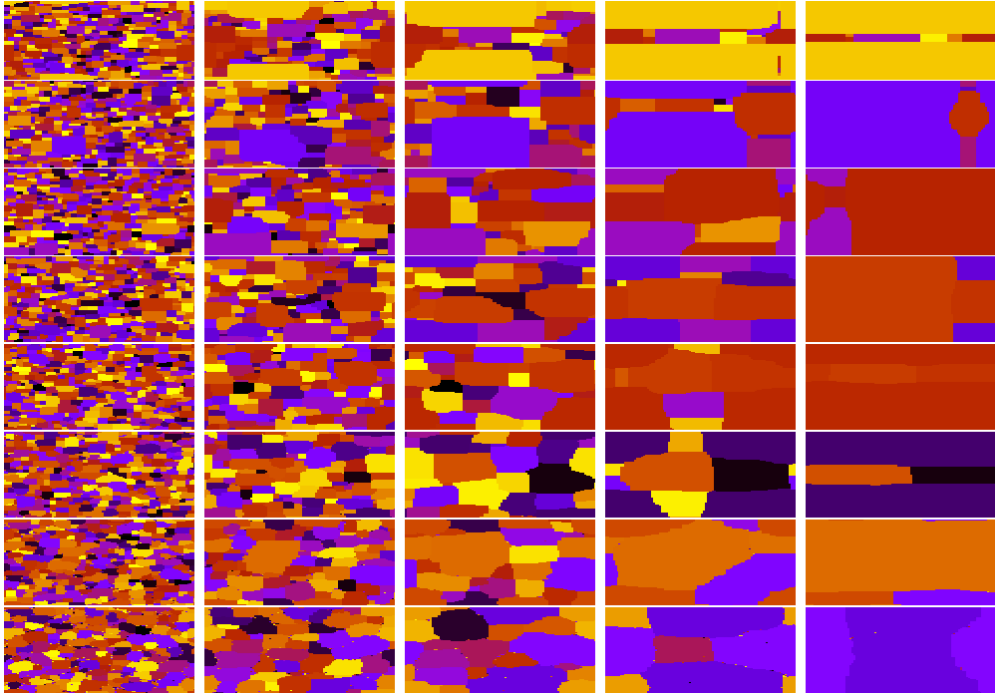


**Figure 3.15:** Snapshots with  $q = 100$  and  $L = 10^2$  at  $R(t) = 5, 10, 20, 40, 80$  from left to right with  $T/T_c = 0.20, 0.25, 0.30, 0.40, 0.50, 0.60, 0.70, 0.80$  from top to bottom.

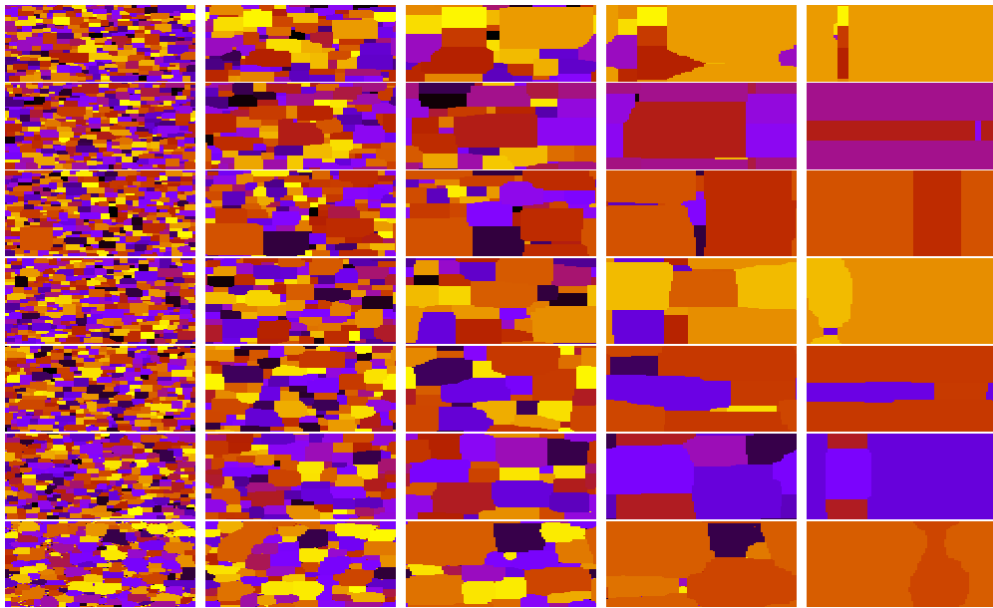


**Figure 3.16:** Snapshots with  $q = 10^3$  and  $L = 10^2$  at  $R(t) = 5, 10, 20, 40, 80$  from left to right with  $T/T_c = 0.25, 0.30, 0.40, 0.50, 0.60, 0.70, 0.80$  from top to bottom.

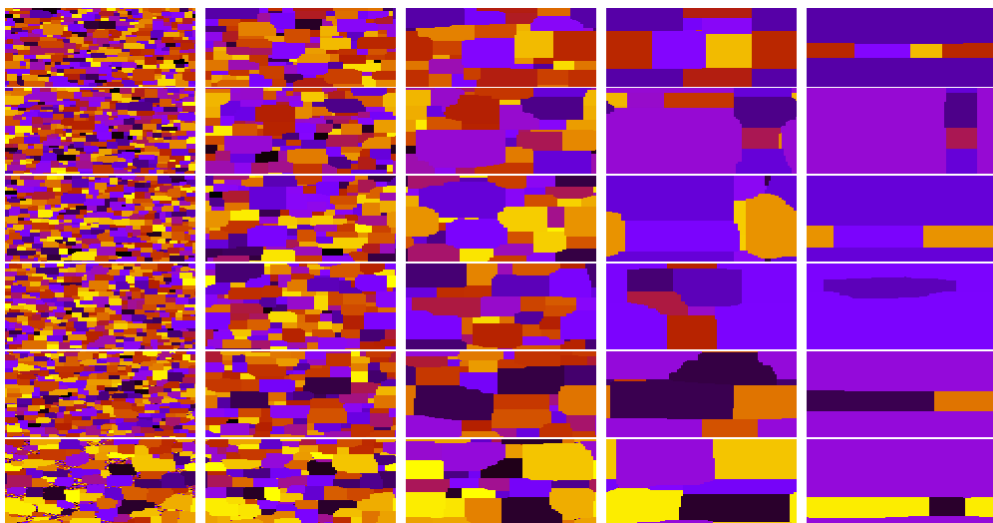


**Figure 3.17:** Snapshots with  $q = 10^4$  and  $L = 10^2$  at  $R(t) = 5, 10, 20, 40, 80$  from left to right with  $T/T_c = 0.3, 0.40, 0.50, 0.60, 0.70, 0.80$  from top to bottom.

From the snapshots, it is evident that, at fixed  $R(t)$  the various lattices looks like the same both for different  $T/T_c$  that for different  $q$ . This is an evident sign of the universality *w.r.t* these parameters.

$T/T_c$	time	$N_{cl}$	$N(1)$	$max_A$	$N(A > 10)$	$N_{col}$
0.20	30906 (60)	461.9 (1)	0.14 (1)	261 (2)	292.9 (1)	99.21 (1)
0.25	2865 (5)	460.9 (1)	0.19 (1)	254 (1)	293.35 (9)	99.17 (1)
0.30	629 (1)	457.5 (1)	0.41 (1)	235 (1)	294.83 (8)	99.14 (1)
0.35	236 (1)	450.5 (1)	1.13 (1)	209 (1)	297.48 (8)	99.07 (1)
0.40	124.5 (2)	440.75 (5)	3.17 (2)	184.7 (5)	300.78 (8)	98.98 (1)
0.45	81.4 (1)	430.95 (5)	8.35 (3)	166.6 (4)	303.20 (7)	98.86 (1)
0.50	61.27 (5)	424.71 (5)	19.77 (5)	155.3 (4)	302.92 (7)	98.81 (1)
0.60	45.66 (3)	440.0 (1)	79.7 (1)	149.0 (3)	286.32 (6)	98.96 (1)
0.70	45.91 (3)	525.7 (2)	225.4 (2)	166.2 (4)	238.21 (6)	99.56 (1)
0.80	64.07 (4)	722.4 (2)	487.7 (2)	232.2 (5)	156.59 (5)	99.94 (1)
0.20	31313 (214)	45719 (28)	0.5 (3)	1322 (250)	29117 (25)	$10^2$
0.25	2942 (8)	45608 (21)	6.9 (7)	784 (32)	29180 (20)	$10^2$
0.30	645 (3)	45233 (23)	26 (2)	652 (69)	29336 (30)	$10^2$
0.35	240 (2)	44586 (25)	108 (3)	551 (40)	29542 (33)	$10^2$
0.40	127.6 (4)	43606 (20)	334 (5)	384 (13)	29889 (20)	$10^2$
0.45	83.4 (3)	42601 (17)	862 (9)	331 (18)	30138 (24)	$10^2$
0.50	62.3 (2)	42029 (18)	2040 (21)	284 (7)	30083 (17)	$10^2$
0.60	46.7 (2)	43666 (26)	8120 (21)	266 (12)	28366 (20)	$10^2$
0.70	47.0 (1)	52420 (41)	22853 (55)	279 (8)	23540 (21)	$10^2$
0.80	65.1 (2)	72727 (53)	49472 (70)	395 (11)	15542 (18)	$10^2$

**Table 3.1:** Measurements of some interesting geometrical observables for  $q = 10^2$  and  $L = 10^2$  and  $L = 10^3$ .

$T/T_c$	time	$N_{cl}$	$N(1)$	$max_A$	$N(A > 10)$	$N_{col}$
0.30	1508100 (5197)	442.7 (2)	0.11 (1)	177 (2)	303.1 (3)	433.1 (2)
0.35	167197(578)	442.4 (2)	0.13 (1)	176 (2)	303.7 (3)	432.9 (2)
0.40	31442 (113)	442.5 (2)	0.11 (1)	176 (2)	303.5 (3)	433.0 (2)
0.45	8251 (30)	441.0 (2)	0.16 (2)	172 (2)	305.4 (3)	431.5 (2)
0.50	2591 (10)	438.8 (2)	0.37 (2)	165 (2)	308.5 (3)	429.6 (2)
0.60	329.5 (14)	434.5 (2)	7.3 (1)	144 (1)	315.9 (3)	425.4 (2)
0.70	66.1 (2)	489.0 (4)	112.7 (5)	134 (1)	292.5 (3)	477.4 (4)
0.80	109.9 (2)	1097.8 (9)	940 (1)	367 (2)	98.8 (2)	1039.8 (8)
0.30	1500748 (3098)	44269 (15)	0.4 (2)	448 (25)	30351 (16)	9881 (4)
0.35	165760 (294)	44252 (17)	0.5 (3)	384 (19)	30389 (37)	9876 (3)
0.40	31578 (114)	44221 (18)	0.7 (3)	399 (32)	30399 (26)	9883 (4)
0.45	8259 (28)	44108 (20)	7 (1)	415 (25)	30569 (30)	9878 (4)
0.50	2589 (13)	43892 (20)	36 (2)	407 (42)	30882 (27)	9876 (3)
0.60	327.7 (6)	43571 (11)	895 (11)	258 (18)	31573 (18)	9875 (5)
0.70	66.4 (1)	49034 (34)	11437 (44)	206 (7)	29239 (18)	9928 (3)
0.80	110.0 (2)	109863 (56)	94186 (60)	572 (20)	9897 (15)	9999.8 (2)

**Table 3.2:** Measurements of some interesting geometrical observables for  $q = 10^4$  and  $L = 10^2$  and  $L = 10^3$ .

Reading these tables we can say that:

- The time that the system needs to reach  $R(t) = 5$  is independent from the linear size  $L$ .
- $N_{cl}$  gains a factor  $10^2$  in the  $L = 10^3$  case *w.r.t* the  $L = 10^2$  one.
- $N(1)$  gains a factor  $10^2$  in the  $L = 10^3$  case *w.r.t* the  $L = 10^2$  one.
- $max_A$  increases since there are much more clusters in the  $L = 10^3$  case.

With these data we can ensure the absence of *finite size correction* for the chosen physical quantities.

## Chapter 4

# Conclusions and future research

To conclude, let us resume all the result found in this research work which aims in the description of the bidimensional large  $q$ -*Potts* model. Beyond the well known general characterization of the dynamics, we found a finite temperature region  $T_c/2 < T \leq T_c$  in which, the  $q \rightarrow \infty$  model, is never able to escape the disordered *metastable* state which, thus, survives forever. In this region but in the finite  $q$  case, the *metastable* states can last forever or can be also escaped, even if this process could be incredibly long. Indeed, to escape, is needed a  $q$  dependent time,  $t_e(q)$ . But, this time, diverges at a  $q$  dependent temperature  $T_m(q)$ , making impossible the ordering process. The most interesting result is, instead, found in the  $0 \leq T \leq T_c/2$  region for  $q \geq 10^3$ . For quenches with final temperature falling in this interval, the model rapidly jumps into a *blocked* state with  $R(t) \simeq R_b = 3.7$  describing the zero temperature or the infinite  $q$  physics<sup>1</sup>. At finite temperature and finite  $q$  these *blocked* states are escaped universally at a rescaled time  $t_b \simeq e^{1/T}$  giving way, in the *coarsening* regime, to the final ordering process. We have also obtained the parameter dependence of the rescaling factor<sup>2</sup>:

$$t_s(q, T/T_c) \simeq ae^{J/T} \simeq aq^{T_c/(2T)} \text{ with } a \text{ constant.}$$

Using the rescaling factor, we can conclude highlighting the universal behaviour of the growing length. Let us do it in a compact way, by means of an universal

---

<sup>1</sup>Which lasts forever only if  $q \rightarrow \infty$  or  $T = 0$ .

<sup>2</sup>Restoring  $J$ .

function  $f(x)$ :

$$R(t; T/T_c, q) \simeq f(e^{-1/T}t) \text{ with } f(x) \simeq \begin{cases} 3.7, & \text{for } x \ll 1 \\ x^{1/2}, & \text{for } x \gg 1 \end{cases}$$

These results will be improved in the PhD thesis, analyzing in a more critic way the  $T > T_c/2$  regime. The aim is to found an eventual rescaling which can light up some particular behaviour of the dynamics. The same analysis could be extended to the tridimensional *Potts* model, exploring the influence of the spatial dimension on the dynamics. Moreover, the dynamics could be interestingly deepen on other kind of lattices and with conservative-*order parameter*.

The most interesting feature, to be deepen for the *Potts* model, is the influence of the *quenched disorder* on the dynamics. A claim of *superuniversality* has been recently done in [46] and this could be tested. Also since the *FOT* becomes a *SOT* it could be pleasing to check the new critical exponents for different  $q$ . Another stimulating aspect, to be analyzed in the presence of disorder, is the study of critical interfaces (*i.e.* geometrical cluster interfaces at the critical point) to determine the *fractal* dimension.

# Bibliography

- [1] Fa-Yueh Wu. «The potts model». In: *Reviews of modern physics* 54.1 (1982), p. 235 (cit. on pp. iii, 1, 15).
- [2] Francesco Chippari - Leticia F. Cugliandolo - Marco Picco. «Dynamics for large  $q$ -Potts model in  $2d$ ». In: *IN PROGRESS* (2020) (cit. on pp. iv, 41, 62).
- [3] RB Potts. «Some generalized order-disorder transformations». In: *Mathematical Proceedings of the Cambridge Philosophical Society*. Vol. 48. 1. Cambridge University Press. 1952, pp. 106–109 (cit. on p. 1).
- [4] Denis Weaire and Nicolas Rivier. «Soap, cells and statistics—random patterns in two dimensions». In: *Contemporary Physics* 25.1 (1984), pp. 59–99 (cit. on p. 2).
- [5] James A Glazier, Michael P Anderson, and Gary S Grest. «Coarsening in the two-dimensional soap froth and the large-Q Potts model: a detailed comparison». In: *Philosophical Magazine B* 62.6 (1990), pp. 615–645 (cit. on p. 2).
- [6] Steffen A Bass, Miklos Gyulassy, Horst Stoecker, and Walter Greiner. «Signatures of quark-gluon plasma formation in high energy heavy-ion collisions: a critical review». In: *Journal of Physics G: Nuclear and Particle Physics* 25.3 (1999), R1 (cit. on p. 2).
- [7] Athanasius FM Marée, Verônica A Grieneisen, and Paulien Hogeweg. «The Cellular Potts Model and biophysical properties of cells, tissues and morphogenesis». In: *Single-cell-based models in biology and medicine*. Springer, 2007, pp. 107–136 (cit. on p. 2).
- [8] T Garel and H Orland. «Mean-field model for protein folding». In: *EPL (Europhysics Letters)* 6.4 (1988), p. 307 (cit. on p. 2).
- [9] Cristian Bisconti, Angelo Corallo, Laura Fortunato, Antonio A Gentile, Andrea Massafra, and Piergiuseppe Pellè. «Reconstruction of a real world social network using the Potts model and loopy belief propagation». In: *Frontiers in psychology* 6 (2015), p. 1698 (cit. on p. 2).

- [10] Rodney J Baxter. *Exactly solved models in statistical mechanics*. Elsevier, 2016 (cit. on p. 4).
- [11] RJ Baxter. «Onsager and Kaufman’s calculation of the spontaneous magnetization of the Ising model». In: *Journal of Statistical Physics* 145.3 (2011), pp. 518–548 (cit. on p. 4).
- [12] Bruria Kaufman and Lars Onsager. «Crystal statistics. III. Short-range order in a binary Ising lattice». In: *Physical Review* 76.8 (1949), p. 1244 (cit. on p. 4).
- [13] Richard Chace Tolman. *The principles of statistical mechanics*. Courier Corporation, 1979 (cit. on p. 10).
- [14] Kerson Huang. «Statistical Mechanics, John Wily & Sons». In: *New York* (1963) (cit. on p. 10).
- [15] Abbas Ali Saberi. «Recent advances in percolation theory and its applications». In: *Physics Reports* 578 (2015), pp. 1–32 (cit. on p. 10).
- [16] Leticia F Cugliandolo. «Advanced Statistical Physics: Phase Transitions». In: (2017) (cit. on pp. 12–14, 54).
- [17] Ulli Wolff. «Collective Monte Carlo updating for spin systems». In: *Physical Review Letters* 62.4 (1989), p. 361 (cit. on p. 14).
- [18] VL Berezinskii. «Zh. É ksp. Teor. Fiz. 59, 907 1970 Sov. Phys». In: *JETP* 32 (1971), p. 493 (cit. on p. 14).
- [19] VL Berezinskii. «Zh. É ksp. Teor. Fiz. 61, 1144 1971 Sov. Phys». In: *JETP* 34 (1972), p. 610 (cit. on p. 14).
- [20] John Michael Kosterlitz and David James Thouless. «Ordering, metastability and phase transitions in two-dimensional systems». In: *Journal of Physics C: Solid State Physics* 6.7 (1973), p. 1181 (cit. on p. 14).
- [21] J Michael Kosterlitz. «Kosterlitz–Thouless physics: a review of key issues». In: *Reports on Progress in Physics* 79.2 (2016), p. 026001 (cit. on p. 14).
- [22] Matthew PA Fisher, Peter B Weichman, Geoffrey Grinstein, and Daniel S Fisher. «Boson localization and the superfluid-insulator transition». In: *Physical Review B* 40.1 (1989), p. 546 (cit. on p. 14).
- [23] Luigi Amico and Vittorio Penna. «Dynamical mean field theory of the Bose-Hubbard model». In: *Physical Review Letters* 80.10 (1998), p. 2189 (cit. on p. 14).
- [24] Yoseph Imry and Michael Wortis. «Influence of quenched impurities on first-order phase transitions». In: *Physical Review B* 19.7 (1979), p. 3580 (cit. on p. 15).

- [25] Kristen A Fichtorn and W Hh Weinberg. «Theoretical foundations of dynamical Monte Carlo simulations». In: *The Journal of chemical physics* 95.2 (1991), pp. 1090–1096 (cit. on p. 18).
- [26] Y Miyatake, M Yamamoto, JJ Kim, M Toyonaga, and O Nagai. «On the implementation of the 'heat bath' algorithms for Monte Carlo simulations of classical Heisenberg spin systems». In: *Journal of Physics C: Solid State Physics* 19.14 (1986), p. 2539 (cit. on pp. 19, 42).
- [27] R Burioni, F Corberi, and A Vezzani. «Complex phase ordering of the one-dimensional Heisenberg model with conserved order parameter». In: *Physical Review E* 79.4 (2009), p. 041119 (cit. on pp. 19, 42).
- [28] Alfred B Bortz, Malvin H Kalos, and Joel L Lebowitz. «A new algorithm for Monte Carlo simulation of Ising spin systems». In: *Journal of Computational Physics* 17.1 (1975), pp. 10–18 (cit. on p. 20).
- [29] M Newman and G Barkema. *Monte carlo methods in statistical physics chapter 1-4*. Vol. 24. Oxford University Press: New York, USA, 1999 (cit. on p. 20).
- [30] Gregory N Hassold and Elizabeth A Holm. «A fast serial algorithm for the finite temperature quenched Potts model». In: *Computers in Physics* 7.1 (1993), pp. 97–107 (cit. on p. 20).
- [31] Alan J Bray. «Theory of phase-ordering kinetics». In: *Advances in Physics* 51.2 (2002), pp. 481–587 (cit. on pp. 22, 33, 63).
- [32] Pavel L Krapivsky, Sidney Redner, and Eli Ben-Naim. *A kinetic view of statistical physics*. Cambridge University Press, 2010 (cit. on pp. 22, 33, 36).
- [33] Federico Corberi, Leticia F Cugliandolo, Marco Esposito, and Marco Picco. «Multinucleation in the first-order phase transition of the 2d Potts model». In: *Journal of Physics: Conference Series*. Vol. 1226. 1. IOP Publishing. 2019, p. 012009 (cit. on pp. 22, 27).
- [34] J Olejarz, PL Krapivsky, and S Redner. «Zero-temperature coarsening in the 2d Potts model». In: *Journal of Statistical Mechanics: Theory and Experiment* 2013.06 (2013), P06018 (cit. on pp. 22, 37).
- [35] Thibault Blanchard, Leticia F Cugliandolo, Marco Picco, and Alessandro Tartaglia. «Critical percolation in the dynamics of the 2d ferromagnetic Ising model». In: *Journal of Statistical Mechanics: Theory and Experiment* 2017.11 (2017), p. 113201 (cit. on pp. 23, 36).
- [36] Pierre Papon, Jacques Leblond, and Paul HE Meijer. *Physics of Phase Transitions*. Springer, 2002 (cit. on pp. 24, 26).
- [37] Ken Kelton and Alan Lindsay Greer. *Nucleation in condensed matter: applications in materials and biology*. Elsevier, 2010 (cit. on p. 26).

- [38] Giuseppe Mussardo. *Statistical field theory: an introduction to exactly solved models in statistical physics*. Oxford University Press, 2010 (cit. on p. 28).
- [39] Wolfhard Janke and Stefan Kappler. «2D Potts-Model Correlation Lengths: Numerical Evidence for  $\xi_0 = \xi_d$  at  $\beta t$ ». In: *EPL (Europhysics Letters)* 31.7 (1995), p. 345 (cit. on p. 29).
- [40] Wolfgang Dreyer and Frank Duderstadt. «On the Becker/Döring theory of nucleation of liquid droplets in solids». In: *Journal of statistical physics* 123.1 (2006), pp. 55–87 (cit. on p. 32).
- [41] Yuri Kondratiev, Eugene Lytvynov, and Michael Röckner. «Equilibrium Kawasaki dynamics of continuous particle systems». In: *Infinite Dimensional Analysis, Quantum Probability and Related Topics* 10.02 (2007), pp. 185–209 (cit. on p. 36).
- [42] Ezequiel E Ferrero and Sergio A Cannas. «Long-term ordering kinetics of the two-dimensional q-state Potts model». In: *Physical Review E* 76.3 (2007), p. 031108 (cit. on pp. 37, 40).
- [43] Marcos PO Loureiro, Jeferson J Arenzon, Leticia F Cugliandolo, and Alberto Sicilia. «Curvature-driven coarsening in the two-dimensional Potts model». In: *Physical Review E* 81.2 (2010), p. 021129 (cit. on p. 40).
- [44] Onofrio Mazzarisi, Federico Corberi, Leticia F Cugliandolo, and Marco Picco. «Metastability in the Potts model: exact results in the large q limit». In: *arXiv preprint arXiv:2003.03126* (2020) (cit. on pp. 43, 44, 53, 56, 57).
- [45] Mário J de Oliveira, Alberto Petri, and Tânia Tomé. «Crystal vs. glass formation in lattice models with many coexisting ordered phases». In: *Physica A: Statistical Mechanics and its Applications* 342.1-2 (2004), pp. 97–103 (cit. on pp. 54, 55).
- [46] Gesualdo Delfino. «Exact results for quenched bond randomness at criticality». In: *Physical Review Letters* 118.25 (2017), p. 250601 (cit. on p. 78).

# Acknowledgements

At first, I would like to thank my thesis advisor Dr. Marco Picco. The door of Prof. Picco's office was always open for interesting discussion which have enriched myself both culturally and humanly. I want to thank him for its constant availability, above all, in the moments in which I used to open its door metaphorically, through Zoom or e-mail, when we were thousands of kilometers far apart for the pandemic. I am extremely grateful to Prof. Leticia Cugliandolo for her enlightening lessons, for giving me the opportunity to know Prof. Picco and for the collaboration to this thesis.

I would also like to acknowledge Dr. Luca Dall'asta as the second reader of this thesis.

I need to say thank you to professors Alfredo Braunstein, Alessandro Pelizzola, Vittorio Penna, Andrea Pagnani and Dominique Mouhanna for all the advice given during my studies.

I am forever indebted to my parents for giving me the opportunities and experiences that have made me who I am. I must express my very profound gratitude to them, this accomplishment would not have been possible without their support and efforts, thank you Mum, Dad, Antonio.

I acknowledge all the other family members for giving me the right motivation, thank you to all the uncles and aunts, all the cousins and all the grandparents.

A particular meaningful thank you goes to all my flatmates and quasi-flatmates that have made my everyday life unforgettable and full of laugh and good cooked meals, making this "journey" unique and unforgettable. Thank you: Paco, Luca, Giacomo, Fraf, Giulione, Matte, Chiare, Silvia.

I wish to express my deepest gratitude to all my friends. They have given me the strength to go further during my study without become completely mad. A huge thank you to my bros: Dario, Luca, Paco, Marco, Stacchio, Fabio, Andrea to be constantly by my side, sharing the happiest moments and giving the best influence on my life.

To my sisters: Daniela, Federica, Viviana, Titti, Anna, Claudia, Ale, Cri and Mari for our fantastic holidays which recharge my "batteries".

To Fiorella for the craziest moments both with the feet on the ground and in the

skies.

To Giovanna for being my french "R" teacher since middle school and for the lucky charm yellow umbrella.

To Chicca with whom I passed the most joyful Erasmus in Paris with "a friccico 'ner core".

To Giulia for our extremely expensive dinners which have enriched me a lot.

To Sara for our sunrises in Paris and for the big hand given to me during the quarantine.

To Cri and Checco, high school and football trainings wouldn't have been so great without you.

To Chiara and Giorgia for the best summer nights which have given me not few difficulties in writing this thesis.

I must also thank all my friends and colleagues from *Politecnico di Torino* and *Sorbonne université* for all the work done together during these beautiful years, I will never forget ours happy and anxious moments in all the libraries and the classrooms. Thank you: Claudia, Vale, Ste, Adri, Eugi, Lore, Sara, Nico, Tim, Bisardi, Ale Favero, Ema, Andre, Ele, Pier, Alex, Caffa, Carola, Davide, SimoD, Rosy, Tommy and above all Fraf, Chiare, Matte, Giulione, Silvia, Andre and Claudia for all the notes and the corrections to my uncountable mistakes.

I hope that this will be enough to reciprocate the love that you shared with me.

Love you all!

Francesco Chippari